All Graduate Theses and Dissertations   Graduate Studies

5-2014

Biophysically-Based Measurement of Plant Water Status Using Canopy Temperature

Christopher K. Parry
Utah State University

UtahStateUniversity
MERRILL-CAZIER LIBRARY

BIOPHYSICALLY-BASED MEASUREMENT OF PLANT WATER STATUS

USING CANOPY TEMPERATURE

by

Christopher K. Parry

A dissertation submitted in partial fulfillment
of the requirements for the degree

of

DOCTOR OF PHILOSOPHY

in

Plant Science
(Crop Physiology)

Approved:

_____   _____
Bruce Bugbee   Brent Black
Crop Physiology   Horticulture Physiology
Major Professor   Committee Member

_____   _____
Lawrence Hipps   Christopher Neale
Biometeorology & Atmospheric Science   Irrigation Engineering
Committee Member   Committee Member

_____   _____
Scott Jones   Mark R. McLellan
Soil Physics   Vice President for Research
Committee Member   and Dean of the School
                                              of Graduate Studies

UTAH STATE UNIVERSTIY
Logan, Utah

2014

ABSTRACT

Biophysically-based Measurement of Plant Water Status

Using Canopy Temperature

by

Christopher K. Parry, Doctor of Philosophy

Utah State University, 2014

Major Professor: Dr. Bruce Bugbee
Department: Plants, Soils, and Climate

Methods that directly determine plant physiological responses to water availability have potential to be significantly more sensitive and accurate than indirect approaches like soil moisture measurement. Stomatal conductance is a rapid physiological response to leaf water potential. Stomatal conductance in single leaves has long been calculated using energy balance and biophysical principles. This same biophysical approach can be extended to plant communities using: 1) standard meteorological measurements, 2) accurate measurement of average canopy temperature, and 3) knowledge of canopy architecture. Here we use a two-source energy balance model designed for the calculation of stomatal conductance (g_c) in row crops with random leaf spatial distribution within rows. The two-source model separates soil and canopy heat sources and accounts for the unique characteristic of vegetation clumped in

rows. The distribution of plants in rows affects not only the wind and radiation penetration in the canopy but also the separation of soil and canopy heat sources. The two-source energy balance model requires measurement or estimation of the soil and canopy temperatures. Several methods can be used to derive these temperatures. This study compares two methods for determining canopy temperature for calculation of canopy stomatal conductance.   The methods are compared for two crops (corn and cotton) in multiple geographic locations. By using the necessary environmental measurements, aerodynamic parameters and model modifications, g_C was continuously determined for multiple locations throughout the Midwest and Southern United States. This g_C value was then compared to a calculated reference g_C for a well-watered crop. This ratio is an indicator of crop water status, which is called the stomatal conductance ratio (SCR). The SCR increased closer to one (one indicating no water stress) after each irrigation or significant precipitation, and steadily declined until the next irrigation event. Significant drought stress occurred in several of the fields. Daily SCR values were weighted to correspond with growth stage sensitivity to drought stress. These weighted values were highly correlated with yield (r^2 values up to 0.79). SCR values for cotton were also highly correlated with yield (r^2 values up to 0.96). This biophysical approach has the potential to provide a powerful tool for precision irrigation management.

(222 pages)

PUBLIC ABSTRACT

Biophysically-based Measurement of Plant Water Status

Using Canopy Temperature

by

Christopher K. Parry, Doctor of Philosophy

Utah State University, 2014

Major Professor: Dr. Bruce Bugbee
Department: Plants, Soils, and Climate

Precision irrigation scheduling is one approach that can conserve water by supplying crops with the minimum amount of water needed for sufficient vegetative growth and final crop yield. Improved methods for irrigation scheduling are needed for arid regions that rely mainly on irrigation for crop water needs, and humid regions that supplement water received from precipitation with added irrigation. Methods that directly determine plant physiological responses to water availability have potential to be significantly more sensitive and accurate than indirect approaches like soil moisture measurement. Stomatal conductance is a rapid physiological response to leaf water potential.

Stomatal conductance in single leaves has long been calculated using biophysical and energy balance principles. This same biophysical approach can be extended to plant communities using: 1) standard meteorological

measurements, 2) accurate measurement of average canopy temperature, and 3) knowledge of canopy architecture.

Here we use a model designed to separate the energy balance of the soil and plant canopy for the calculation of stomatal conductance (g_c) in row crops. This model is modified for application in row crops which differ in their spatial distribution when compared to more uniform crops such as turfgrass or alfalfa. The energy balance model requires measurement or estimation of the soil and canopy temperatures. Various methods can be used to derive these temperatures, i.e., using a composite temperature of the two and either directly measuring or estimating one of the temperatures to derive the other, or directly measuring both component temperatures. This study compares two methods to determine which one is more appropriate in determining canopy temperature for calculation of canopy stomatal conductance for the measurements taken on the fields studied.

By using the necessary environmental measurements, and model modifications, g_c was continuously determined for 10 corn and 6 cotton crops throughout the Midwest and Southern United States. This g_c value was then compared to a calculated reference g_c for a well-watered crop. This reference g_c represents the stomatal conductance of a well-watered crop experiencing no water stress. The ratio of the calculated and reference g_c is an indicator of crop water status, which is called the stomatal conductance ratio (SCR). The SCR increased closer to one (indicating minimal water stress) after each irrigation or

significant precipitation event, and steadily declined until the next irrigation event. Significant drought stress occurred in several of the fields.

Daily SCR values were weighted to correspond with growth stage sensitivity to drought stress. These weighted values were highly correlated with yield (r^2 values up to 0.79). SCR values for cotton were also highly correlated with yield (r^2 values up to 0.96).

This biophysical approach has the potential to provide a powerful tool for precision irrigation management. Growers can more efficiently apply water to their crops and more accurately determine when to apply irrigation.

ACKNOWLEDGMENTS

CONTENTS

LIST OF FIGURES

CHAPTER 1

INTRODUCTION AND LITERATURE REVIEW

1.1. Introduction

As the world population increases so does its demand for fresh water. The demand for fresh water for domestic, industrial, and agricultural use is beginning to exceed its supply. People are becoming aware of the problem and are looking for solutions to conserve water usage. Irrigation is the largest user of fresh water and this is why conservation of water use should begin with improving the efficiency of crop irrigation. Precision irrigation scheduling is one approach that can conserve water by supplying crops with the minimum amount of water needed for sufficient vegetative growth and final crop yield. Improved methods for irrigation scheduling are needed for arid regions that rely mainly on irrigation for crop water needs, and humid regions that supplement water received from precipitation with added irrigation.

Knowing when to irrigate is crucial to maximize crop yield and minimize over application of water over the growth cycle of a crop. Three general approaches for deciding when to irrigate to minimize crop water stress include measuring the soil water content, using a water budget approach, and by directly measuring the physiological crop water status. There are several ways to measure the soil water content. Some of these methods are more labor intensive and others can be automatically measure and record the data.

Most irrigation scheduling indicators require automated measurements of surrounding environmental conditions and may even include direct measurements of the plant such as canopy temperature. The Utah State University solar-powered Environmental Observatory (www.weather.usu.edu) was constructed using state-of-the-art sensors and programming to provide research grade measurements and examples to the public. The task of constructing and programming this weather station was supplemental to the primary research of this dissertation. The program includes measurement of multiple types of sensor outputs, and algorithms to manage the power during the winter months. This program implements special storage saving instructions to retain variables necessary for climate data when a new program is sent or if the station was to re-power (see program in APPENDIX A).

Numerous studies have been performed on the relation between chlorophyll, plant health, and water content. These studies often use vegetation indices to determine the chlorophyll content of the crop being studied. These indices are often validated using handheld chlorophyll content meters that provide an index related to the chlorophyll content of the plant. The relationship between these optically-measured chlorophyll indices and absolute chlorophyll concentration was studied as supplemental research to the primary research in this dissertation (APPENDIX B).

Estimates of canopy stomatal conductance can be used to determine the onset of crop water stress and can be used to determine irrigation scheduling. Accurate estimates of canopy stomatal conductance can also be used to

supplement crop water use models that estimate surface evapotranspiration or canopy transpiration rates.

The objective of this study is to determine daily and seasonal crop water status of corn and cotton using canopy stomatal conductance estimates. Crop water status will be determined using the stomatal conductance model developed by Blonquist et al. (2009). This model has been developed and tested on homogeneous crop canopies (turfgrass alfalfa) and needs to be modified for application on row crops. Row crops differ from the random spatial distribution of crops like turfgrass and alfalfa because they are non-randomly distributed in rows. This unique planting distribution allows for open space between the rows until the plants grow wide enough to fill in these gaps. It is possible that full canopy closure may never happen by the end of the season due to water supply or other management practices determined by the grower. The partial covered canopies due to the spatial distribution of row crops affects the calculations of canopy and soil net radiation which is required for the calculation of canopy stomatal conductance. Improved estimates of canopy and soil net radiation are needed when applying energy balance derived approaches to row crops, as is intended for this study.

The canopy stomatal conductance model used in this study requires the calculation of the energy balance for the canopy. Canopy temperature is a key component in calculating the energy balance. A composite soil and canopy surface temperature be measured with an infrared thermometer. This composite temperature will need to be separated into a soil and canopy temperature.

Separation of these temperatures can be done either by modeling or directly measuring soil or canopy temperature. The unknown temperature (soil or canopy) can then be derived using the measured composite temperature. This study will determine with method yields temperatures that result in more correct values of canopy stomatal conductance. The robustness of the SCR index will also be examined as it is applied to row crops grown in different regions and climates.

1.2. Literature review

1.2.1. Irrigation scheduling

Irrigation scheduling is the decision of when and how much water to apply to a crop. Its primary purpose is to maximize the irrigation efficiency by applying the exact amount of water needed to replenish the soil moisture to a level that meets the water demands of the crop. Irrigation scheduling can minimize water loss common with overwatering and can save the energy required for irrigation. Irrigation scheduling requires monitoring indicators that determine when to irrigate. The most common monitoring indicators use water-balance, soil moisture-based approaches, or measure plant physiological response to water deficit (Jones, 2004).

Plant water status indicators also have the potential for use in "regulated deficit irrigation." This is the practice of allowing a slight plant water deficit to improve the carbohydrate portioning to reproductive structures as well as minimize excessive vegetative growth (Chalmers et al., 1981). This method of irrigation relies on accurate measurements of soil moisture or plant stress

indicators and the ability to irrigate often in small increments on demand.

Another method similar to regulated deficit irrigation in controlling growth and

allocation of carbohydrates to reproductive structures is partial root-zone drying.

This method supplies water alternatively to different parts of the root system (Dry

and Loveys, 1998). The dry roots provide a signal to modify growth and stomatal

aperture while the well-watered roots provide water adequate water to the plant

(Stoll et al., 2000).

Jones (2008) discussed the features that an ideal irrigation monitoring

system would have. These features include: (a) sensitive to small changes in the

system, (b) rapid response measurement in "real time" to the surrounding

conditions affecting plant water status and continual measurement, (c) readily

adaptable to different crops, growth stages, environments, and environmental

and meteorological conditions without the need of extensive recalibration, (d)

robust and reliable, (e) easy to use with little training or knowledge of the

measurement system, (f) automated to reduce labor requirements, and (g) low

setup and running costs.

1.2.2. Soil-moisture-based methods

Irrigation scheduling approaches based on soil moisture can be direct

measurements such as measuring soil water content or soil water potential, or

indirectly by making calculations of the soil water content by using a water

balance (book-keeping) approach that accounts for water inputs (precipitation or

irrigation events) and water losses (evapotranspiration, run-off and drainage)

from the soil.

Many different soil moisture sensors exist and they can be classified into two groups, those that measure soil water content (neutron probe and dielectric sensors) and those that measure the energy status or soil water availability to the plants (tensiometers and psychrometers).

The advantages of measuring the soil water potential or soil water content are that they are easy to apply, they are precise, are a good indication of how much water to apply, and can be readily automated. Disadvantages include measuring a small sampling area which requires the use of many sensors to account for soil heterogeneity, difficulty in placing in an area representative of the root-zone, and the sensors do not measure water status at the root surface (Jones, 2004).

The water budget approach is easy to apply in principle and gives the grower an idea of how much water to apply. This approach requires knowledge of how much water is added to and taken out of the plant available water reservoir. Measurement of weather variables for inputs into an evapotranspiration model for estimation of water taken from the reservoir, as well as estimates or models to predict run-off and drainage are required. Input of water into the reservoir is estimated by measuring the amount of water applied from precipitation and irrigation events. This approach is not as accurate as direct plant status measurements. It also has the disadvantage of needing accurate local estimates of precipitation and runoff, good estimates of crop coefficients for evapotranspiration estimates, and regular calibration is often needed due to errors being cumulative (Jones, 2004).

One of the problems with using the soil water status and the water budget approach is that while they are both good indicators of plant water usage they are not direct indicators of a crops water needs. Being able to detect the stress condition of a crop is considered a better method for managing irrigation scheduling since it is a direct indication of the crops water status.

1.2.3. Plant-based methods

Plants physiologically respond directly to changes in the water status in the plant tissues and not to changes in the bulk soil water content. The tissue water potential depends on both the soil moisture status and the rate of water flow through the plant. The plant response to the amount of available soil water is a complex function of the evaporative demand (Jones, 2004). This makes plant-based-methods, particularly those based on physiological plant responses more accurate in determining plant water status.

Plant based methods used for irrigation scheduling can be categorized into those that depend directly or indirectly on leaf or shoot water status, and those that rely on measurement of plant physiological response to changes in water status (Jones, 2008).

1.2.4. Physiological measurement of crop water stress

1.2.3.1. Plant water status

A common approach to identify when a plant is water stressed is to observe the plant for signs of visible wilting. The disadvantage of this method is that wilting is not an early indicator of the plant undergoing water stress and by the time wilting is apparent the impact on potential yield could be substantial. It

is generally agreed upon that water potential is a more rigorous and applicable measure of plant water status (Jones, 1990).

Two common water potential measurements are made for the leaf and the stem. Interpretation of leaf water status as an indicator of plant water status is difficult due to it being sensitive to stomatal aperture and other regulatory mechanisms, as well as environmental conditions (Jones, 2004). Stem water potential is a more useful and robust indicator of plant water status. Stem water potential is thought to more closely resemble soil water status than leaf water potential. Unfortunately these plant-based methods are not easily automated and since they closely related to soil water status they do not pose a real advantage over directly measuring soil water potential. Although soil water potential measurements do not give very accurate readings at the root surface during the day for an actively transpiring plant.

1.2.3.2. Water status of crop using canopy temperature

For any given environmental conditions, leaf or canopy temperature is directly related to the rate of transpiration from the canopy surface. Measurement of canopy temperature can be used to infer stomatal conductance or estimate transpiration rates (Jackson, 1982; Jones, 1999; Jones et al., 2002; Merlot et al., 2002). Validation of using canopy temperatures as a stress indicator relies on two basic assumptions. The first assumption is that under ideal and well watered conditions, plants will transpire at a maximum rate, which uses enough internal energy to keep leaf temperature below air temperature. This is only true if there is advected sensible heat from the surroundings to the plant canopy The

second assumption is that as the water available to the plant decreases so does the rate of transpiration, which then causes an increase of leaf temperature (Jackson, 1982).

Monteith and Szeicz (1962) and Tanner (1963) were some of the earliest researchers to measure canopy temperature as an indicator of plant drought stress. Plant leaf temperature was initially measured with thermocouples but with improved technology the more common method is to use infra-red radiometers to represent canopy temperature (Jackson, 1982). Advances in remote sensing and infrared radiometry have made it possible to apply plant-based methods for monitoring plant water status to a field scale for monitoring crop water status (Gonzalez-Dugo et al., 2006).

Measurements of leaf or canopy temperature alone are not enough to make estimates of stomatal conductance and transpiration rates or use for estimates of plant water status. Canopy temperature is influenced not only by stomatal aperture and transpiration rates but also by radiation, turbulence, air temperature, and humidity. For this reason many attempts have been made to normalize leaf and canopy temperature to account for the influence of the environment.

Air temperature was one of the first and is still widely used for normalization of environmental factors. Jackson et al. (1977) accumulated differences between leaf and air temperature as a measure of plant stress. Increased normalization was done by Idso et al. (1981) with the development of the crop water stress index (CWSI). This index relates the observed temperature

to the temperature of non-stressed and non-transpiring (stressed) crops under similar environmental conditions. This empirical approach was later modified by Jackson et al. (1981) to be more theoretically correct by using canopy and leaf temperature along with measurements of vapor pressure deficit, and a function of solar radiation.

Around the same time that the CWSI was introduced, the temperature stress day (TSD) was developed (Gardner et al., 1981). The TSD shows the difference in temperature between a stressed plot and a well-watered plot. This is not always practical in a commercial environment. The empirical CWSI becomes less accurate with a higher noise to signal ratio in environments with high humidity or where radiation or wind speed fluctuates (Jones, 2008). To further account for more of the environmental conditions more indices were developed. An attempt to account for some of these conditions was made by Jones (1999) by using wet or dry references. This method is still subject to the difficulty of making a reference surface that is similar to the measured surface, such as radiation exposure and similar radiation absorption properties.

Canopy to air temperature differences has been correlated to soil water content and stem water potential for potential use in managing deficit irrigation of peach orchards (Wang and Gartung, 2010). Wang and Gartung (2010) obtained correlations with r^2 vales of 0.67 to 0.70 between stem water potential and canopy to air temperature difference.

Another use of canopy temperature to estimated crop water stress is to measure the temperature variability of a crop (Gonzalez-Dugo et al., 2006).

Using the deviation of mid-day canopy temperatures as an irrigation scheduling

tool was suggested by Aston and Van Bavel (1972) and has been implemented

in various studies (Clawson and Blad, 1982; Clawson et al., 1989). The theory

behind this method is that plants deplete the available water around their roots at

different rates due to variability of soil properties, rooting depth and irrigation

application. The spatial variability in canopy temperature should be low for a

well-watered, non-stressed crop but increase as plant water stress increases.

Gonzalez-Dugo et al. (2006) compared canopy temperature variability with CWSI

and determined that temperature variability was sensitive to variations in plant

water stress for moderately stressed crops and was a poor indicator of crop

water stress at high levels of water stress.

1.2.5. Stomatal conductance

Changes in stomatal conductance that are sensitive to incipient water

deficits have the potential to provide an accurate indication of plant water status.

Stomatal conductance can be accurately measured using portable diffusion

porometers, but they are labor intensive and unsuitable for automation. Infrared-

thermometry and thermography can be used as alternates to porometers in

estimating stomatal aperture as it responds to water stress. These approaches

have the advantage of viewing a larger sampling area as well as being able to

automate for real-time measurements. Measurement of stomatal conductance

gives effective comparisons across a range of environmental conditions. The

ability to calculate stomatal conductance from canopy temperature would

overcome the limitations imposed by the difficulty of getting reference surfaces

with similar properties to the measured canopy leaves, but requires additional accurate meteorological data, especially when dealing with radiation interception and canopy energy balance (Jones, 2008). Blonquist et al. (2009) calculated canopy stomatal conductance for turfgrass (*Poa pratensis* L.) and alfalfa (*Medicago sativa* L.) by solving for stomatal conductance from energy balance equations. Estimates of stomatal conductance were compared to a reference stomatal conductance calculated from the Ball, Woodrow, Berry model. This comparison gave an indication of the current water status of the crop. Under well watered conditions when the crop was assumed to be under little or no water stress, the calculated canopy stomatal conductance was near or over the reference value. It was observed that stomatal conductance generally decreased throughout the day in response to a depletion of available water to the plant throughout the day. Stomatal conductance modeled by Blonquist et al. (2009) also responded to water application indicating decreased water status in response to increased water availability.

1.2.6. Measurement of canopy temperature

Leaf temperatures can vary by several degrees because of differences in angle, position, radiation capture, and size. For this reason it is suggested that an aggregated measurement of many leaves be used as a representation of canopy temperature (Jones et al., 2009). When measuring canopy temperature the target temperature is most often a composite of several objects other than the leaves themselves. The target temperature could be influenced by stems, branches, as well as the soil surface. The major concern is separating the soil

and canopy temperatures while assuming all other components are negligible.
The relation between the composite radiometric temperature ($T_{Radiometric}$,
temperature after correction for emissivity of the target object), canopy
temperature T_{Canopy}, and soil temperature T_{Soil}, is based on the Stephan-
Boltzman relationship between radiation and temperature:

$$T_{Radiometric}^4 = f_C(\theta_R)T_{Canopy}^4 + (1 - f_C(\theta_R))T_{Soil}^4 \qquad 1.1$$

Assuming a random canopy, the fraction of the radiometer field of view occupied
by the canopy ($f_C(\theta_R)$) can be calculated using a simple extinction equation:

$$f_C(\theta_R) = 1 - e^{-\left(\frac{Kdir*LAI}{cos\theta_R}\right)}$$

1.2

where LAI is the leaf area index (m^2_{leaf} m^{-2}_{ground}), θ_R is the zenith angle of the
radiometer, and K_{dir} is the direct radiation extinction coefficient for light
transmission through plant canopy. The extinction coefficient (K_{dir}) is the ratio of
the area projected onto the horizontal from the viewing direction θ to the hemi-
surface area projection of a 3-D object determined by the leaf angle distribution
of a canopy. The most useful distribution is ellipsoidal (Campbell and Norman,
1998). The simple calculation of the canopy fraction within the radiometer field of
view is intended for use with homogeneous, randomly spaced canopies.
Canopies that exhibit a sparse, non-random spatial distribution such as crops
early in the growth season or row crops require modified extinction equations or
geometrically based equations to account for their unique canopy cover. Another
option is to wait until the canopy has reached full coverage and assume that the
target temperature is composed only of the canopy. This may not be possible for

some crops such as cotton that depending on water availability and growing conditions may never reach full canopy coverage. Increasing the infrared radiometer zenith angle will also maximize the fraction of canopy within the radiometer field of view but has the potential of not measuring an acceptable portion of both sunlit and shaded canopy leaf temperatures. Weighting sunlit or shaded leaves more in the composite temperature of the canopy will not give an adequate representation of the canopy temperature as a whole.

1.2.7. Review of Blonquist et al. (2009)

Blonquist et al. (2009) combined energy balance and heat flux equations for a transpiring plant canopy and rearranged them to derive an equation for stomatal conductance (See derivation of this equation Appendix C):

$$g_C = \frac{g_V P_B \left[(R_{nC} - A_n) - g_H C_P (T_{Canopy} - T_{Air}) \right]}{g_V \lambda (e_{SC} - e_A) - P_B \left[(R_{nC} - A_n) - g_H C_P (T_{Canopy} - T_{Air}) \right]} \qquad 1.3$$

where g_c is canopy stomatal conductance (mol m^{-2} leaf area s^{-1}), g_V and g_H are the boundary layer conductance to water vapor and heat respectively (mol m^{-2} s^{-1}), P_B is the barometric pressure (kPa), R_{nc} is the net radiation divergence in the canopy (W m^{-2}), A_n is net assimilation (W m^{-2}), C_P is the heat capacity of air (29.17 J mol^{-1} C^{-1}), T_{Canopy} is the aerodynamic canopy temperature (°C), T_{Air} is the air temperature (°C), λ is the latent heat of vaporization (J mol^{-1}), e_{SC} is the saturated vapor pressure (kPa), at $T_{Canopy,}$ and e_A is the vapor pressure (kPa), of air.

This equation is an improvement over other equations that treat the canopy as a "big-leaf" because it uses only the canopy layer as opposed to a composite of both the soil and canopy layers. To use this equation, a value for T_{Canopy} and $R_{ncanopy}$ must be calculated. It is difficult to measure these variables directly due to the difficulty of eliminating the soil component from the view of infrared and net radiometers. Blonquist et al. (2009) used the two-source model of Norman et al. (1995) and later refined by Kustas and Norman (1999) to separate the surface energy balance into soil and canopy layers. A major assumption is made that the radiometric canopy temperature (T_{Canopy}) value used for the stomatal conductance equation is equal to aerodynamic canopy temperature, and does not include soil temperature seen by the radiometer (Blonquist et al., 2009).

Blonquist et al. (2009) performed a model response and sensitivity test of equation (1.3) as a function of each measured variable and the stability corrections needed for the calculation of heat and water vapor boundary layer conductance. The analysis showed that sensitivity increased for all variables as the conditions changed from sunny, warm, and dry to cloudy cool and humid. They emphasized the importance of accurate canopy and air temperature measurements. Sensitivity of equation (1.3) is especially high for small errors in these two variables under cloudy, cool, and humid conditions.

Blonquist et al. (2009) made the necessary measurements for calculation of g_c using equation (1.3) over alfalfa (*Medicago sativa* L.) and turfgrass (*Poa pratensis* L.) canopies during the summer. The calculated g_c was compared to a

"potential canopy stomatal conductance" (g_{cp}) or rather a reference canopy stomatal conductance to have an indication of the plant water status. The g_{cp} was calculated by scaling up maximum shaded and sunlit leaf stomatal conductance values (g_{LSun} and g_{Lshade}). These leaf stomatal conductance values were calculated using the Ball, Woodrow, Berry model (Ball et al., 1987):

$$g_L = m \frac{A_{nL} RH_L}{C_{CO_2 L}} + b \qquad\qquad 1.4$$

where A_{nL} is the leaf net assimilation (mol m^{-2} leaf area s^{-1}), RH_L and $C_{CO_2 L}$ are the relative humidity (kPa kPa^{-1}) and CO_2 mole fraction (mol mol^{-1}) of the air at the leaf surface, respectively, and m and b are the slope and intercept specific to the plants type of photosynthesis (C$_3$ or C$_4$).

Blonquist et al. (2009) observed that the ratio of the calculated to potential stomatal conductance for the alfalfa crop generally decreased throughout the day. This is an indication that the alfalfa crop was unable to supply the water needed by the leaves with stomata fully open during the afternoon. The stomata closed in response to available water at the time. The typical daily ratio values for turfgrass were similar to those of alfalfa. They also saw an increase in g_c for alfalfa and turfgrass as the stomata responded to an application of water.

1.2.8. Model for calculation of a stomatal conductance

To calculate stomatal conductance (g_C) from equation (1.3) measurements or estimates of canopy temperature, air temperature, barometric pressure, relative humidity, net radiation, wind speed, and plant canopy height are needed.

This equation calculates a stomatal conductance that does not include the soil component and is not a calculated conductance for the surface as a whole. The two-source energy balance model developed by Norman et al. (1995) is used to separate the surface energy balance into soil and canopy layers. This approach allows T_{Canopy} to be calculated from a surface radiometric temperature and net radiation of the canopy (R_{NC}) to be calculated from measurements of net radiation (R_N) of the surface or from the components of the surface radiation balance.

1.2.9. Use of two-source model

Norman et al. (1995) proposed a two-source energy balance model (TSM) where the sensible heat and latent heat flux can be calculated separately for both the canopy and soil layer. A parallel and a series resistance network model to account for coupling between the soil and canopy were both described in detail. In the parallel network, turbulent fluxes occur as separate interactions between the soil and the atmosphere and the canopy and the atmosphere, without a direct interaction between the soil and canopy. The series network accounts for interaction between the soil and canopy with the introduction of a within-canopy air temperature term (T_{AC}). Li et al. (2005) concluded that the parallel network formulation was more sensitive to vegetation cover estimates and that the errors from these uncertainties are minimized by using the series network and its T_{AC} term. The series network was deemed more preferable over the parallel network for heterogeneous landscapes that can vary in canopy cover (Kustas and Norman, 1999; Li et al., 2005).

This two-source model requires a single measurement for radiometric temperature (T_Radiometric), basic vegetation information, and meteorological variables that are readily available from weather stations equipped to calculate reference evapotranspiration (ET) (air temperature, vapor pressure deficit, wind speed, and incoming solar radiation). The relationship between T_Radiometric, canopy temperature T_Canopy, and soil temperature T_Soil, is based on the Stephan-Boltzman relationship between radiation and temperature (see equation 1.1).

To separate canopy and soil temperatures from the composite radiometric temperature, Norman et al. (1995) proposed making an initial estimate of T_Canopy by separating canopy net radiation into latent and sensible heat fluxes using a modified Priestly-Taylor approximation equation:

$$\Delta R_{NC} = LE_{Canopy} + H_{Canopy} \qquad\qquad 1.5$$

$$LE_{Canopy} = PT\alpha f_g \frac{S}{S+\gamma}\Delta R_{NC} \qquad\qquad 1.6$$

$$H_{Canopy} = g_H C_P (T_{Canopy} - T_{Air}) \qquad\qquad 1.7$$

$$T_{Canopy} = \frac{\Delta R_{NC}\left[1 - 1.3 f_g \frac{S}{S+\gamma}\right] R_A}{\rho C_P} + T_{Air} \qquad\qquad 1.8$$

where ΔR_{NC} is the net radiation for the canopy (W m^{-2}), LE_{Canopy} is the canopy latent heat flux (W m^{-2}), H_{Canopy} is the canopy sensible heat flux (W m^{-2}), $PT\alpha$ is the Priestley-Taylor coefficient, f_g is the fraction of green vefgetation, S is the

slope of the saturation vapor pressure to temperature relation (kPa C^{-1}), γ is the psychrometric constant (kPa C^{-1}), and g_H is the aerodynamic boundary layer heat conductance (mol m^{-2} s^{-1}), T$_{Soil}$ is then calculated from T$_{Canopy}$ and T$_{Radiometric}$ by the rearrangement of equation 1.1, resulting in:

$$T_{Soil} = \sqrt[4]{\frac{T_{Radiometric}^4 - f(\theta)T_{Canopy}^4}{(1 - f(\theta))}} \qquad 1.9$$

The remaining soil and canopy energy fluxes are calculated to assure that the energy balance equations for soil and canopy are satisfied. If the soil latent heat flux results in a negative number, it can be set to zero and heat fluxes, T$_{Canopy}$, and T$_{Soil}$ are recalculated until a reasonable energy balance is obtained. It has also been proposed that the Priestley-Taylor coefficient be reduced gradually, reflecting a reduction in potential transpiration, until a reasonable energy balance is obtained (Agam et al., 2010).

The Norman et al. (1995) two-source energy balance model only uses a single measurement of T$_{Radiometric}$ and generally does not require additional information than that required for most single layer energy balance models.

1.2.10. Sensible heat flux

Canopy sensible heat flux (H$_{Canopy}$) cannot be measured directly with the sensors on the station so H$_{Canopy}$ is estimated using the equation:

$$H_{Canopy} = g_H C_p \left(T_{Canopy} - T_{Air} \right) \qquad 1.10$$

It is similar to the bulk aerodynamic sensible heat equation (1.7). The difference is the use of T$_{Canopy}$ in place of the aerodynamic temperature (T$_O$).

The aerodynamic temperature cannot be directly measured. T_O represents the temperature of the apparent source/sink of sensible heat flux or the effective temperature of the surface that that satisfies the sensible heat equation based on observed values of H (Kustas and Norman, 2000). If H was measured with an eddy covariance station then it could be solved by inverting the sensible heat equation and using the conductance term derived using measurements of H, wind speed, and air temperature (Chavez et al., 2005).

Radiometric surface temperature ($T_{Surface}$) is often instead of T_O. Surface temperature ($T_{Surface}$) is usually 2-3 ^{0}C higher than T_O for uniform canopies and up 10 to 15 ^{0}C higher for incomplete canopies (Chavez et al., 2010). This is due to the influence that soil temperature has on $T_{Surface}$. T_O is the contribution of all transpiring canopy layers. The more layers that are included in the radiometric temperature measurement will result in T_{canopy} being closer to T_O. This would mean that T_{canopy} measured at an angle perpendicular to the canopy would be further from T_O than using a viewing measurement angle that looks into multiple canopy layers. An optimum viewing angle is considered to be between 50 and 70 degrees from nadir.

Many approaches have been developed to more accurately estimate T_O. These approaches include using adjustment parameters or replacing the roughness length for sensible heat exchange with a "radiometric" roughness length. The radiometric roughness length was unreliable for partial canopies and adjustment parameters are limited in their accuracy when the difference between $T_{Surface}$ and T_O is large (Maes and Steppe, 2012). This would mean that if $T_{Surface}$

was used instead of T_O in estimating sensible heat flux, the surface would have

to be uniform and homogeneous (full canopy cover) and the $T_{Surface}$ and T_O

difference would need to be low. For low $T_{Surface}$ and T_O differences to occur the

canopy would need to be complete and T_{Soil} and $T_{Surface}$ differences would need

to be relatively low, since T_{Soil} influences $T_{Surface}$. Also, assuming the surface is a

crop canopy, using view angles of 50 to 70 degrees to measure the radiometric

temperature will give closer values of $T_{Surface}$ to T_O.

The difference between $T_{Surface}$ and T_O in partial canopies, such as row

crops, has been addressed using two-source energy balance models. The

surface is divided into a soil and canopy layer and the energy fluxes are

computed for each. Using this two-source model takes out the soil component of

a surface measured surface radiometric temperature. Because T_O is largely

influenced by the transpiring canopy layers, using T_{Canopy} instead of $T_{Surface}$ for T_O

results in better estimates of canopy sensible heat flux. Using a "series" network

approach that has the heat fluxes from the soil and canopy layers influence the

canopy air space temperature (T_{AC}), the surface sensible heat flux is divided into

the soil and canopy heat flux as follows:

$$H_{Surface} = H_{Soil} + H_{Canopy} \qquad\qquad 1.11$$

$$H_{Soil} = g_H C_p (T_{Soil} - T_{AC}) \qquad\qquad 1.12$$

$$H_{Canopy} = g_H C_p (T_{Canopy} - T_{AC}) \qquad\qquad 1.13$$

$$H_{Surface} = g_H C_p (T_{AC} - T_{Air}) \qquad\qquad 1.14$$

where H is the sensible heat flux of the surface, soil, and canopy; T is the

temperature of the air, soil, canopy, or air within the canopy (T_{AC}); and all other

variables previously defined.

This network permits interaction between soil and canopy components,

allowing the approximated T_{AC} to be a better substitute for T_O.

1.2.11. Measuring radiometric surface temperature

Early techniques of using thermocouples to measure plant temperature

are not suitable to obtain canopy temperatures representative of a community of

plants. Infrared thermometry has the advantage over contact temperature

sensors because they only measure a limited area or volume and can interfere

with the temperature measurement.

Infrared thermometry is a non-contact method of estimating the surface

temperature of a target ($T_{Surface}$). The sensor measures the radiation (E (W m^{-2}))

emitted by an object and relates this radiation to the temperature of this object

using the Stefan-Boltzmann law:

$$E = \varepsilon \sigma T^4$$
1.15

ε is the surface emissivity, σ is the Stefan-Boltzmann constant, T is the

temperature of the object (K), and E is the radiance (W m^{-2}) emitted by an object.

In actuality, because the target surface is most likely not a blackbody emitting

and absorbing the theoretical maximum energy based on temperature, the

infrared sensor is measuring the radiation emitted by the surface and the

background radiation being reflected from the surface:

$$E_{sensor} = \varepsilon E_{Surface} + (1 - \varepsilon)E_{Background} \qquad \text{1.16}$$

By using the Stefan-Boltzmann law this equation can be written in terms of temperature:

$$\sigma T_{Sensor}^4 = \varepsilon \sigma T_{Surface}^4 + (1 - \varepsilon)\varepsilon \sigma T_{Background}^4 \qquad \text{1.17}$$

The derived radiometric surface temperature can then be portioned into its separate components (soil and canopy) and used in a two-source energy balance model.

Equations 1.17, 1.18, and 1.19 assume that the radiance being measured is emitted by a blackbody with would be the sum of all wavelengths, and that the emissivity is constant over all wavelengths. These assumptions are not valid because the infrared radiometers being used correspond to an atmospheric window of 8 to 18 µm, and emissivity (ε) varies with wavelength. According to Blonquist et al (2009) the errors for emissivity correction are negligible because a large portion of the radiation emitted by terrestrial objects is in the 8 to 14 µm waveband, making the power of 4 a reasonable approximation. Also, the emissivity for most terrestrial objects does not vary significantly within the 8 to 14 µm waveband.

1.2.12. Calculation of reference stomatal conductance

Plant water measurements are of little use unless compared to values of that measurement that assume well watered plants under the same environmental conditions. This is done by establishing a reference or baseline

value that represents plants under non-water limiting conditions (Goldhamer, 2003).

Blonquist et al. (2009) used the Ball-Woodrow-Berry equation (Ball et al., 1987; Collatz et al., 1991) to calculate a "potential" stomatal conductance to which they compared the calculated g_C:

$$g_L = m \frac{A_{nL} RH_L}{CO_{2L}} + b \qquad\qquad 1.18$$

where A_{nL} is the leaf net assimilation (mol m^{-2} leaf area s^{-1}), RH_L and CO_{2L} are the relative humidity (kPa kPa^{-1}) and CO_2 mole fraction (mol mol^{-1}) of the air at the leaf surface, and m and b (mol m^{-2} s^{-1}) are the slope and intercept empirically calculated for a specific species. The leaf stomatal conductance (g_L) was scaled to the canopy using estimates of sunlit and shaded leaf area indexes (LAI$_{Sun}$, LAI$_{Shade}$) and calculated sunlit and shaded stomatal conductance (g_{Lsun}, g_{LShade}).

$$g_L = (g_{LSun} * LAI_{Sun}) + (g_{LShade} * LAI_{Shade}) \qquad\qquad 1.19$$

LAI$_{Sun}$ was calculated using estimated total LAI and the previously defined canopy radiation extinction coefficient (K$_{dir}$):

$$LAI_{Sun} = \frac{1 - e^{-K_{dir} * LAI}}{K} \qquad\qquad 1.20$$

LAI$_{Shade}$ is LAI-LAI$_{Sun}$.

For this study the reference stomatal conductance was calculated using a modified version of the Ball-Woodrow-Berry model developed by Leuning (1995):

$$g_L = m \frac{A_{nL}}{(C_{CO_2L} - \Gamma)(1 + \frac{D_s}{D_0})} + b \qquad \text{1.21}$$

where m and b are the same as the Ball-Woodrow-Berry model, Γ is the CO_2 compensation point, Ds is the vapor pressure deficit (VPD) at the leaf surface, and D_0 is an empirical coefficient.

For calculation of g_{Lsun} and g_{Lshade} a maximum value of A_{nL} was assumed as 0.000030 mol m^{-2} for cotton (C$_3$ plant), and 0.000045 for corn (C$_4$ plant). These values assume a peak value with the actual value calculated as a response to radiation intensity using a light response curve approximated from shapes given in Chapter 14 of Campbell and Norman (Campbell and Norman, 1998). A_{nL} was calculated using the assumed light response curve as a function of absorbed PPF (μmol m^{-2} s^{-1}) for shaded and sunlit leaves.

Ds and CO_{2L} were calculated following the procedures of Blonquist et al. (2009) by coupling equation (1.18) with leaf boundary layer equations for water vapor and CO2 found in chapter 7 of Campbell and Norman (1998) and the aerodynamic boundary layer conductance:

$$g_H = \frac{u \rho_{Mol} k^2}{\left[\ln\left(\frac{z_{m-d}}{z_m}\right) - \psi_M\right]\left[\ln\left(\frac{z_{Ta-d}}{z_h}\right) - \psi_H\right]} \qquad \text{1.22}$$

where u is wind speed (m s^{-1}), k is the von Karman constant (assumed at 0.41), z_u and z_{Ta} are the reference heights (m) where wind speed and air temperature are measured, d is the zero plane displacement height (m), z_m is roughness length (m) for momentum transfer, and z_h is roughness length (m) for heat

transfer, and ψ_H and ψ_M are the stability parameters for heat and momentum

transfer, respectively.

Iteration is required to calculate D_S and CO_{2L} because the equations are

dependent on each other.

When calculating the reference stomatal conductance for cotton we set

m= 8.0 and b= 0.03, D_0 = 2, and Γ = 40. For corn m = 3.23 and b= 0.06, D_0 = 5,

and Γ = 5.0.

The reference g_c that is calculated using this method assumes maximum

g_c for the same time period in which actual g_c is calculated and serves as a

comparison. The ratio of actual to reference g_c serves as a water status index

value indicating the degree of stress that a crop is under. A value of zero being

extremely stressed and a value of one being well watered and unstressed. The

ratio will be referred as the stomatal conductance ratio (SCR) from here on out.

1.3. References

Agam, N., Kustas, W.P., Anderson, M.C., Norman, J.M., Colaizzi, P.D., Howell, T.A., Prueger, J.H., Meyers, T.P., Wilson, T.B., 2010. Application of the Priestley-Taylor Approach in a Two-Source Surface Energy Balance Model. Journal of Hydrometeorology 11, 185-198.

Aston, A.R., Van Bavel, C.H.M., 1972. Soil surface water depletion and leaf temperature Agronomy 64, 368-373.

Ball, J.T., Woodrow, I., Berry, J., 1987. A Model Predicting Stomatal Conductance and its Contribution to the Control of Photosynthesis under Different Environmental Conditions, Progress in Photosynthesis Research. Springer Netherlands, pp. 221-224.

Blonquist, J.M., Norman, J.M., Bugbee, B., 2009. Automated measurement of canopy stomatal conductance based on infrared temperature. Agricultural and Forest Meteorology 149, 2183-2197.

Campbell, G.S., Norman, J.M., 1998. An Introduction to Environmental Biophysics. Springer-Verlag, New York, NY, USA.

Chalmers, D.J., Mitchell, P.D., Vanheek, L., 1981. Control of Peach-Tree Growth and Productivity by Regulated Water-Supply, Tree Density, and Summer Pruning. Journal of the American Society for Horticultural Science 106, 307-312.

Chavez, J.L., Howell, T.A., Gowda, P.H., Copeland, K.S., Prueger, J.H., 2010. Surface Aerodynamic Temperature Modeling over Rainfed Cotton. Transactions of the Asabe 53, 759-767.

Chavez, J.L., Neale, C.M.U., Hipps, L.E., Prueger, J.H., Kustas, W.P., 2005. Comparing aircraft-based remotely sensed energy balance fluxes with eddy covariance tower data using heat flux source area functions. Journal of Hydrometeorology 6, 923-940.

Clawson, K.L., Blad, B.L., 1982. Infrared Thermometry for Scheduling Irrigation of Corn. Agronomy Journal 74, 311-316.

Clawson, K.L., Jackson, R.D., Pinter, P.J., 1989. Evaluating Plant Water-Stress with Canopy Temperature Differences. Agronomy Journal 81, 858-863.

Collatz, G.J., Ball, J.T., Grivet, C., Berry, J.A., 1991. Physiological and Environmental-Regulation of Stomatal Conductance, Photosynthesis and Transpiration - a Model That Includes a Laminar Boundary-Layer. Agricultural and Forest Meteorology 54, 107-136.

Dry, P.R., Loveys, B.R., 1998. Factors influencing grapevine vigour and the potential for control with partial rootzone drying. Australian Journal of Grape and Wine Research 4, 140-148.

Gardner, B.R., Blad, B.L., Maurer, R.E., Watts, D.G., 1981. Relationship between Crop Temperature and the Physiological and Phenological Development of Differentially Irrigated Corn. Agronomy Journal 73, 743-747.

Goldhamer, D.A., 2003. Irrigation scheduling with plant indicators: field applications. . In: B.A. Stewart and T.A. Howell (Editors), Encyclopedia of Water Science. Marcel Dekker Inc., New York, pp. 512-518.

Gonzalez-Dugo, M.P., Moran, M.S., Mateos, L., Bryant, R., 2006. Canopy temperature variability as an indicator of crop water stress severity. Irrigation Science 24, 233-240.

Idso, S.B., Jackson, R.D., Pinter, P.J., Reginato, R.J., Hatfield, J.L., 1981. Normalizing the Stress-Degree-Day Parameter for Environmental Variability. Agricultural Meteorology 24, 45-55.

Jackson, R.D., 1982. Canopy Temperature and Crop Water Stress., Adv. Irr., pp. 43-85.

Jackson, R.D., Idso, S.B., Reginato, R.J., Pinter, P.J., 1981. Canopy Temperature as a Crop Water-Stress Indicator. Water Resources Research 17, 1133-1138.

Jackson, R.D., Reginato, R.J., Idso, S.B., 1977. Wheat Canopy Temperature - Practical Tool for Evaluating Water Requirements. Water Resources Research 13, 651-656.

Jones, H.G., 1990. Physiological-Aspects of the Control of Water Status in Horticultural Crops. Hortscience 25, 19-26.

Jones, H.G., 1999. Use of infrared thermometry for estimation of stomatal conductance as a possible aid to irrigation scheduling. Agricultural and Forest Meteorology 95, 139-149.

Jones, H.G., 2004. Irrigation scheduling: advantages and pitfalls of plant-based methods. Journal of Experimental Botany 55, 2427-2436.

Jones, H.G., 2008. Irrigation scheduling- comparison of soil, plant and atmosphere monitoring approaches. Acta Horticulturae (ISHS) 792, 391-403.

Jones, H.G., Serraj, R., Loveys, B.R., Xiong, L.Z., Wheaton, A., Price, A.H., 2009. Thermal infrared imaging of crop canopies for the remote diagnosis and quantification of plant responses to water stress in the field. Functional Plant Biology 36, 978-989.

Jones, H.G., Stoll, M., Santos, T., de Sousa, C., Chaves, M.M., Grant, O.M., 2002. Use of infrared thermography for monitoring stomatal closure in the field: application to grapevine. Journal of Experimental Botany 53, 2249-2260.

Kustas, W.P., Norman, J.M., 1999. Evaluation of soil and vegetation heat flux predictions using a simple two-source model with radiometric temperatures for partial canopy cover. Agricultural and Forest Meteorology 94, 13-29.

Kustas, W.P., Norman, J.M., 2000. A two-source energy balance approach using directional radiometric temperature observations for sparse canopy covered surfaces. Agronomy Journal 92, 847-854.

Leuning, R., 1995. A Critical-Appraisal of a Combined Stomatal-Photosynthesis Model for C-3 Plants. Plant Cell and Environment 18, 339-355.

Li, F.Q., Kustas, W.P., Prueger, J.H., Neale, C.M.U., Jackson, T.J., 2005. Utility of remote sensing-based two-source energy balance model under low- and high-vegetation cover conditions. Journal of Hydrometeorology 6, 878-891.

Maes, W.H., Steppe, K., 2012. Estimating evapotranspiration and drought stress with ground-based thermal remote sensing in agriculture: a review. Journal of Experimental Botany 63, 4671-4712.

Merlot, S., Mustilli, A.C., Genty, B., North, H., Lefebvre, V., Sotta, B., Vavasseur, A., Giraudat, J., 2002. Use of infrared thermal imaging to isolate Arabidopsis mutants defective in stomatal regulation. Plant Journal 30, 601-609.

Monteith, J.L., Szeicz, G., 1962. Radiative temperature in the heat balance of natural surfaces. Quarterly journal Royal Meteorological Society 88, 496-507.

Norman, J.M., Kustas, W.P., Humes, K.S., 1995. Source Approach for Estimating Soil and Vegetation Energy Fluxes in Observations of Directional Radiometric Surface-Temperature. Agricultural and Forest Meteorology 77, 263-293.

Stoll, M., Loveys, B., Dry, P., 2000. Hormonal changes induced by partial rootzone drying of irrigated grapevine. Journal of Experimental Botany 51, 1627-1634.

Tanner, C.B., 1963. Plant Temperatures. Agronomy Journal 55, 210-211.

Wang, D., Gartung, J., 2010. Infrared canopy temperature of early-ripening peach trees under postharvest deficit irrigation. Agricultural Water Management 97, 1787-1794.

CHAPTER 2

EFFECT OF USING MEASURED VS. MODELED SOIL

TEMPERATURE TO DERIVE CANOPY TEMPERATURE:

IMPLICATIONS FOR CALCULATION OF

CANOPY STOMATAL CONDUCTANCE

2.1. Abstract

Canopy temperature is a crucial measurement in the use of biophysically based methods and equations to calculate stomatal conductance. The most common surface measurement is a composite of both vegetation and soil temperatures. Canopy temperature needs to be separated from this composite temperature to compute the energy balance for the canopy and from this the canopy stomatal conductance. This separation can be done with either a measurement or an estimation of canopy or soil temperature. Canopy stomatal conductance was calculated using both methods to separate soil and canopy temperature from the composite surface temperature. The calculated canopy stomatal conductance using a derived canopy and soil temperature from a composite radiometric temperature was less variable. The daily and seasonal canopy stomatal conductance behavior was more theoretically correct than the stomatal conductance calculated using direct soil measurement and derived canopy temperature.

2.2. Introduction

2.2.1. Objectives and hypotheses

The objective of this study was to determine whether direct measurements of soil temperature could replace estimation of soil temperature using the Priestley-Taylor approach to obtain more accurate stomatal conductance values. We hypothesized that direct measurement of soil temperature with the use of infrared thermometers would lead to more correct values of canopy temperature and thus more accurate stomatal conductance values. We also hypothesized that decreasing the Priestley-Taylor coefficient to correspond with canopy cover over the growth season because of less advective influence from the sensible heat flux from bare soil, would yield more correct canopy temperatures and thus more correct stomatal conductance values.

2.2.2. Background

Calculation of an energy balance for a plant canopy requires a measurement or estimate of canopy temperature. A single composite temperature of the soil and canopy is often the only available surface temperature measurement available if one is available at all. The canopy and soil temperatures can be derived using this composite temperature either by taking a direct measurement or estimating the other temperature. This way you can solve for the unknown temperature. The appropriate method to obtain the most accurate soil and canopy temperatures is often dependent on the degree of canopy closure and radiometer zenith angle.

The two-source energy balance model (TSM) of Norman et al. (1995) partitions the observed radiometric surface temperature into soil and canopy contributions using an estimate of canopy fraction within the radiometer field of view:

$$T^4_{Radiometric} = f(\theta)T^4_{Canopy} + (1 - f(\theta))T^4_{Soil} \qquad 2.1$$

where $T_{Radiometric}$, T_{Canopy}, and T_{Soil} are the target surface, canopy and soil temperatures (C), respectively, and f(θ) is the fraction of canopy in the field of view of the radiometer. In this example a single emissivity is used to represent the combined soil and vegetation.

After each component temperature is calculated the soil and canopy sensible heat fluxes are calculated along the temperature gradients regulated by transport resistances that are calculated. With a measurement or approximation of net radiation within the canopy (R_{NC}) and above the soil surface, the energy balance can be calculated for both the canopy and soil layers. A single radiometric temperature composed of soil and canopy temperature is usually the only surface temperature measurement readily available. Another equation or measurement is needed of T_{Canopy} or T_{Soil} along with equation (2.1) to obtain the sensible heat fluxes for the soil and canopy. Direct measurement of canopy or soil temperatures may be considered impractical over wide spatial and temporal scales (Agam et al., 2010). Kustas found that predictions of H and LE using the Norman et al. (1995) two-source model with observed T_{Canopy} and T_{Soil} measurements were comparable to those using the Priestley-Taylor (PT) method

but were more scattered and had higher root-mean-squared-error (RMSE) values.

Another method to separate soil and canopy temperatures uses infrared radiometers at different angles (Otterman et al., 1992; Francois, 2002). Kustas and Norman (1997) compared observed latent and sensible heat flux values to modeled values from the Norman et al. (1995) two-source model using a "two angle," a "two angle PT" and a "one angle PT" method to separate canopy and soil energy balances. The "two angle" model used two radiometers at two different view angles to simultaneously derive a soil and canopy temperature. This method eliminates the need for the Priestley-Taylor approximation and an estimate of f_g. The "two angle PT" model uses the Priestley-Taylor approach to partition R_{NC} between H_C and LE_C with the two radiometers at different view angles to eliminate the need of air temperature in the calculation of the soil and canopy energy fluxes. Kustas and Norman (1997) found the performance of the "two angle PT" model in predicting H and LE to be significantly better than the two-source model, but not as good as the original "one angle PT" model suggested by Norman et al. (1995). This study used radiometric temperatures measured from satellites and results may be different for ground-based radiometric temperatures.

Norman et al. (1995) suggested estimating T_{Canopy} by partitioning net radiation of the canopy (R_{NC}) into canopy sensible (LE_{Canopy}) and latent heat (H_{Canopy}) fluxes using a Priestly-Taylor approximation (Priestley and Taylor, 1972):

$$\Delta R_{NC} = LE_{Canopy} + H_{Canopy} \qquad\qquad 2.2$$

$$LE_{Canopy} = 1.3 f_g \frac{S}{S+\gamma} \Delta R_{NC} \qquad\qquad 2.3$$

$$H_{Canopy} = \rho C_P \frac{T_{Canopy} - T_{Air}}{R_A} \qquad\qquad 2.4$$

$$T_{Canopy} = \frac{\Delta R_{NC} \left[1 - \alpha PT * f_g \frac{S}{S+\gamma}\right] R_A}{\rho C_P} + T_{Air} \qquad\qquad 2.5$$

where f_g is the fraction of leaf are index (LAI) that is green, S is the slope of the saturation vapor pressure versus temperature curve, γ is the psychrometric constant, ρC_P is the volumetric heat capacity of air, and αPT is the Priestly-Taylor coefficient. T_{Soil} is then calculated by rearranging equation (2.1) to:

$$T_{Soil} = \sqrt[4]{\frac{T_{Radiometric}^4 - f_C(\theta) T_{Canopy}^4}{(1 - f_C(\theta))}} \qquad\qquad 2.6$$

2.2.3. Priestley-Taylor method

The Priestley-Taylor (1972) approach is a simplification of Penman's formulation of evapotranspiration, with the assumption that the equilibrium term (λE_{eq}) of Penman's equation is significantly larger than the aerodynamic term (λE_a). The Priestley-Taylor approximation empirically estimates evapotranspiration by eliminating the need for input data other than radiation. Under ideal conditions evapotranspiration would eventually attain a rate of equilibrium for an air mass moving across the surface of vegetation with an abundant supply of water. Once the air mass was saturated the actual rate of

evapotranspiration would equal the potential rate calculated by the Penman equation. The imposed transpiration term in the Penman equation approaches zero and the radiation terms dominate. Priestley and Taylor (1972) found that the actual evapotranspiration rate exceeded the equilibrium potential rate for well watered vegetation. This is best explained by the entrainment of air above the convective boundary layer (CBL). This entrainment imports heat and saturation deficit and exports saturation deficit from the mixed boundary layer. They found that the potential rate could be estimated by multiplying the equilibrium potential rate by a coefficient (α) equal to 1.26 to calculate ET:

$$\lambda E = \alpha \lambda E_{eq}$$

2.7

For two-source models the Priestley-Taylor approximation is modified to calculate only the canopy component of latent heat flux:

$$\lambda E_c = \alpha_c \lambda E_{eqc}$$ 2.8

This approach is considered to be more conservative than the bulk system (soil +canopy) (Agam et al., 2010). Many values have been reported for the Priestly-Taylor coefficient (Jury and Tanner, 1975; Flint and Childs, 1991; Castellvi et al., 2001; Pereira, 2004; Diaz-Espejo et al., 2005; Baldocchi and Xu, 2007). Once soil moisture decreases and the soil and vegetation can no longer transpire at the equilibrium potential rate, the surface conductance to λE decreases and α decreases (Flint and Childs, 1991). Kustas and Norman (1999) concluded from their study that when sensible heat is being advected from a significant bare soil source, α must be significantly higher. This led us to believe that as the canopy

cover closes, α decreases accordingly due to less advective heat influence from bare soil.

2.3. Materials and Methods

2.3.1. Data collection

Weather stations were deployed over corn and cotton fields in the following locations: Corn: Sparta, IL; Lawrence, KS; Qulin, MO; Portland, IN; Rockwood, IL; North Platte, NE; Memphis, TN; Cotton: Maricopa, AZ; Memphis, TN; and Qulin, MO. Each cotton location had a weather station setup on an irrigated and non-irrigated field trial. These stations made the required measurements to monitor crop water status by calculating canopy stomatal conductance. Each station was equipped with a datalogger (model CR1000, Campbell Scientific, Logan, UT), a pyranometer (Model SP-110, Apogee Instruments, Logan, UT), a relative humidity probe (Model CS215, Campbell Scientific, Logan, UT), two thermistors (Model ST-100, Apogee Instruments), a cup anemometer (Model Wind Sentry, RM Young Co., Traverse City, MI), and four infrared (IR) radiometers (Model SI-111 or SI-1H1, Apogee Instruments, Logan, UT). Four extendable poles were used as masts for IR sensor placement. The datalogger, anemometer, RH probe, pyranometer, and one of the thermistors were mounted on the "center" mast. The thermistor and RH probe were each placed in naturally ventilated louvered-radiation shields two meters above the crop canopy. The anemometer was also placed two meters above the crop canopy. The pyranometer was mounted at the top of the center mast. The other thermistor was buried approximately 10 cm below the soil

surface. Three of the infrared radiometers measured surface brightness temperature and each were placed on their own mast at an angle of 68 degrees (Models SI-111) or 72 degrees (SI-1H1) from nadir, at a height above canopy that allows the maximum view of the trial plot. The fourth infrared radiometer measured soil brightness temperature and was placed at an angle of 68 degrees above nadir and approximately 30 cm above the soil surface. A tipping bucket rain gauge (Model TE525WS, Campbell Scientific, Logan, UT) was installed at the edge of the crop fields to insure no obstructions from the crop for precipitation measurements.

Measurements of RH, air temperature, soil and canopy brightness temperature, wind speed, soil temperature at 10 cm, and incoming solar radiation were made every ten seconds and averaged over a 30-minute interval. The canopy height was measured at the time of setup and was periodically measured throughout the season. The growth stage of each crop was also periodically recorded over the season.

An example of the sensor arrangement can be seen in Fig. 2-2 over a stressed cotton field. A typical research cotton field can be seen in Fig. 2-3.

2.3.2. Experimental outline

The Qulin, MO irrigated cotton site was chosen as a representative site to illustrate the effects of measured and calculated soil temperature, as well as changes in the Priestley-Taylor coefficient on the stomatal conductance ratio index.

The stomatal conductance ratio (SCR) was calculated as outlined in Chapter 1, with the incorporation of the two-source energy balance model (Fig. 2-4) using data from the six cotton and ten corn sites with the necessary modifications needed to account for sparse canopy coverage using the clumping index (Kustas and Norman, 1999; Kustas and Norman, 2000; Anderson et al., 2005). Stomatal conductance calculations were performed using canopy temperature derived from soil temperature measurements directly measured between the corn and cotton rows, and then made using canopy temperature derived from the composite radiometric surface temperature using the Priestly-Taylor approximation (equation 2.3). The soil and canopy temperatures derived using the Priestley-Taylor approach were compared with the measured soil temperature and the canopy temperatures derived using measured soil temperature. Due to constraints of the trial sites most radiometers measuring the surface temperature were faced in the same general compass direction. This is true with all sites except the irrigated cotton site in Qulin, MO. This site had two radiometers facing west and one facing east. The soil and canopy temperature comparisons described above between the two methods to derive canopy temperature were compared for the east and west facing radiometers.

The use of varying Priestley-Taylor coefficients over the season to account for decreased advection from bare soil inter-rows was also studied. An equation was implemented to decrease α from 1.5 to 1.26 dependent on the fraction of canopy viewable (canopy width (m)/row spacing (m)) from a nadir view. As the viewable canopy fraction increased, as a result of the canopy

growing and the width increasing, α decreased reflecting less advective sensible heat influence from the soil surface on the canopy temperature. This decreases the potential canopy latent heat flux in the Priestley-Taylor equation the lower α gets towards the end of the season. This is done by increasing the derived canopy temperature from the composite (soil and canopy) radiometric temperature higher than what it would be if remained constant at a typical value of 1.3. The stomatal canopy conductance ratio (SCR) is compared using the varying α from 1.5 to 1.3 and the constant α of 1.3 over the season.

2.3.3. Calculating daily average stomatal conductance ratio

Daily averages of the stomatal conductance ratio (SCR) were calculated to summarize the water status of a crop over a season. These values were calculated as outlined in CHAPTER 1 using equations 1.3, 1.19, and 1.20. The 30-minute values were averaged for each day. This values are graphed with the standard deviation of these 30-minute values (Fig. 3-1).

Figure 2-1 is an example of how the stomatal conductance ratio is calculated using the calculated canopy stomatal conductance values and the reference canopy stomatal conductance values. This graph shows three days that vary in the solar intensity, with water being applied between the second and third day. The stomatal conductance ratio shows the crop at moderate water stress days two and three with an average daily SCR ratio at approximately 0.56 and 0.60, respectively. The decreased solar radiation of the second day decreases the water stress of the canopy. After the irrigation event the canopy is shown to have little water stress with an average SCR at 0.90.

2.4. Results and Discussion

2.4.1. Measured and derived soil temperature comparisons

The measured soil temperature (T_{Soil}) is lower than the T_{Soil} derived from the west-facing radiometric temperature and the Priestley-Taylor approximation early on in the growth season (Fig. 2-6) when canopy coverage is low (27%). Mid-season, the canopy coverage has increased (65%) and the derived and measured T_{Soil} take on different shapes throughout the day. Both temperatures increase during the early morning with the derived temperature higher than the measured. As the day gets closer to solar noon the derived T_{Soil} decreases and then increases after solar noon. This decrease in temperature from morning to afternoon is best explained by the change in sunlit and shaded soil that the radiometer is viewing as the day moves on. Early on in the day the majority of the soil viewed by the west-facing radiometer is sunlit leading to a higher soil temperature than when the soil become more shaded as the sun position changes.

The measured soil temperature increases to about solar noon and decreases over the rest of the day. This increase during mid-day is most likely due to a spatial sampling error. It appears that the measured T_{Soil} is influenced by the incident solar radiation on the soil, as it follows the trend of net shortwave radiation at the soil surface, just lagging behind it (Fig. Appendix D-3). It is likely that the infrared radiometer measuring more of the space between the rows and not integrating an equal portion between the rows and under the canopy. Towards the end of the season as the canopy coverage is more complete (94%)

the difference between the derived soil temperature and the measured temperature is smaller but the shapes still similar to how they were mid-season.

The T_{Soil} derived from the east-facing radiometric temperature and the Priestley-Taylor approximation was lower, but close together measured T_{Soil} early on in the growth season (Fig. 2-6) when canopy coverage is low (27%). Mid-season, the canopy coverage has increased (65%) and the derived and measured T_{Soil} are similar in the morning but diverge mid-day most likely to the large influence that solar radiation has on measured T_{Soil}. Towards the end of the season as the canopy cover is nearly closed (94%) the two temperatures follow similar shapes, indicating that the measured T_{Soil} is probably less influenced mid-day by the incoming solar radiation. There is still a difference between the temperatures showing that the shaded soil that the east-facing radiometer is viewing in the morning is cooler and then warmer in the afternoon as the radiometer is viewing more sunlit soil.

A comparison was made between the soil and canopy temperature derived using the Priestley-Taylor approximation and the measured composite surface temperature of the east and west-facing radiometers (Fig. D-1 and Fig. D-2). This comparison shows how the direction of the radiometer measuring the composite surface temperature can affect the derived soil and canopy temperatures. As expected, the soil and canopy temperatures derived from the composite temperature of the east facing radiometer is cooler in the morning and warmer in the afternoon.

The temperature spatial variability of the soil which appears not to be accounted for in the measured soil temperature is most likely due to shading and soil moisture variability of the field. It is also possible that the soil under the canopy is more wet than the inter-row and the derived soil temperature is measuring this soil that may be cooler due to larger soil evaporation rates than the inter row soil. It is also possible that the discrepancy between the derived and measured soil temperature is largely due to differences in shading of the soil that is in the field of view of the radiometer measuring the composite temperature and the radiometer measuring the soil temperature. With the high zenith viewing angle of the composite-temperature radiometer it is possible that it is viewing soil that is a different temperature than the soil-temperature radiometer due to differences in shading.

2.4.2. Canopy temperature comparisons

Early on in the growth season when the canopy coverage is low (27%), the T_{Canopy} derived using the measured T_{Soil} is higher than the T_{Canopy} derived from the Priestley-Taylor approximation in the morning and both temperatures come together towards the latter part of the day. This is true for canopy temperature derived from both east and west-facing radiometric temperatures (Fig. 2-7). The difference is that the canopy temperature derived from the west-facing radiometer is warmer in the morning and cooler in the afternoon the canopy temperature derived from the east facing radiometric temperature. This is due to the same reason that the soil temperature was higher for the west than the east.

The viewed leaves are shaded in the morning for the east facing radiometer and sunlit for the west radiometer, switching after solar noon.

The two soil temperatures most likely come together toward the end of the day, for both east and west facing radiometers, due temperature of the canopy being more influenced by the canopy energy balance than the degree of shading.

As the canopy begins to fill in mid-season (65%) the fraction of canopy in the radiometer field of view is significantly higher than the fraction of soil. This attributes more of the composite radiometric temperature to canopy temperature (equation 2.1) and derivation of the canopy temperature is less influenced by the measured soil temperature. This is evident by the canopy temperature not having a significant decrease in the middle of the day, following the big increase for the measured soil temperature (Fig. 2-7). During the end of the season when the canopy cover is high (94%) the fraction of canopy within the radiometer field of view is very close to one. This attributes the majority of the composite temperature to the derived canopy temperature. Even though the two soil temperatures differed at this time the two canopy temperatures (T_{Canopy} derived from Priestley-Taylor and T_{Canopy} derived from measured T_{Soil} and composite surface temperature) are very close together due to soil temperature having little influence on the measured composite temperature (Fig. 2-7).

It is interesting that the east facing canopy temperature is closer to the canopy temperature derived from the measured soil temperature, especially as the canopy fills in.

2.4.3. SCR comparisons

The stomatal conductance ratio was calculated using the derived canopy temperatures from the composite radiometric surface temperatures of an east facing, west-facing, and combined east and west-facing radiometers. The 30-minute averages of the SCR, and the daily average from the 30-minute averages were compared against each other (Fig. 2-8). The SCR values of the west-facing radiometers increase to about mid-day and then decrease again. This "parabolic" shape would represent a canopy that was stressed in the morning and became less stressed to mid-day and gradually became more stressed towards the end of the day. The lower SCR values in the morning that gradually increase are due to the canopy temperatures being higher and gradually decreasing. This temperature change is most likely due to the leaves in the west-facing radiometer being sunlit early on and then gradually changing to being composed of more shaded leaves.

The SCR values of the east-facing radiometer start high in the morning and decrease towards the end of the day. This would represent a canopy that is well watered and non-stressed in the morning and gradually becomes more stressed throughout the day as the water availability to the plant decreases. Towards the end of the season the error bars in Fig. 2-8 for the SCR values of the east-facing radiometer are very large. This is due to very high SCR values early in the morning that are not seen on the graph showing the 30-minute values due to the graph scaling.

The SCR values from the combined east and west canopy temperatures is more strongly affected by the west-facing canopy temperature in the mornings for early and mid-season days, but influenced more by the east-facing canopy temperatures towards the end of the season. The combined SCR daily shape is more "parabolic" in nature for the early and mid-season days and more linearly shaped latter on in the season.

The daily average SCR values (average of each 30-minute SCR value) are very similar for the three different radiometric temperatures compared. The difference in the daily shapes is represented by the error bars, which is the standard deviation of the daily average. The most appropriate method would be the combined canopy temperatures which represents both the shaded and sunlit leaves of the canopy. The standard deviation for the combined method is also smaller or equal to the other two methods.

The daily SCR values of the three canopy temperature approaches were graphed over the season for the time the data was collected (Fig. 2-9). The three SCR values follow each other very closely with little deviation throughout the season. The SCR values respond well to precipitation/irrigation events with an increase in the value, and the value decreasing when water availability is decreasing due to no precipitation/irrigation events or not enough to supply the crop with its high demand at that time.

The average 30-minute and daily SCR values calculated from the temperature derived from the Priestley-Taylor approximation were compared to the SCR calculated with the canopy temperature derived from the measured soil

temperature and combined east and west composite radiometric surface temperatures (Fig. 2-10). Early on in the season with a low canopy coverage (27%) and mid-season (65% canopy coverage) the SCR values calculated from the canopy temperature derived from measured soil temperature are more erratic and higher in magnitude than the SCR values calculated from the Priestley-Taylor derived canopy temperatures. As the canopy coverage increases and is almost closed (94%) towards the latter part of the season, the two SCR values are closer together with similar daily shapes and standard deviations. The less erratic SCR values from the derived Priestley-Taylor canopy temperature are noticeable in the season comparison of the two methods (Fig. 2-11).

2.4.4. Varying Priestley-Taylor coefficients

It was hypothesized that reducing the Priestley-Taylor coefficient from 1.5 (suggesting high influence from advective sensible heat flux from the bare soil to the canopy energy balance which increases potential canopy transpiration) to 1.0 (suggesting little advective influence from the soil sensible heat flux to the canopy energy balance due to no bare soil and full canopy coverage) would provide more theoretically correct SCR values. The average 30-minute and daily values (Fig. 2-12) and daily seasonal trend (Fig. 2-13) show that reducing the coefficient values reduce absolute SCR values from mid-season to late-season. There is not enough difference between the two values or a reference standard to compare the values, to suggest using one method over the other.

2.4.5. SCR comparisons for all cotton and corn sites

A comparison for all of the cotton (Fig. 2-14,) and corn (Fig. 2-15, Fig. 2-16, and Fig. 2-17) daily average SCR values using the two canopy and soil derivation methods showed different results between the corn and cotton values over the season. The SCR values, calculated using the canopy temperature derived from measured soil temperature and a composite surface temperature, were more erratic with bigger error bars for the cotton fields than they were for the corn fields. This is because the majority of the corn fields were already at complete canopy cover when the weather stations used for data collection were deployed. The corn canopies fill in quicker than the cotton canopies because of the smaller row spacing (0.76 m compared to 1.02 m) and because the ratio of their width to height before canopy closure is larger (1.0:1.0 compared to 0.75:1.0). When a full canopy coverage is reached in the cotton fields the two methods to calculate SCR result in similar values for Memphis, TN and Qulin, MO (Fig. 2-14).

2.5. Conclusions

This study observed the effect that canopy temperature derivation approaches had on the calculation of stomatal conductance. The effect of changing the Priestley-Taylor coefficient over the season for one of the approaches was also observed. No direct measurements of canopy or leaf stomatal conductance were available for any of the sites used in this study. This makes it difficult to validate the daily and seasonal corn and cotton canopy stomatal conductance values calculated. Due to this limitation we determined

which approach led to better estimates of canopy stomatal conductance by observing the behavior of the calculated values. Stomatal conductance values were assessed on their response to irrigation/precipitation events, expected daily and seasonal behavior, and the variability throughout the day. Leaf stomatal conductance measurements made with a leaf porometer are the most commonly made measurements of stomatal conductance in the field. For comparison to the calculated canopy stomatal conductance values made in this study, leaf stomatal conductance measurements would need to be scaled up. There is error and uncertainty associated with the multiple methods used to scale up leaf to canopy stomatal conductance. Even if 30-minute or once-a-day leaf stomatal conductance measurements were made, which would be labor and time intensive, there is no certainty that these values would be the best reference. They could however provide a good relative indication of the expected daily and seasonal trends.

These results do not support the hypothesis that a direct measurement of soil temperature would lead to better estimates of canopy temperature and from those estimates, more correct values of stomatal conductance. There was also not enough evidence to show that reducing the Priestley-Taylor coefficient from a high value to a low value that corresponds with the canopy coverage would lead to more correct values of stomatal conductance.

Results did show that the derived canopy temperature from the composite radiometric surface temperature is dependent on the direction of the radiometer relative to the sun direction. Crop row orientation will largely affect the sun

position relative to the radiometer since radiometers are most often pointed perpendicular to the crop row. The results suggest that a more correct method of measuring the composite surface temperature is combining the measured temperatures from radiometers facing in opposite directions in order to get a more appropriate measurement of canopy temperature that integrates both sunlit and shaded leaves.

Temperature measurements from north and south-facing radiometers were not available in this current study. It is likely that similar results would be seen between north and south-facing radiometers but without as much dependence on the time of day. For the northern hemisphere, the north facing radiometer would most likely see more shaded leaves than the south-facing radiometer for the majority of the day (the south-facing radiometer seeing more sunlit leaves). This would result in the north-facing radiometer reading lower canopy temperatures than the south-facing radiometer.

The large difference between the Priestley-Taylor derived and the measured soil and composite temperature derived canopy temperatures might be reduced by using smaller zenith view angles for the radiometric composite temperature. This may seem counter intuitive because if the radiometer is angled lower than the 68 degrees used in this study then it would be viewing more soil and have a smaller overall sampling area, however, this could result in more accurate canopy temperatures using the composite and soil temperature measurements because more of the measured soil temperature would be in the radiometers field of view. One of the biggest problems is that the soil

temperature in the radiometer field of view is most likely different than the soil

temperature in the inter rows that is being directly measured. By increasing the

viewing zenith angle of the radiometer measuring the composite temperature of

the soil and canopy the error in deriving the canopy temperature can be reduced.

2.6. References

Agam, N., Kustas, W.P., Anderson, M.C., Norman, J.M., Colaizzi, P.D., Howell,
T.A., Prueger, J.H., Meyers, T.P., Wilson, T.B., 2010. Application of the
Priestley-Taylor Approach in a Two-Source Surface Energy Balance
Model. Journal of Hydrometeorology 11, 185-198.

Anderson, M.C., Norman, J.M., Kustas, W.P., Li, F.Q., Prueger, J.H., Mecikalski,
J.R., 2005. Effects of vegetation clumping on two-source model estimates
of surface energy fluxes from an agricultural landscape during SMACEX.
Journal of Hydrometeorology 6, 892-909.

Baldocchi, D.D., Xu, L.K., 2007. What limits evaporation from Mediterranean oak
woodlands - The supply of moisture in the soil, physiological control by
plants or the demand by the atmosphere? Advances in Water Resources
30, 2113-2122.

Castellvi, F., Stockle, C.O., Perez, P.J., Ibanez, M., 2001. Comparison of
methods for applying the Priestley-Taylor equation at a regional scale.
Hydrological Processes 15, 1609-1620.

Diaz-Espejo, A., Verhoef, A., Knight, R., 2005. Illustration of micro-scale
advection using grid-pattern mini-lysimeters. Agricultural and Forest
Meteorology 129, 39-52.

Flint, A.L., Childs, S.W., 1991. Use of the Priestley-Taylor Evaporation Equation
for Soil-Water Limited Conditions in a Small Forest Clear-Cut. Agricultural
and Forest Meteorology 56, 247-260.

Francois, C., 2002. The potential of directional radiometric temperatures for
monitoring soil and leaf temperature and soil moisture status. Remote
Sensing of Environment 80, 122-133.

Jury, W.A., Tanner, C.B., 1975. Advection Modification of Priestley and Taylor
Evapotranspiration Formula. Agronomy Journal 67, 840-842.

Kustas, W.P., Norman, J.M., 1997. A two-source approach for estimating
turbulent fluxes using multiple angle thermal infrared observations. Water
Resources Research 33, 1495-1508.

Kustas, W.P., Norman, J.M., 1999. Evaluation of soil and vegetation heat flux predictions using a simple two-source model with radiometric temperatures for partial canopy cover. Agricultural and Forest Meteorology 94, 13-29.

Kustas, W.P., Norman, J.M., 2000. A two-source energy balance approach using directional radiometric temperature observations for sparse canopy covered surfaces. Agronomy Journal 92, 847-854.

Norman, J.M., Kustas, W.P., Humes, K.S., 1995. Source Approach for Estimating Soil and Vegetation Energy Fluxes in Observations of Directional Radiometric Surface-Temperature. Agricultural and Forest Meteorology 77, 263-293.

Otterman, J., Brakke, T.W., Susskind, J., 1992. A Model for Inferring Canopy and Underlying Soil Temperatures from Multidirectional Measurements. Boundary-Layer Meteorology 61, 81-97.

Pereira, A.R., 2004. The Priestley-Taylor parameter and the decoupling factor for estimating reference evapotranspiration. Agricultural and Forest Meteorology 125, 305-313.

Priestley, C.H.B., Taylor, R.J., 1972. On the Assessment of Surface Heat Flux and Evaporation Using Large-Scale Parameters. Monthly Weather Review 100, 81-92.
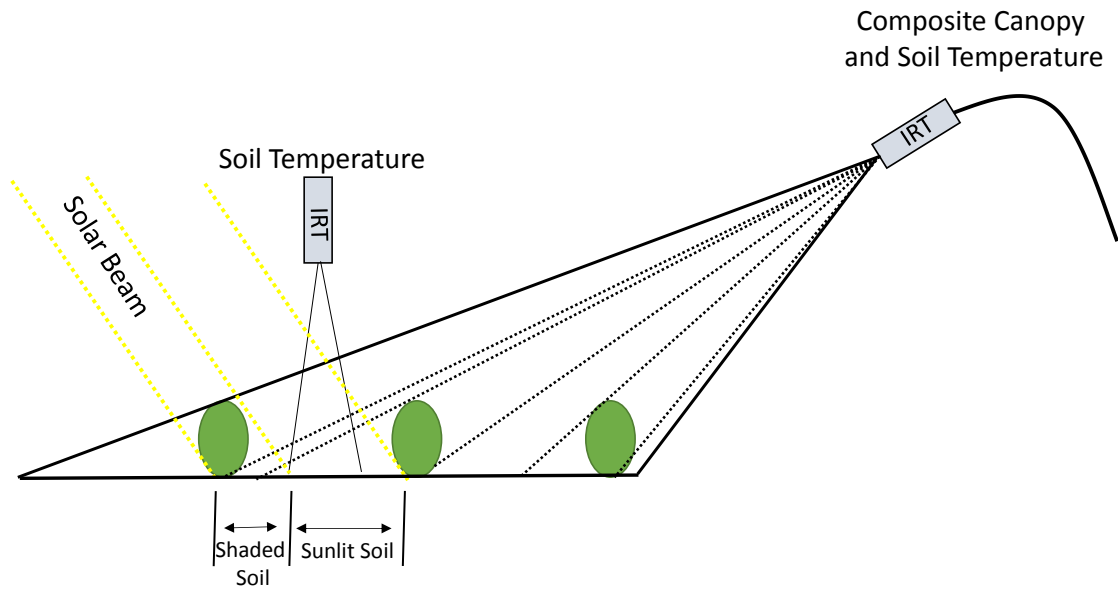
Fig. 2-1: Diagram portraying the sunlit and shaded soil in the view of the composite temperature measuring radiometer and the soil surface measuring radiometer.

Fig. 2-2: Typical sensor arrangement in a stressed corn field. Three infrared thermometers mounted at 68 degrees (zenith angle), 22 degrees below horizontal. These sensors measured canopy temperature. The leaves in this field are beginning to roll, indicating water stress.

Fig. 2-3: Typical cotton research field showing variability in the sunlit and shaded soil surface.
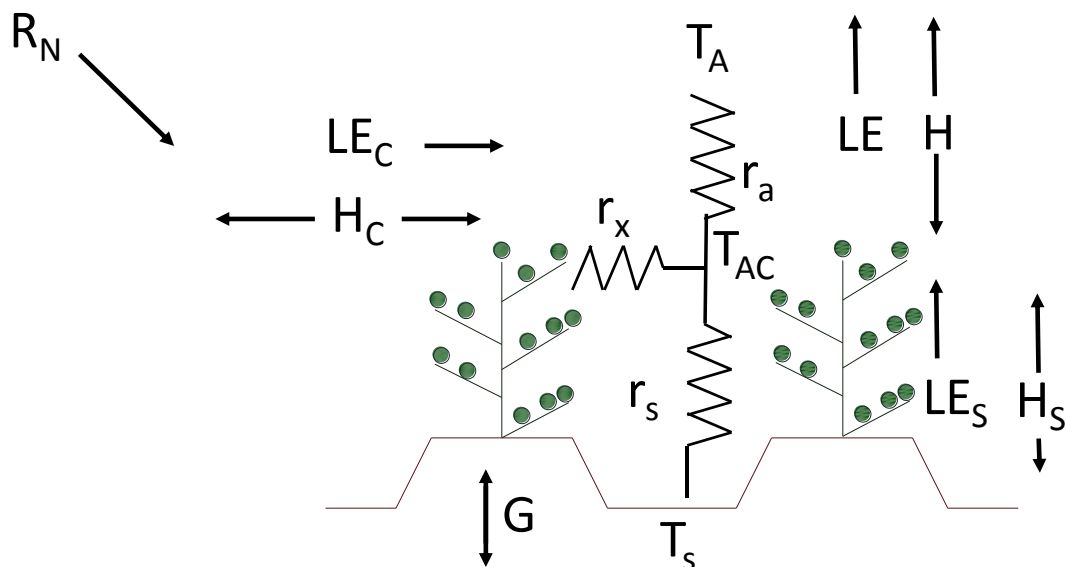
Fig. 2-4: Two-source energy balance model (series resistance model) used to separate energy fluxes for soil and canopy layers of the surface (Adopted from Norman et al (1995), Figure 11, and Colaizzi et al (2012b), Figure 1). Net radiation is depicted as R_N, LE is the latent heat flux, H is the sensible heat flux, G is the soil heat flux, T_A is the air temperature, T_{AC} is the air temperature within the canopy, subscripts C and S denoting the energy fluxes for the canopy and soil respectively. The boundary layer resistances above the soil surface, combination of the canopy leaves, and above the canopy are denotes as r_s, r_x, and r_a.
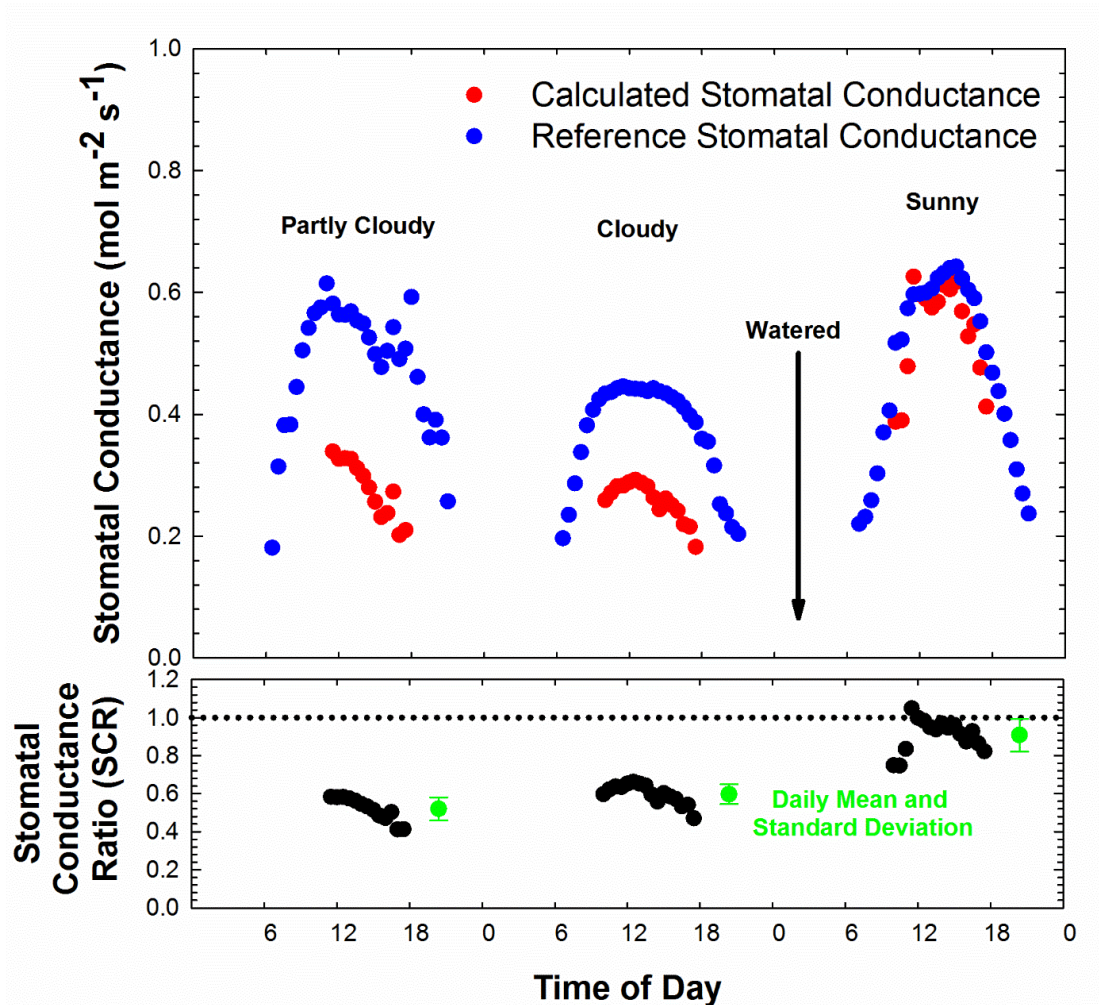
Fig. 2-5: Calculated 30-minute stomatal conductance ratio (SCR) values. The SCR is a ratio of the measured actual stomatal conductance to the reference stomatal conductance. The daily average is shown with error bars representing the standard deviation of each of the 30-minute SCR values.
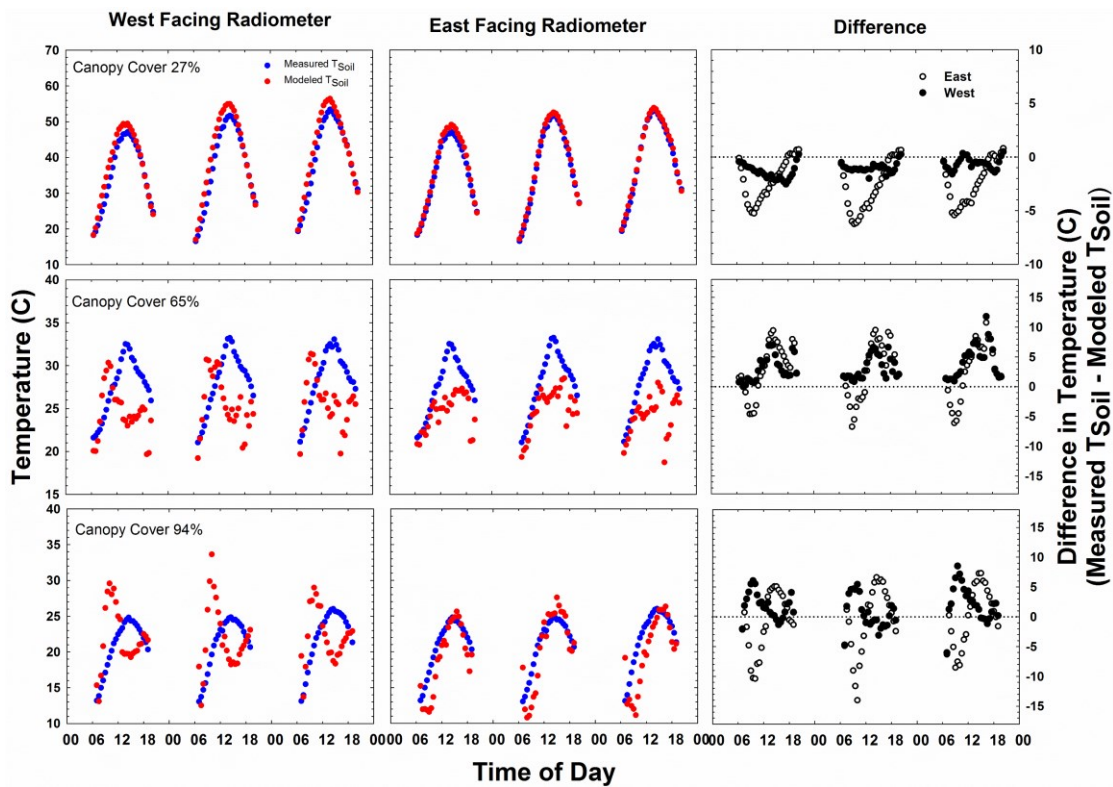
Fig. 2-6: Measured soil temperature (T$_{Soil}$) compared with T$_{Soil}$ derived from canopy temperature (T$_{canopy}$) modeled with the Priestley-Taylor approximation and the composite radiometric temperature of a west and east-facing radiometer. Comparisons are shown for three different times of the growth season: early, mid, and late season.
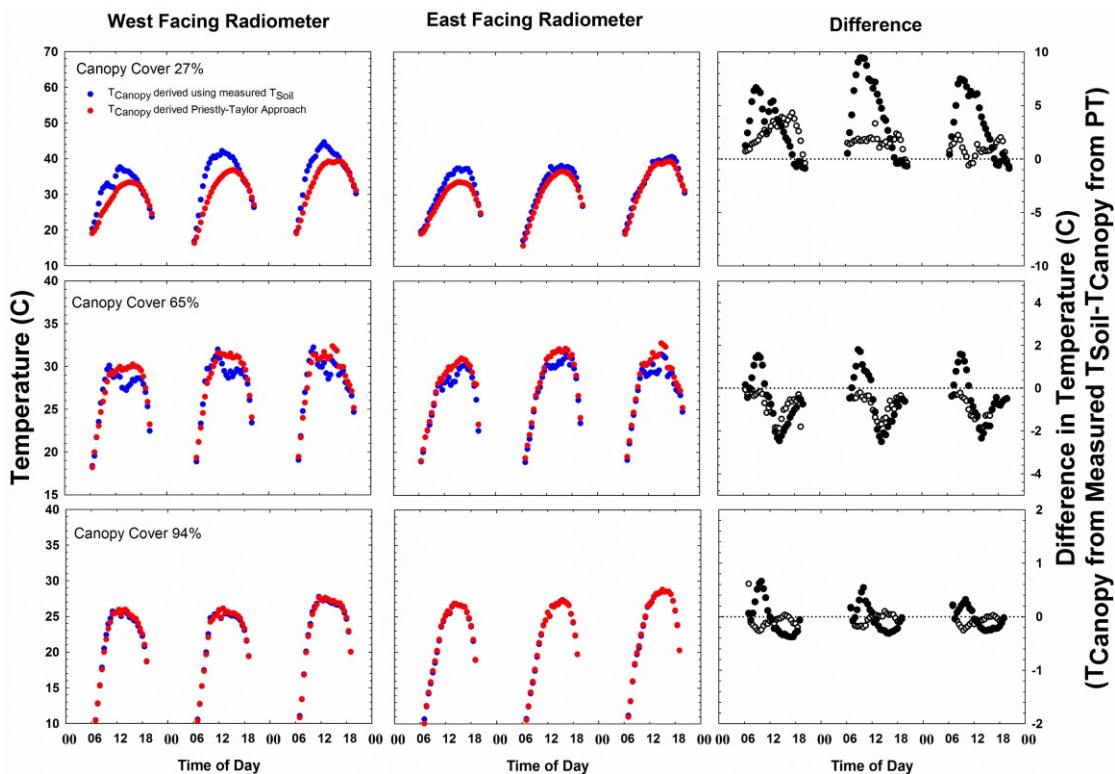
Fig. 2-7: Canopy temperature (T_{Canopy}) derived from measured T_{Soil} compared with T_{Canopy} modeled with the Priestley-Taylor approximation and the composite radiometric temperature of an east and west-facing radiometer. Comparisons are shown for three different times of the growth season: early, mid, and late season.
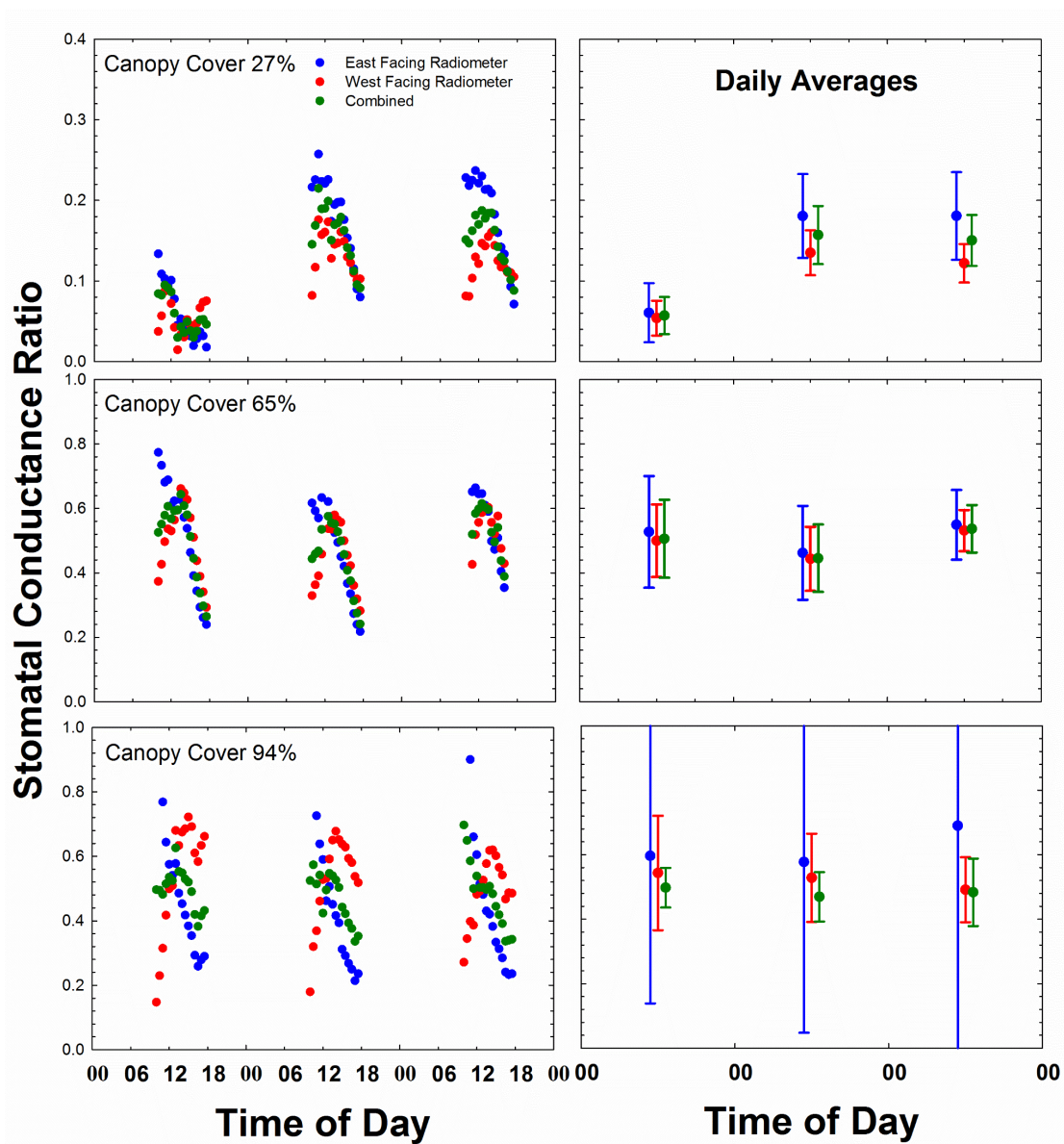
Fig. 2-8: The calculated stomatal conductance ratio using radiometric temperatures from east-facing, west-facing, and combined radiometers. Results are shown for the 30-minute averages made throughout the day and the daily averages for these 30-minute averages.
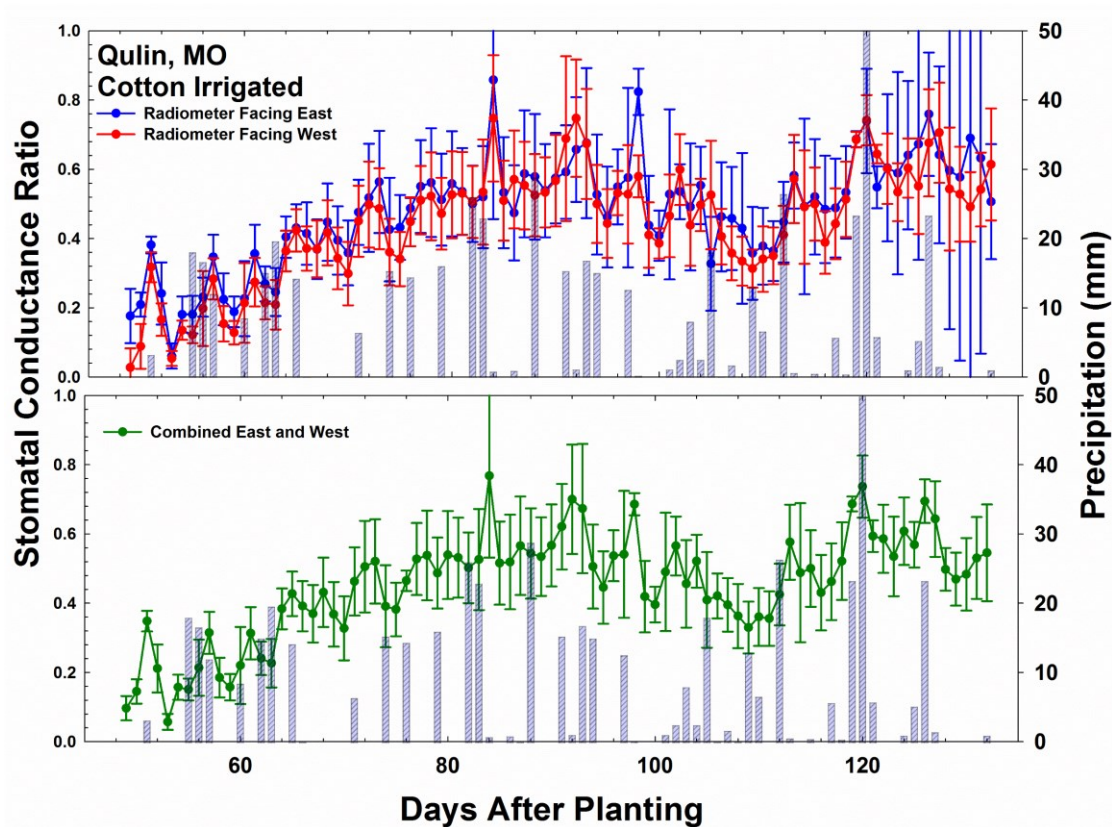
Fig. 2-9: The seasonal stomatal conductance ratio (SCR) average was calculated using the derived canopy temperature from the Priestley-Taylor approximation using composite radiometric temperatures measured by radiometers facing east, west, and combining east and west.
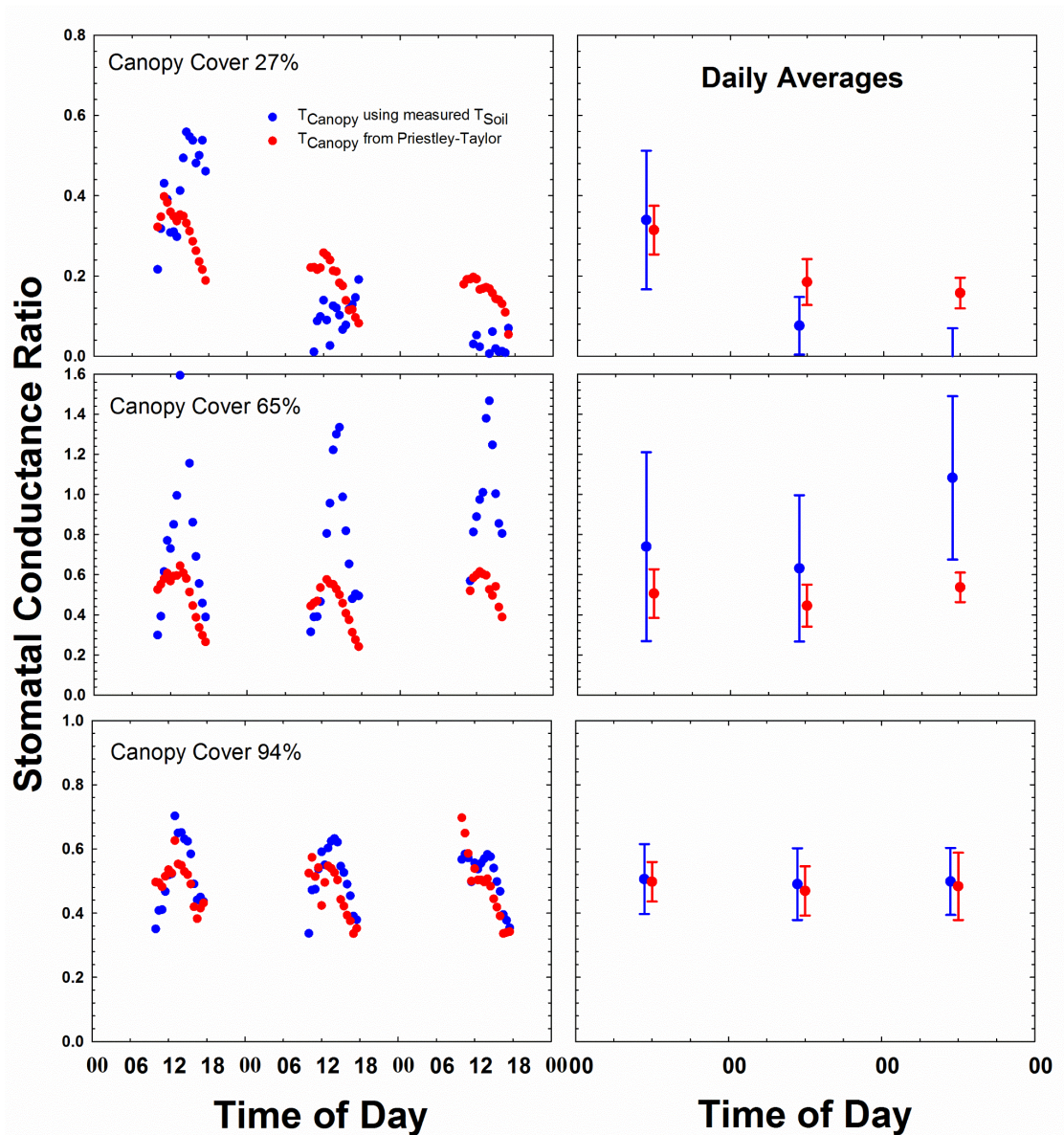
Fig. 2-10: The 30-minute and daily averaged stomatal conductance ratios (SCR) calculated using the modeled canopy temperature from the Priestley-Taylor approximation was compared to the SCR values calculated using canopy temperature derived from measured soil temperature and a composite radiometric surface temperature.
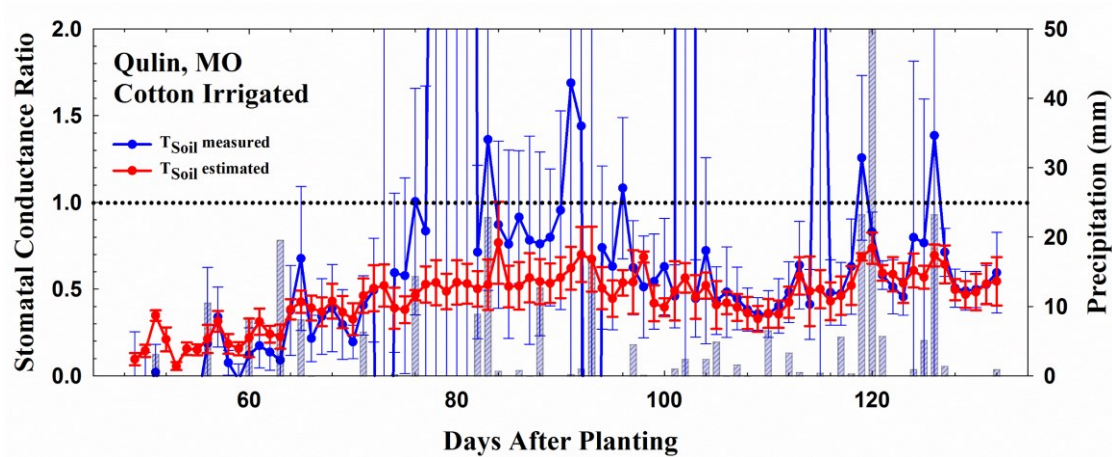
Fig. 2-11: The seasonal stomatal conductance ratio (SCR) averages calculated using the modeled canopy temperature from the Priestley-Taylor approximation was compared to the SCR values calculated using canopy temperature derived from measured soil temperature and a composite radiometric surface temperature.
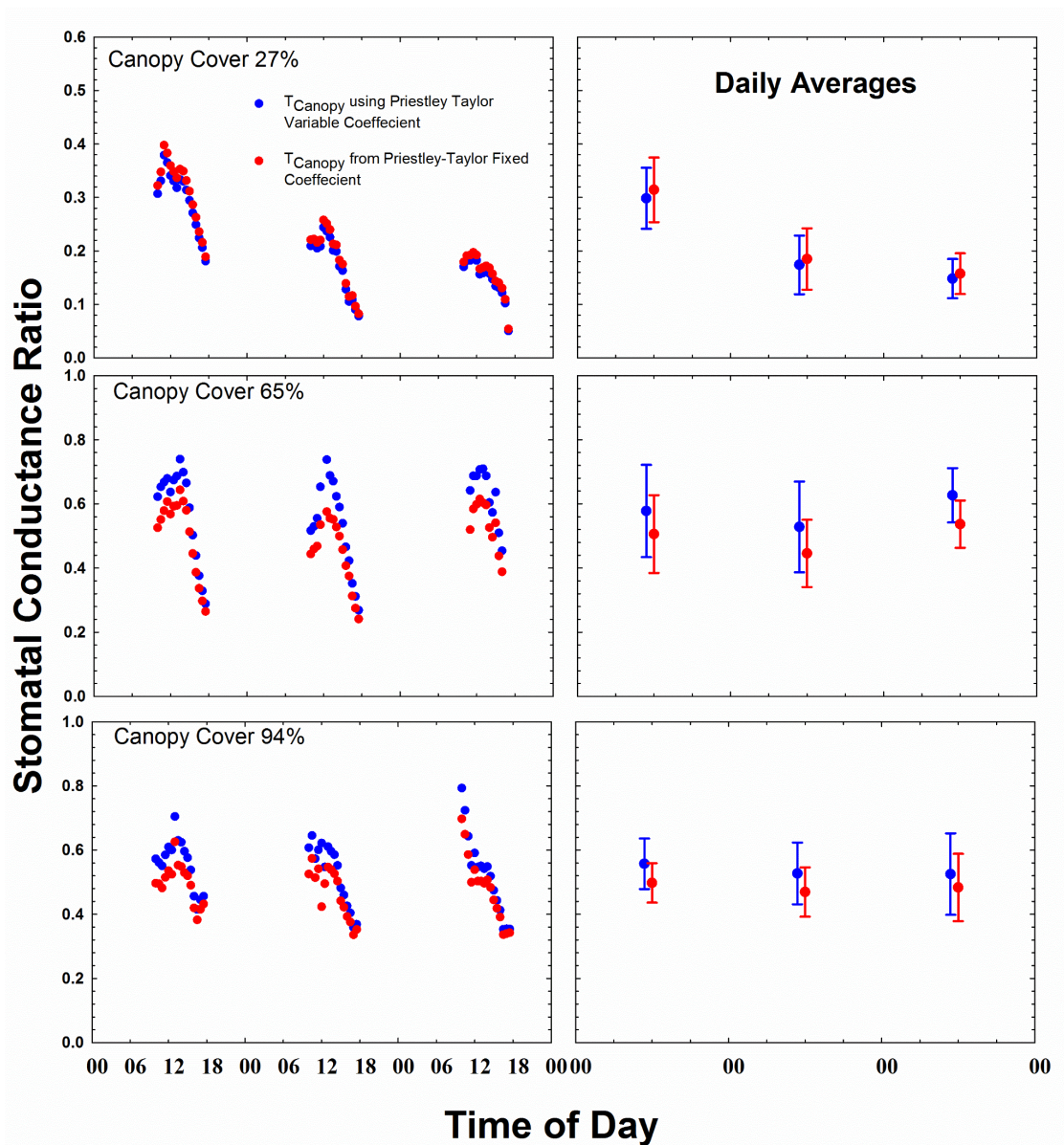
Fig. 2-12: The 30-minute and daily averaged stomatal conductance ratio (SCR) using canopy temperature derived using the Priestley-Taylor approximation using a constant Priestley-Taylor coefficient of 1.3 throughout the season was compared to the SCR calculated using a Priestley-Taylor coefficient that decreased from 1.5 to 1.3 depending on canopy coverage.
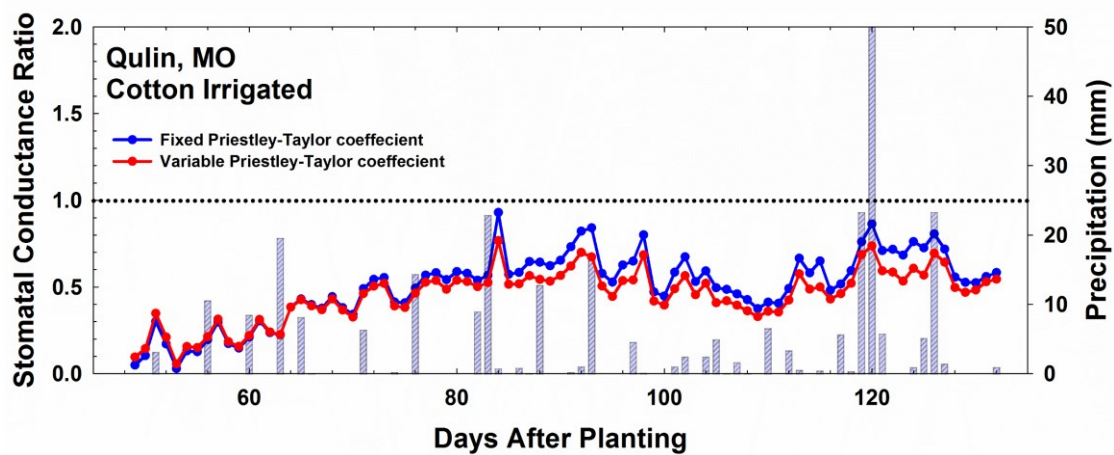
Fig. 2-13: The seasonal stomatal conductance ratio (SCR) using canopy temperature derived using the Priestley-Taylor approximation using a constant Priestley-Taylor coefficient of 1.3 throughout the season was compared to the SCR calculated using a Priestley-Taylor coefficient that decreased from 1.5 to 1.3 depending on canopy coverage.
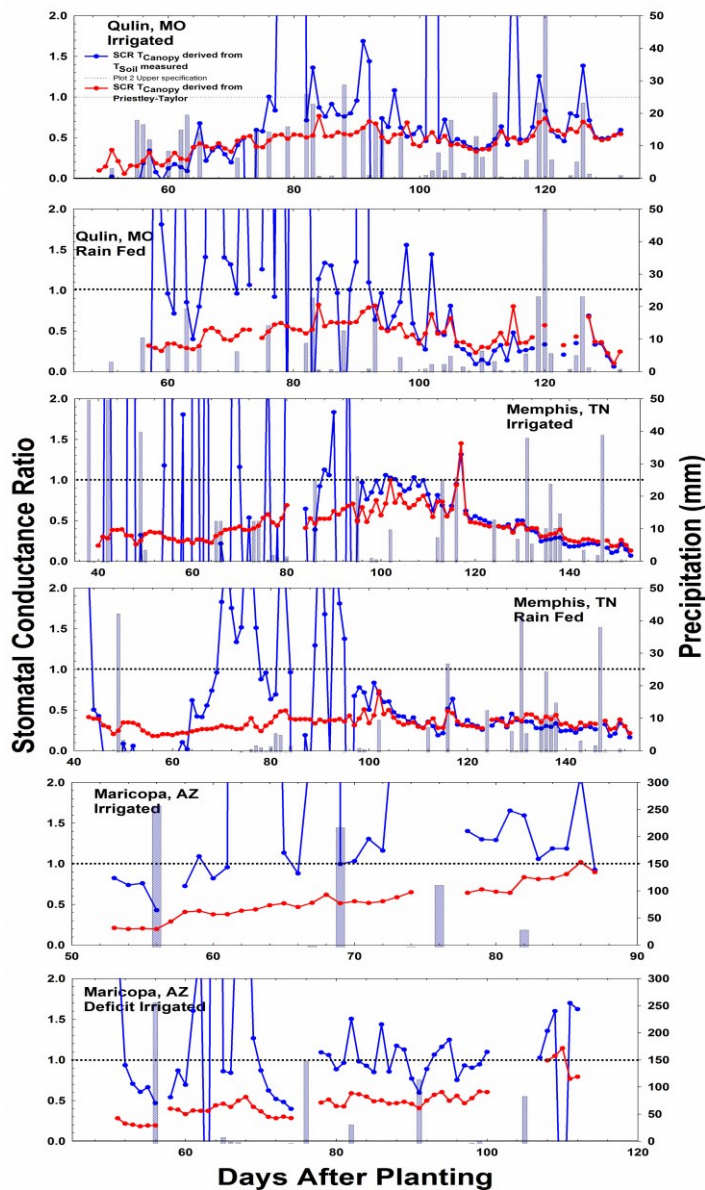
Fig. 2-14: The seasonal stomatal conductance ratio (SCR) average for an irrigated and rain fed/deficit irrigated cotton field in Qulin, MO, Memphis, TN, and Maricopa AZ. SCR using canopy temperature derived from the Priestley-Taylor approximation is compared to SCR calculated using canopy temperature derived from measured soil temperature and a composite radiometric surface temperature.
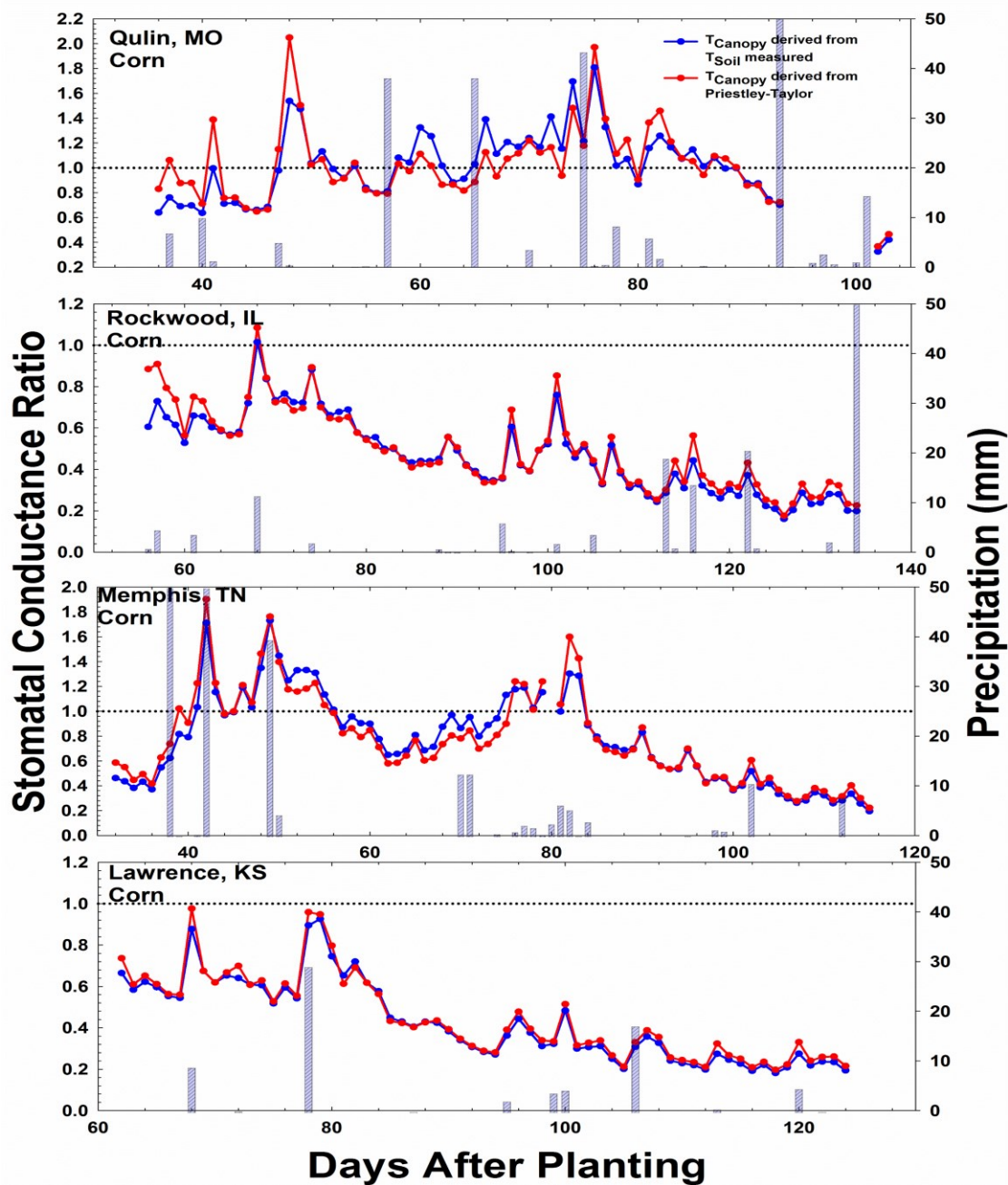
Fig. 2-15: The seasonal stomatal conductance ratio (SCR) average corn fields located in Quilin, MO, Rockwood IL, Memphis, TN and Lawrence, KS. SCR using canopy temperature derived from the Pirestley-Taylor approximation is compared to SCR calculated using canopy temperature derived from measured soil temperature and a composite radiometric surface temperature.
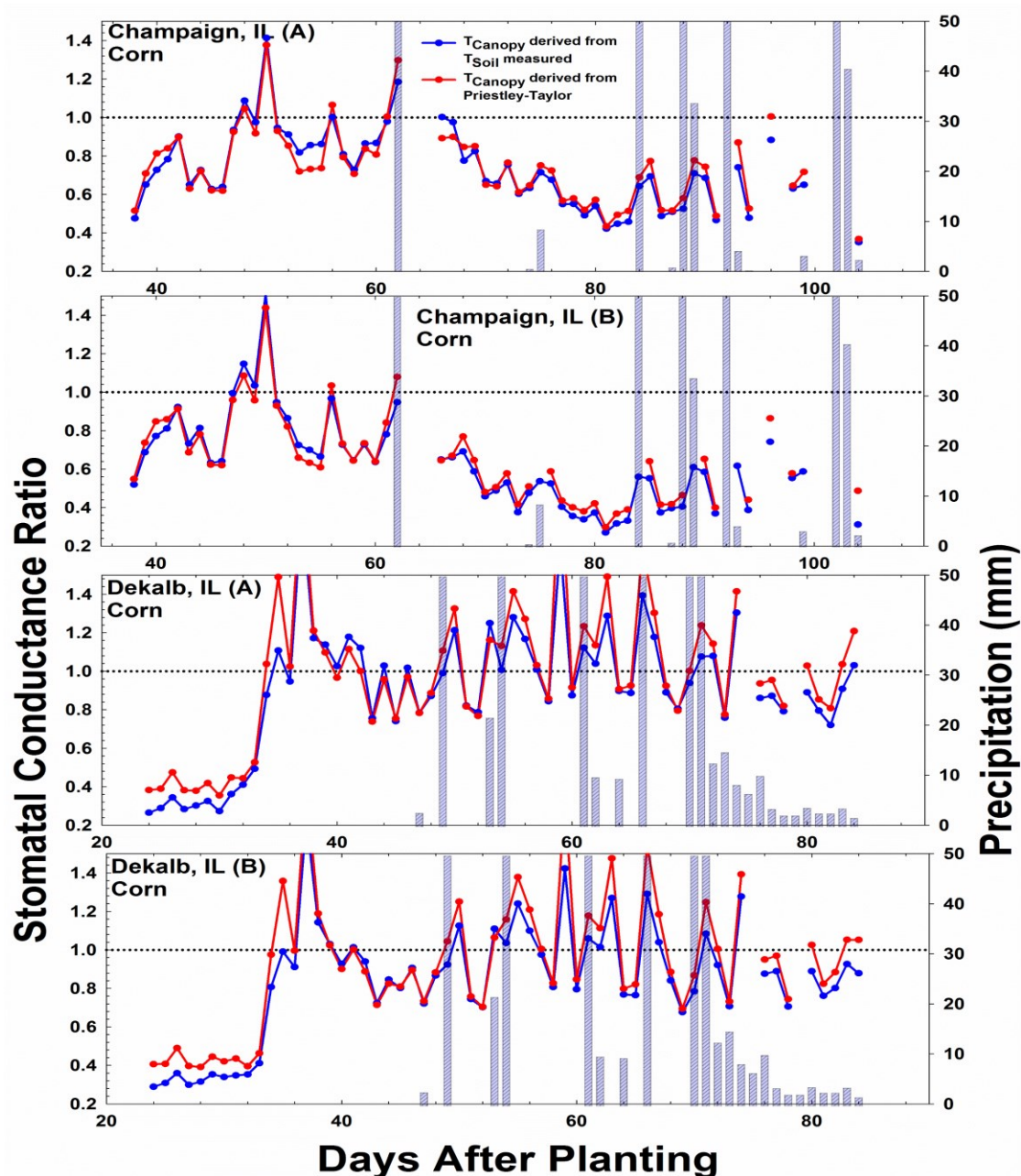
Fig. 2-16: The seasonal stomatal conductance ratio (SCR) average corn fields located in Champaign, IL (two sites, A and B), and Dekalb, IL (two sites, A and B). SCR using canopy temperature derived from the Pirestley-Taylor approximation is compared to SCR calculated using canopy temperature derived from measured soil temperature and a composite radiometric surface temperature.
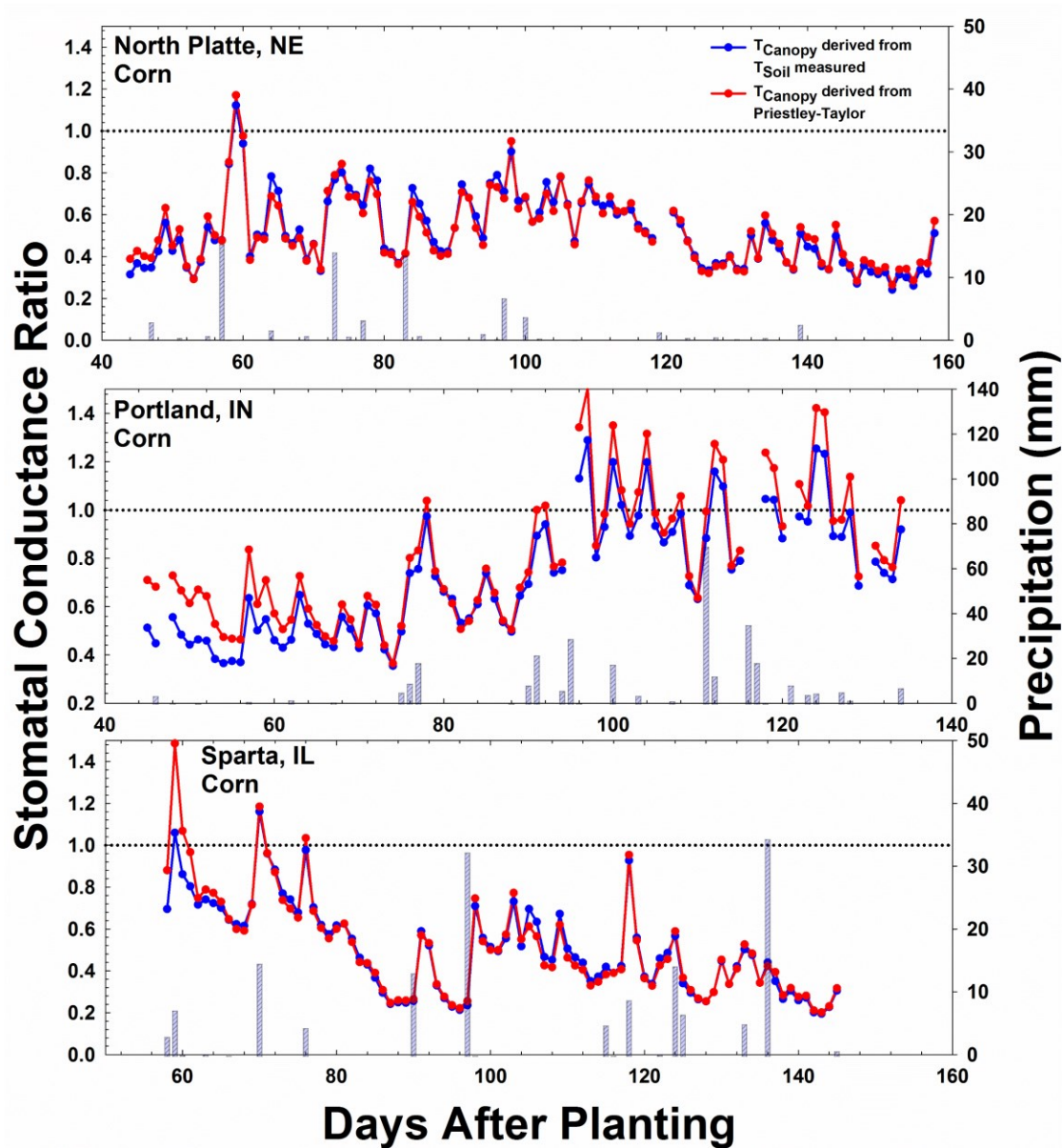
Fig. 2-17: The seasonal stomatal conductance ratio (SCR) average corn fields located in North Platte, NE, Portland, IN, and Sparta, IL. SCR using canopy temperature derived from the Priestley-Taylor approximation is compared to SCR calculated using canopy temperature derived from measured soil temperature and a composite radiometric surface temperature.

CHAPTER 3

NON-UNIFORM DISTRIBUTION OF NET RADIATION IN ROW CROPS:

IMPLICATIONS FOR CALCULATION OF CANOPY STOMATAL

CONDUCTANCE

3.1. Abstract

Canopy stomatal conductance can be calculated with application of biophysical principles from the energy balance of a plant canopy. Distribution of net radiation between the plants and soil within the canopy (R_{nc}) is a crucial parameter in the calculation of canopy stomatal conductance. The net radiation of the surface can be separated into soil and canopy components. The clumping, non-random spatial distribution of row crops needs to be accounted for when calculating these net radiation components. A clumping index was used to account for these special attributes of cotton and corn canopies. We found that incorporating the clumping index in the radiation divergence algorithms resulted in more reasonable and less erratic canopy stomatal conductance values for thirty minute average values over a day and daily average values over a season.

3.2. Introduction

The energy balance for a plant canopy needs to be calculated for the use of many bio-physically based plant water status indicators. The equation used in this study developed by Blonquist et al. (2009) for the calculation of canopy stomatal conductance is no exception. A two-source energy balance model is used to separate the absorbed radiation and energy fluxes of the soil and canopy layers. This two-source model is intended for use on homogeneous canopies

that are uniform in canopy coverage. Crops grown in rows, corn and cotton for example, have sparse canopy coverage for the majority of their growth season and the unique spatial distribution of these crops needs to be accounted for when calculating the energy balance and energy fluxes. Error in the calculation of water stress indices, such as canopy stomatal conductance, are very likely if a homogenous canopy is assumed when making these calculations for row crops.

Modifications need to be made to algorithms involved in the two-source energy balance model to account for the unique spatial distribution of sparse canopies and row crops (Colaizzi et al., 2012b). The radiation divergence within the canopy algorithms in the original two-source model were developed for canopies of randomly distributed leaves over the entire surface. The clumping characteristic of row crops needs to be accounted for when calculating radiation interception of the canopy and soil layers. These "clumped" crop canopies may only intercept 70 % to 80 % of the radiation compared to the same crop that is randomly distributed over the surface (Campbell and Norman, 1998). The calculation of the fraction of the radiometer field of view occupied by the canopy $f_c(\theta_R)$ is also affected by the clumping distribution of row crops.

3.2.1. Canopy fraction in radiometer field of view

3.2.1.1. Clumping index approach

The measured radiometric temperature used to calculate soil and canopy temperature is a composite temperature of the two layers. Separation of the composite radiometric temperature to a composite soil and canopy temperature requires an estimation of the fraction of the radiometer field of view occupied by

the canopy.   For a randomly spatially distributed (homogeneous) canopy it can be estimated using LAI (leaf are index (m²m⁻²)) and the radiometer zenith view angle (θ_R):

$$f_c(\theta_R) = 1 - e^{-(Kdir(\theta_R)*LAI)}$$

3.1

The exponential term is the "gap fraction" as calculated from the Beer-Lambert law, $Kdir(\theta_R)$ is the extinction coefficient for direct beam radiation calculated using the ellipsoid leaf angle distribution model of Campbell and Norman (1998).

The non-random spatial distribution must be accounted for when estimating the fraction of canopy in the radiometer's field of view for a row crop. This can be done by using the semi-empirical clumping index approach or a three-dimensional model of the canopy structure. The clumping index approach is considered to be robust for a variety of canopy structural types when a separation of sunlit and shaded components for the soil and canopy vegetation is not needed (Colaizzi et al., 2010). Three dimensional models of the canopy structure are needed to partition the soil and vegetation into their sunlit and shaded components.

The clumping index has been used to characterize the unique spatial distribution of forest canopies (Chen, 1996; Kucharik et al., 1999), and has been adapted for use with row crops such as cotton (Kustas and Norman, 1999), and corn and soybean (Anderson et al., 2005).

The clumping index $\Omega(\theta)$ is one way of defining the heterogeneity of a plant canopy. When the leaves are not randomly positioned, the canopy is considered homogeneous. The clumping index is incorporated into the extinction equations by multiplying it by the average leaf area index (LAI). The clumping index being dependent on zenith angle (θ). For random canopies $\Omega(\theta)$ =1, clumped vegetation has $\Omega(\theta)$<1.

Campbell and Norman (1998) suggested that the apparent clumping index $\Omega(\theta)$ is a function of the zenith view angle (θ) and Anderson et al. (2005) express it as:

$$\Omega(\theta) = \frac{\Omega_0 * \Omega_{max}}{\Omega_0 + (\Omega_{max} - \Omega_0) * exp(-k * \theta^p)} \qquad 3.2$$

where Ω_0 the clumping index when the canopy is viewed from nadir, θ=0:

$$\Omega_0 = \frac{ln\left((1 - f_{veg}) + f_{veg} * f_{gap}\right)}{-kdir(0) * LAI} \qquad 3.3$$

f_{veg} is the fraction of the total area within a field that is covered by the canopy:

$$f_{veg} = \frac{CanopyWidth(meters)}{RowSpacing(meters)} \qquad 3.4$$

f_{gap} is the area where soil is seen through the gaps of the canopy viewing at nadir ($\theta = 0$):

$$f_{gap} = exp(-kdir(0) * LAI_{local}) \qquad 3.5$$

LAI_{local} is the leaf area index of the canopy within a crop row:

$$LAI_{local} = \frac{LAI}{f_{veg}}$$
$$3.6$$

Ω_{max} is the maximum clumping index value, and accounts for the effect that the radiometer azimuth angle (ϕ) has on the calculated canopy fraction:

$$\Omega_{max} = \Omega_0 + (1 - \Omega_0)(sin\phi)^{0.05}$$
$$3.7$$

ϕ is the azimuth angle of the radiometer relative to the crop row.

k controls the response of the clumping index to changing radiometer azimuth angle:

$$k = -(0.3 + [1.7 * \Omega_0 * (sin\phi)^{0.1}]^{14})$$
$$3.8$$

$$p = 3.8 - 0.46 * D$$
$$3.9$$

$$D = \frac{CanopyHeight}{CanopyWidth}$$
$$3.10$$

The calculations for k and Ω_{max} used in this study were empirically developed by Anderson et al. (2005) to account for the azimuth dependence of these parameters that reproduce the expected behavior of $\Omega(\theta)$.

Colaizzi et al. (2010) proposed a geometric model for estimating the area fraction of sunlit and shaded soil and vegetation appearing in an elliptical or circular radiometer footprint that views over a row crop. Like the clumping index approach this model takes into account the radiometer zenith and azimuth viewing angles. Colaizzi et al. (2010) compared the total vegetation components (sunlit and shaded) from the geometric model to total vegetation predicted from the clumping index approach and found the geometric model to perform slightly better than the clumping index approach.

3.2.1.2 Radiation partitioning model

For sparse or incomplete canopies, radiation divergence within the canopy

models usually use some form of a view factor to account for differences in

radiation interception for the canopy and soil caused by the nonrandom spatial

distribution of the crop (Colaizzi et al., 2012a). Geometric modeling of the canopy

and the semi-empirical clumping index approaches are the more commonly used

approaches to account for the nonrandom spatial distribution of row crop

vegetation (Kustas and Norman, 1999; Annandale et al., 2004; Anderson et al.,

2005; Pieri, 2010b; Pieri, 2010a; Colaizzi et al., 2012b)

Campbell and Norman (1998) gave procedures to estimate shortwave

radiation transmittance and reflectance of a vegetated surface taking into

account wavelength and beam angle, leaf angle distribution, and the spatial

distribution of the vegetation. This procedure has been used in many studies

that use two-source energy balance models for estimation of evapotranspiration

(Kustas and Norman, 1999; Anderson et al., 2005; Li et al., 2005; French et al.,

2007). Shortwave transmittance and reflectance are calculated by calculating

their separate components of photosynthetically active radiation (PAR), near

infra-red radiation (NIR) and direct beam and diffuse components. The extinction

and scattering of shortwave radiation for a vegetated surface is dependent on the

radiation wavelength and beam angle. Vegetation absorbs greater PAR than

NIR incident radiation on leaves which is why it is important to use a radiation

transfer/partitioning model that accounts for these subcomponents. Diffuse

radiation is calculated by integrating the direct-beam components over a half-sphere.

Colaizzi et al. (2012c) compared measured irradiance fluxes with fluxes that were calculated using the Campbell and Norman (1998) radiation model. The model was modified to use the clumping index approach and a geometric view factor approach modeled as an elliptical hedgerow.   These measurements and calculations were made on corn, cotton, and sorghum throughout their growth cycle with vegetation cover changing over the season. They found that both approaches resulted in similar good agreement between the calculated and measured irradiance fluxes. Although the elliptical hedgerow approach did result in slightly but consistently smaller root mean squared error (RMSE) and mean absolute error (MAE) compared with the clumping index approach.

3.2.2. Objectives and hypotheses

The objective of this study was to determine if better estimates of canopy stomatal conductance could be achieved by accounting for the spatial distribution in row crops, as calculated in CHAPTER 1. The clumping spatial distribution of row crops will be accounted for in the calculation of canopy fraction in the radiometer field of view $\left(f_c(\theta_R)\right)$, and in the radiation partitioning algorithms for corn and cotton. This study also sought to determine the amount of influence measured and estimated variables have in the calculation of the clumping index. This was done by determining the sensitivity of the clumping index to the variables needed for its calculation. The behavior response of the stomatal

conductance will be assessed to determine whether these modifications improve the stomatal conductance estimates.

3.3. Materials and Methods

3.3.1. Data collection

Weather stations were deployed over corn and cotton fields in the following locations: Corn: Sparta, IL; Lawrence, KS; Qulin, MO; Portland, IN; Rockwood, IL; North Platte, NE; Memphis, TN; Cotton: Maricopa, AZ; Memphis, TN; and Qulin, MO. Each cotton location had a weather station setup on an irrigated and non-irrigated field trial. These stations made the required measurements to monitor crop water status by calculating canopy stomatal conductance. Each station was equipped with a datalogger (model CR1000, Campbell Scientific, Logan, UT), a pyranometer (Model SP-110, Apogee Instruments, Logan, UT), a relative humidity probe (Model CS215, Campbell Scientific, Logan, UT), two thermistors (Model ST-100, Apogee Instruments), a cup anemometer (Model Wind Sentry, RM Young Co., Traverse City, MI), and four infrared (IR) radiometers (Model SI-111 or SI-1H1, Apogee Instruments, Logan, UT). Four extendable poles were used as masts for IR sensor placement. The datalogger, anemometer, RH probe, pyranometer, and one of the thermistors were mounted on the "center" mast. The thermistor and RH probe were each placed in naturally ventilated louvered-radiation shields two meters above the crop canopy. The anemometer was also placed two meters above the crop canopy. The pyranometer was mounted at the top of the center mast. The other thermistor was buried approximately 10 cm below the soil

surface. Three of the infrared radiometers measured surface brightness temperature and each were placed on their own mast at an angle of 68 degrees (Models SI-111) or 72 degrees (SI-1H1) above nadir, at a height above canopy that allows the maximum view of the trial plot. The fourth infrared radiometer measured soil brightness temperature and was placed at an angle of 68 degrees above nadir and approximately 30 cm above the soil surface. A tipping bucket rain gauge (Model TE525WS, Campbell Scientific, Logan, UT) was installed at the edge of the crop fields to insure no obstructions from the crop for precipitation measurements.

Measurements of RH, air temperature, soil and canopy brightness temperature, wind speed, soil temperature at 10 cm, and incoming solar radiation were made every ten seconds and averaged over a 30-minute interval. The canopy height was measured at the time of setup and was periodically measured throughout the season. The growth stage of each crop was also periodically recorded over the season.

3.3.2. Experimental outline

The Qulin, MO irrigated cotton site was chosen as a representative site to illustrate the effects of the clumping index on the calculations of net radiation and on the stomatal conductance ratio index.

The stomatal conductance ratio (SCR) was calculated as outlined in CHAPTER 1 using data from the six cotton and ten corn locations. These calculations were made using canopy temperature derived using the Priestley-Taylor approach as described in CHAPTER 2.

3.3.3.   Calculating daily average stomatal conductance ratio

Daily averages of the stomatal conductance ratio (SCR) were calculated to summarize the water status of a crop over a season. These values were calculated as outlined in CHAPTER 1 using equations 1.3, 1.19, and 1.20. The 30-minute values were averaged for each day. This values are graphed with the standard deviation of these 30-minute values (Fig. 3-1).

Figure 3-1 is an example of how the stomatal conductance ratio is calculated using the calculated canopy stomatal conductance values and the reference canopy stomatal conductance values. This graph shows three days that vary in the solar intensity, with water being applied between the second and third day. The stomatal conductance ratio shows the crop at moderate water stress days two and three with an average daily SCR ratio at approximately 0.56 and 0.60, respectively. The decreased solar radiation of the second day decreases the water stress of the canopy. After the irrigation event the canopy is shown to have little water stress with an average SCR at 0.90.

3.3.4. Applying clumping index approach to radiometer field of view

The clumping index approach was used for calculation of the fraction of canopy in the infra-red radiometer field of view. The resulting canopy fraction ($f_{c(\Omega)}$) was compared to the calculated canopy fraction that assumes a homogeneous, randomly distributed canopy (f_c) for corn and cotton over time. A sensitivity analysis was performed on the clumping index and its dependence on Ω_0 and the dependence of Ω_0 on f_{veg} and the viewing zenith angle.

3.3.5. Applying View Factors to Radiation Partitioning Model

Net radiation for the canopy and soil were calculated by summing up their respective shortwave and longwave components:

$$R_{nc} = SW_{nc} + LW_{nc}$$

<div align="right">3.11</div>

$$R_{ns} = SW_{ns} + LW_{ns}$$

<div align="right">3.12</div>

where R_{nc} and R_{ns} are the net canopy and soil radiation, SW_{nc} and LW_{nc} are the net canopy shortwave and longwave radiation, and SW_{ns} and LW_{ns} are the net soil shortwave and longwave radiation. The shortwave radiation components include visible and near infrared radiation which are partitioned into direct beam and diffuse components. Each of these subcomponents have different reflectance and transmittance properties. Radiation components were calculated following the method and equations of Colaizzi et al. (2012b). Their approach was based on the procedures of Campbell and Norman (1998) which calculate reflectance and transmittance separately for each subcomponent (NIR, PAR, direct-beam, and diffuse radiation). This radiation partitioning model is usually coupled with a clumping index or view factor for sparse or incomplete canopies.

The following equations and methods were used to calculate R_{nc} with the clumping index incorporated. Campbell and Norman (1998) radiation partitioning model modification for sparse crops:

$$SW_{nc} =$$

$$SW_{nc,PAR,DIR} + SW_{nc,PAR,DIFF} + SW_{nc,NIR,DIR} + SW_{nc,NIR,DIFF}$$

3.13

where SW$_{nc}$ is the net shortwave radiation within the canopy and PAR, NIR, DIR, and DIFF refer to the photosynthetically active radiation, near infrared radiation, direct beam, and diffuse shortwave subcomponents, respectively, with:

$$SW_{nc,PAR,DIR} =$$

$$R_S f_{PAR} \left[K_{b,PAR} \left(1 - \tau_{c,DIR,PAR} \right) \left(1 - \rho_{s,PAR} \right) - \rho_{c,DIR,PAR} \right]$$

3.14

$$SW_{nc,PAR,DIFF} =$$

$$R_S f_{PAR} \left[\left(1 - K_{b,PAR} \right) \left(1 - \tau_{c,DIFF,PAR} \right) \left(1 - \rho_{s,PAR} \right) - \rho_{c,DIFF,PAR} \right]$$

3.15

$$SW_{nc,NIR,DIR} =$$

$$R_S \left(1 - f_{PAR} \right) \left[K_{b,NIR} \left(1 - \tau_{c,DIR,NIR} \right) \left(1 - \rho_{s,NIR} \right) - \rho_{c,DIFF,NIR} \right]$$

3.16

$$SW_{nc,NIR,DIFF} =$$

$$R_S \left(1 - f_{PAR} \right) \left[\left(1 - K_{b,NIR} \right) \left(1 - \tau_{c,DIFF,NIR} \right) \left(1 - \rho_s \right) - \rho_{c,DIFF,NIR} \right]$$

3.17

where R_S is the incoming shortwave radiation (W m^{-2}), f_{PAR} is the ratio of photosynthetically active radiation to total incoming shortwave radiation (approximately 0.45), K_b is the fraction of direct beam irradiance for visible or near infrared radiation, τ_c is the canopy transmittance, ρ_s is the soil reflectance, and ρ_c is the canopy reflectance. The τ_c, ρ_s, and ρ_c variables are for each

calculated for the photosynthetically active radiation (PAR), near infrared radiation (NIR), direct beam (DIR), and diffuse (DIFF) shortwave subcomponents subcomponent..

The procedures for calculating K_b, τ_c and ρ_c (with the clumping index included) can be found in (Colaizzi et al., 2012a):

$$\tau_{c,DIR,PAR} =$$

$$\frac{(\rho_{c,PAR}^{*2} - 1)\exp(-\sqrt{\zeta_{PAR}}K_{dir}(\Omega(\theta_{SW}))LAI)}{(\rho_{c,PAR}^{*}\rho_{s,PAR} - 1) + \rho_{c,PAR}^{*}(\rho_{c,PAR}^{*} - \rho_{s,PAR})\exp(-2\sqrt{\zeta_{PAR}}K_{dir}(\Omega(\theta_{SW}))LAI)} \qquad 3.18$$

where $\rho_{c,PAR}^{*}$ is the beam PAR reflection coefficient for a canopy with nonhorizontal leaves, ζ_{PAR} is the PAR absorption of leaves, K$_{dir}$ is the extinction coefficient for direct beam radiation, $(\Omega(\theta_{SW})$ is the clumping index to account for the nonrandom spatial distribution of vegetation at the solar zenith angle (θ_{SW}), and $\rho_{s,PAR}$ is the PAR reflectance of the soil. The reflectance terms $\rho_{c,PAR}^{*}$ and $\rho_{s,PAR}$ account for down welling radiation that is reflected from the soil and reflected by the canopy leaves. Goudriaan (1988) calculated $\rho_{c,PAR}^{*}$ as:

$$\rho_{c,PAR}^{*} = \frac{2K_{dir}\rho_{PHOR,PAR}}{K_{dir} + 1} \qquad 3.19$$

where $\rho_{PHOR,PAR}$ is the beam radiation coefficient for a canopy with horizontal leaves calculated as:

$$\rho_{PHOR,PAR} = \frac{1 - \sqrt{\zeta_{PAR}}}{1 + \sqrt{\zeta_{PAR}}} \qquad 3.20$$

Direct beam NIR transmittance ($\tau_{c,DIR,NIR}$) was calculated in the same manner as

$\tau_{c,DIR,VIS}$, replacing ζ_{PAR} with ζ_{NIR} (NIR absorption) and $\rho_{s,PAR}$ was replaced with

$\rho_{s,NIR}$. The diffuse transmittance ($\tau_{c,DIFF,NIR}$ and $\tau_{c,DIFF,PAR}$) was calculated by

numerically integrating $\tau_{c,DIR,NIR}$ and $\tau_{c,DIR,PAR}$ over a half spere.

The canopy beam extinction coefficient (K_{dir}) was calculated as:

$$K_{dir} = \frac{\sqrt{\chi^2 + tan^2\theta_{SW}}}{\chi + 1.774(\chi + 1.182)^{-0.733}} \qquad 3.21$$

where χ is the ratio of horizontal to vertical projected unit are of leaves. The χ

parameter quantifies the average leaf angle and is species specific (Colaizzi et

al., 2012a).

The net longwave component for the canopy is calculated as follows:

$$LW_{nc} = \left[\varepsilon_c L_{sky} + \varepsilon_c L_s - (1 - \varepsilon_c)L_c\right](1 - \theta_{LW}) \qquad 3.22$$

where

$$\theta_{LW} = exp(-K_{LW}LAI\frac{row}{w_c}) \qquad 3.23$$

where w_c is the canopy width (m), row is the crop row spacing (m), ε_c is the

canopy emittance (0.96), L_{sky} is the longwave irradiance from the sky (W m^{-2}), L_s

and L_c are the longwave irradiance from the soil and canopy respectively (W m^{-2}),

K_{LW} is the extinction coefficient for longwave irradiance (0.95), and L_{sky}, L_s, and

L_c are calculated using the Stephan-Boltzmann relation:

$$L_{sky} = \varepsilon_{ATM}\sigma T_{Air}^4 \qquad 3.24$$

$$L_s = \varepsilon_s \sigma T_{soil}^4$$

3.25

$$L_c = \varepsilon_c \sigma T_{canopy}^4$$

3.26

where ε_{ATM} is the atmospheric emittance, σ is the Stephan-Boltzmann constant (5.67×10^{-8} W m^{-2} K^{-4}). ε_{ATM} was calculated according to Idso et al. (1981).

The stomatal conductance ratio (SCR) was calculated as described in CHAPTER 1 using the clumping index ($\Omega(\theta)$) for calculation of the canopy shortwave and longwave components.

3.4. Results and Discussion

3.4.1. Clumping index response to measured or estimated variables

Calculation of the clumping index $\Omega(\theta)$ requires measurements or estimates of canopy height and canopy width, along with a knowledge of the row spacing. Observation of the response of $\Omega(\theta)$ to the variables that go into its calculation has led us to conclude that $\Omega(\theta)$ is most sensitive to the clumping index from the nadir view $\Omega(0)$. The $\Omega(0)$ value was varied from a minimum of zero to a maximum of one to show the sensitivity of $\Omega(\theta)$ to changes in $\Omega(0)$. This relationship was shown for four zenith view angles ($\theta = 0, 30, 45,$ and 70) (Fig. 3-2). Analysis showed that $\Omega(\theta)$ could vary as much as 15% with an error in $\Omega(0)$ of 0.1.

The clumping index at nadir $\Omega(0)$ is sensitive to the measured or estimated ratio of canopy width to canopy height (w/h) (Fig. 3-3). An analysis has shown that an error in w/h of 0.5 can result in as much as a 10% change in $\Omega(0)$.

These results show the importance of having accurate canopy width and height measurements for calculation of $\Omega(0)$ and thus $\Omega(\theta)$. Often when height and width measurements are not made they are estimated using empirical equations relating height to a growth degree unit and width to height. These results suggests that estimates using these equations may introduce significant errors in the clumping index calculation.

3.4.2. Fraction of canopy in radiometer field of view

For the radiometer zenith view angle of $68°$ used for each study location the estimated ($f_{c(\Omega)}$) starts out smaller than the estimated (f_c) and the difference between the two gradually decreases as the canopy cover fills in, as seen in the irrigated Memphis, TN cotton trial (Fig. 3-4). The ($f_{c(\Omega)}$) value never reached 1.0, signifying 100% canopy fraction in the radiometer field of view, for this particular location because the canopy was estimated to stop growing at a height that allowed a fraction of soil to still be viewed.

3.4.3. Clumping index effect on shortwave radiation calculation

The clumping index was incorporated into the canopy net shortwave and net longwave radiation calculations. These resulting values were compared to canopy net shortwave (SW_{nc}) (Fig. 3-5) and net longwave (LW_{nc}) (Fig. 3-6) radiation calculated without using the clumping index to account for the unique spatial distribution of the crop. Comparisons between the values of two calculation methods are shown for three different time periods (early, mid, and late season). The SW_{nc} was higher for the method not using the clumping index for each time period as was expected. As the canopy filled in over the season,

the two SW_{nc} values came closer together as expected. If the canopy was to reach full coverage the two values would be the same because the clumping index would equal a value of one and would have no impact on the calculated components of SW_{nc}. Comparisons of LW_{nc} showed the LW_{nc} values calculated using the clumping index to be higher for all three time periods. This is due to the conversion of an averaged LAI to a local LAI in equation (3.23). This conversion is the same as the f_{veg} (equation 3.4) variable used in the clumping index. This conversion increases the LAI and thus LW_{nc} in equation (3.22). These comparisons show that there is a considerable difference between the net radiation values calculated with and without the clumping index. All variables dependent on net shortwave and net longwave radiation of the canopy are likely to vary greatly as well depending on which value is used. This can be seen with the difference between the calculated stomatal conductance values calculated with and without the clumping index.

3.4.4. Clumping index effect on stomatal conductance ratio

The clumping index affects the calculated values of net shortwave and net longwave radiation at the canopy as seen in section (3.4.3). These net radiation values are added together to yield a total net radiation value (R_{nc}) that is used in the stomatal conductance equation (1.3). The stomatal conductance ratio (SCR) was calculated with and without the clumping index incorporated into the radiation algorithms and compared in (Fig. 3-7) over three time periods (early, mid, and late season). These values were calculated using 30-minute average measurements. As expected the increased R_{nc} from not incorporating the

clumping index in the radiation algorithms results in higher SCR values than the SCR using the clumping index derived R_{nc}. The difference between the two methods for calculation of SCR over the season can be seen on the representative field trial in Qulin, MO (Fig. 3-8). The calculation of SCR with the clumping index incorporated is determined to be the most correct method. Determining which method gives the most realistic results is based on their response to irrigation/precipitation events, expected daily and seasonal behavior, and the variability throughout the day. The average daily SCR values respond to precipitation/irrigation events by showing less stressed plants while increasing in stress during such events. The values remain steady with consistent watering and the crop appears to have been more stressed at the beginning of the season compared to mid and late season. This may be due to the root system not going as deep into the soil at the beginning of the season and having less water available to its root system than it does later on in the season. There also is the possibility that the clumping index overcompensates in the reduction of R_{nc} when the plants are smaller and canopy architecture components (height, width, LAI) are more difficult to calculate or measure.

As the canopy coverage closes over the season the two calculated SCR values (with and without incorporating the clumping index) come closer together, as do there corresponding daily averages and error bars. This supports the hypothesis that modification needs to be done for radiation algorithms calculated for row crops that are unique in there spatial distribution with their "clump" like behavior. Once the canopy has closed such modifications are not necessary.

There are conditions that result in the stomatal conductance ratio (SCR) exceeding the theoretical limit of one. This occurs when the calculated canopy stomatal conductance value exceeds the reference value. Decreasing the estimated radiation absorbed by the canopy, using the clumping index, reduces theses occurrences, although it still happens occasionally even with this incorporation. It is possible that the canopy stomatal conductance model used does not accurately account for certain conditions or the measurements used are not reliable during these times. It is also possible that the reference value used is not accounting for particular conditions accordingly and reads lower that what it should at times. This question of why the SCR exceeds one at times needs to be investigated in future studies, perhaps finding a better method to calculate the reference value.

3.4.5. Seasonal SCR comparisons for all cotton and corn sites

A comparison for all of the cotton (Fig. 3-9) and two representative corn (Fig. 3-10) daily average SCR values calculate with and without incorporation of the clumping index in the radiation showed different results between the corn and cotton values over the season. The SCR values, calculated without incorporation of the clumping index were more erratic with bigger error bars for the cotton fields than they were for the corn fields. This is because the majority of the corn fields were already at complete canopy cover when the weather stations use for data collection were deployed. This canopy coverage resulted in a clumping index value of one, thus making no changes in the radiation partitioning algorithms. The corn canopies fill in quicker than the cotton canopies because of the smaller

row spacing (0.76 m compared to 1.02 m) and because the ratio of their width to height before canopy closure is larger (1.0:1.0 compared to 0.75:1.0). When a full canopy coverage is reached in the cotton fields the two methods to calculate SCR result in similar values (Memphis, TN, Fig. 3-9).

3.5. Conclusions

No direct measurements of canopy or leaf stomatal conductance were available for any of the sites used in this study. This makes it difficult to validate the daily and seasonal corn and cotton canopy stomatal conductance values calculated. Due to this limitation we determined which approach led to better estimates of canopy stomatal conductance by observing the behavior of the calculated values. Stomatal conductance values were assessed on their response to irrigation/precipitation events, expected daily and seasonal behavior, and the variability throughout the day. Leaf stomatal conductance measurements made with a leaf porometer are the most commonly made measurements of stomatal conductance in the field. For comparison to the calculated canopy stomatal conductance values made in this study, leaf stomatal conductance measurements would need to be scaled up. There is error and uncertainty associated with the multiple methods used to scale up leaf to canopy stomatal conductance. Even if 30-minute or once-a-day leaf stomatal conductance measurements were made, which would be labor and time intensive, there is no certainty that these values would be the best reference. They could however provide a good relative indication of the expected daily and seasonal trends.

The hypothesis that the incorporating the clumping index into the radiation partitioning algorithms for calculation of the stomatal conductance ratio (SCR) would improve the SCR values is supported by the findings of this chapter. The values show expected behavior over the course of the day with the magnitude of the highest to lowest values not overwhelmingly large. This behavior results in less erratic daily average values over the season with smaller standard deviations. The SCR with the incorporated clumping index gives daily values that respond well and less erratic to precipitation/irrigation events over the course of the season.

The use of the Leuning model (Leuning, 1995) for the reference stomatal conductance value may not be the most appropriate method to determine maximum stomatal conductance. It would be wise to investigate other methods to determine the best approximation of a reference stomatal conductance.

3.6. References

Anderson, M.C., Norman, J.M., Kustas, W.P., Li, F.Q., Prueger, J.H., Mecikalski, J.R., 2005. Effects of vegetation clumping on two-source model estimates of surface energy fluxes from an agricultural landscape during SMACEX. Journal of Hydrometeorology 6, 892-909.

Annandale, J.G., Jovanovic, N.Z., Campbell, G.S., Du Santoy, N., Lobit, P., 2004. Two-dimensional solar radiation interception model for hedgerow fruit trees. Agricultural and Forest Meteorology 121, 207-225.

Blonquist, J.M., Norman, J.M., Bugbee, B., 2009. Automated measurement of canopy stomatal conductance based on infrared temperature. Agricultural and Forest Meteorology 149, 2183-2197.

Campbell, G.S., Norman, J.M., 1998. An Introduction to Environmental Biophysics. Springer-Verlag, New York, NY, USA.

Chen, J.M., 1996. Optically-based methods for measuring seasonal variation of leaf area index in boreal conifer stands. Agricultural and Forest Meteorology 80, 135-163.

Colaizzi, P.D., Evett, S.R., Howell, T.A., Li, F., Kustas, W.P., Anderson, M.C., 2012a. Radiation Model for Row Crops: I. Geometric View Factors and Parameter Optimization. Agronomy Journal 104, 225-240.

Colaizzi, P.D., Kustas, W.P., Anderson, M.C., Agam, N., Tolk, J.A., Evett, S.R., Howell, T.A., Gowda, P.H., O'Shaughnessy, S.A., 2012b. Two-source energy balance model estimates of evapotranspiration using component and composite surface temperatures. Advances in Water Resources 50, 134-151.

Colaizzi, P.D., O'Shaughnessy, S.A., Gowda, P.H., Evett, S.R., Howell, T.A., Kustas, W.P., Anderson, M.C., 2010. Radiometer Footprint Model to Estimate Sunlit and Shaded Components for Row Crops. Agronomy Journal 102, 942-955.

Colaizzi, P.D., Schwartz, R.C., Evett, S.R., Howell, T.A., Gowda, P.H., Tolk, J.A., 2012c. Radiation Model for Row Crops: II. Model Evaluation. Agronomy Journal 104, 241-255.

French, A.N., Hunsaker, D.J., Clarke, T.R., Fitzgerald, G.J., Luckett, W.E., Pinter, P.J., 2007. Energy balance estimation of evapotranspiration for wheat grown under variable management practices in central Arizona. Transactions of the Asabe 50, 2059-2071.

Goudriaan, J., 1988. The Bare Bones of Leaf-Angle Distribution in Radiation Models for Canopy Photosynthesis and Energy Exchange. Agricultural and Forest Meteorology 43, 155-169.

Idso, S.B., Jackson, R.D., Pinter, P.J., Reginato, R.J., Hatfield, J.L., 1981. Normalizing the Stress-Degree-Day Parameter for Environmental Variability. Agricultural Meteorology 24, 45-55.

Kucharik, C.J., Norman, J.M., Gower, S.T., 1999. Characterization of radiation regimes in nonrandom forest canopies: theory, measurements, and a simplified modeling approach. Tree Physiology 19, 695-706.

Kustas, W.P., Norman, J.M., 1999. Evaluation of soil and vegetation heat flux predictions using a simple two-source model with radiometric temperatures for partial canopy cover. Agricultural and Forest Meteorology 94, 13-29.

Leuning, R., 1995. A Critical-Appraisal of a Combined Stomatal-Photosynthesis Model for C-3 Plants. Plant Cell and Environment 18, 339-355.

Li, F.Q., Kustas, W.P., Prueger, J.H., Neale, C.M.U., Jackson, T.J., 2005. Utility of remote sensing-based two-source energy balance model under low- and high-vegetation cover conditions. Journal of Hydrometeorology 6, 878-891.

Pieri, P., 2010a. Modelling radiative balance in a row-crop canopy: Cross-row distribution of net radiation at the soil surface and energy available to clusters in a vineyard. Ecological Modelling 221, 802-811.

Pieri, P., 2010b. Modelling radiative balance in a row-crop canopy: Row-soil surface net radiation partition. Ecological Modelling 221, 791-801.
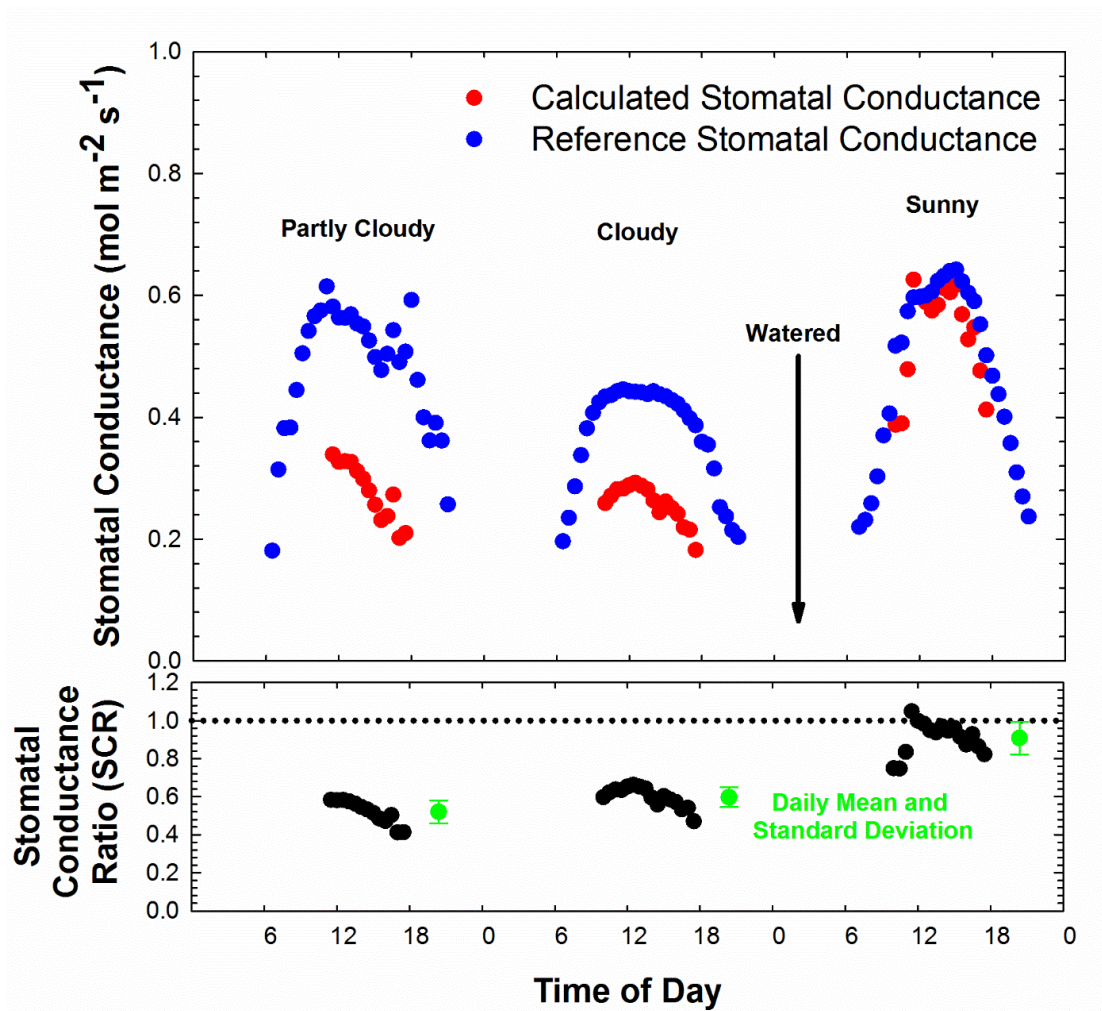
Fig. 3-1: Calculated 30-minute stomatal conductance ratio (SCR) values. The SCR is a ratio of the measured actual stomatal conductance to the reference stomatal conductance. The daily average is shown with error bars representing the standard deviation of each of the 30-minute SCR values.
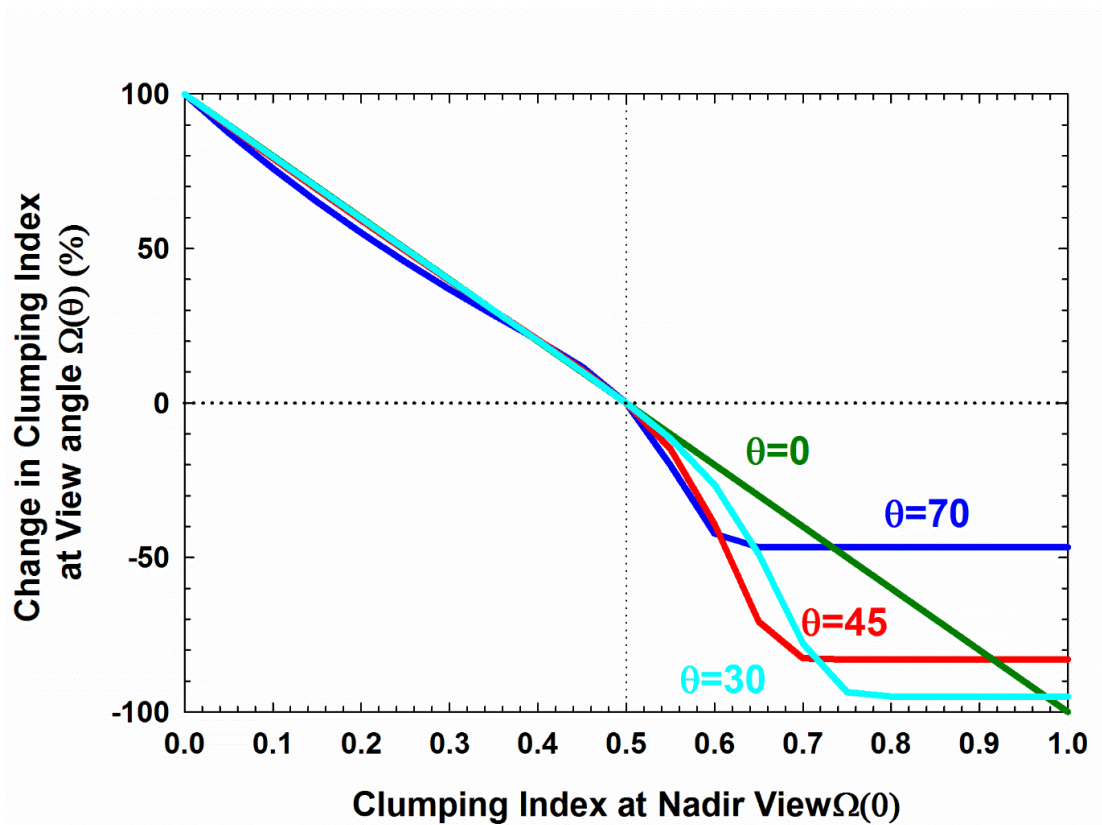
Fig. 3-2: Percentage change in zenith viewing angle (θ) clumping index (Ω(θ)) in response to changes in nadir view clumping index (Ω(0)) at different zenith viewing angles (θ).
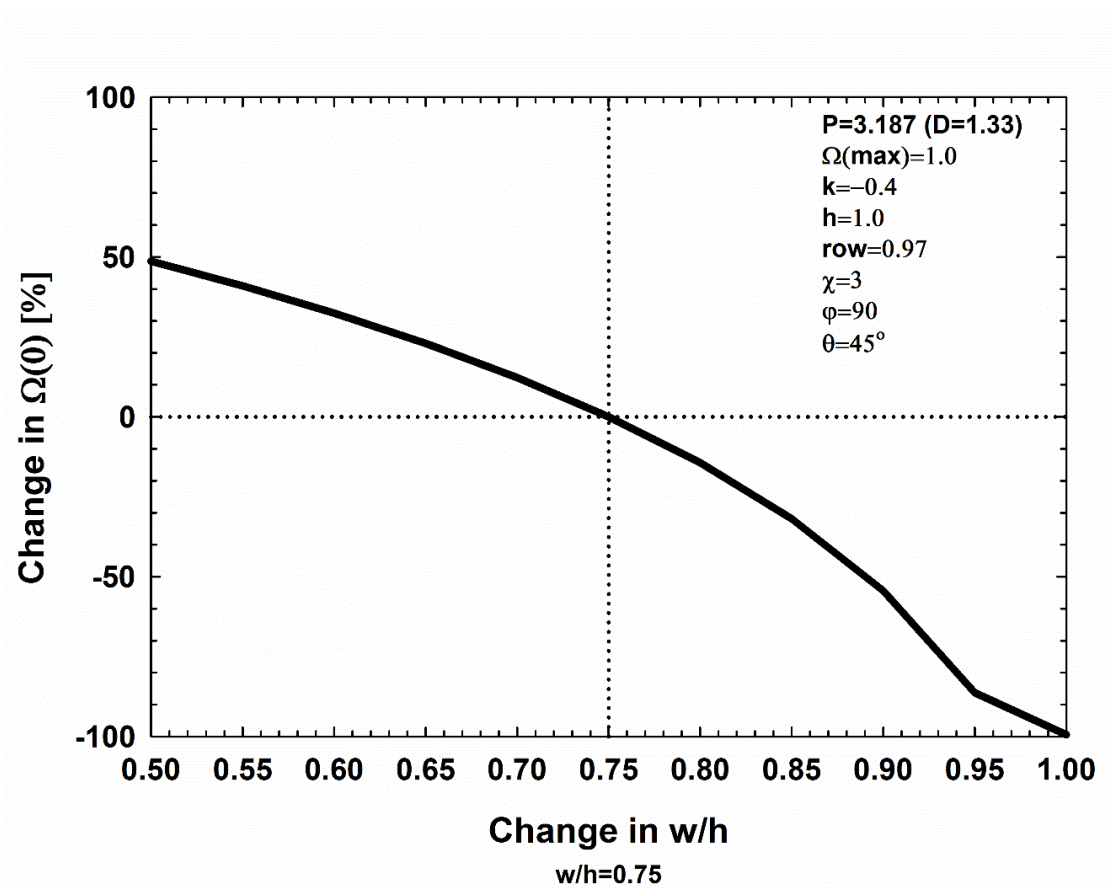
Fig. 3-3: Percentage change in nadir view clumping index ($\Omega(0)$) in response to changes in canopy width (w) to height (h) ratio.
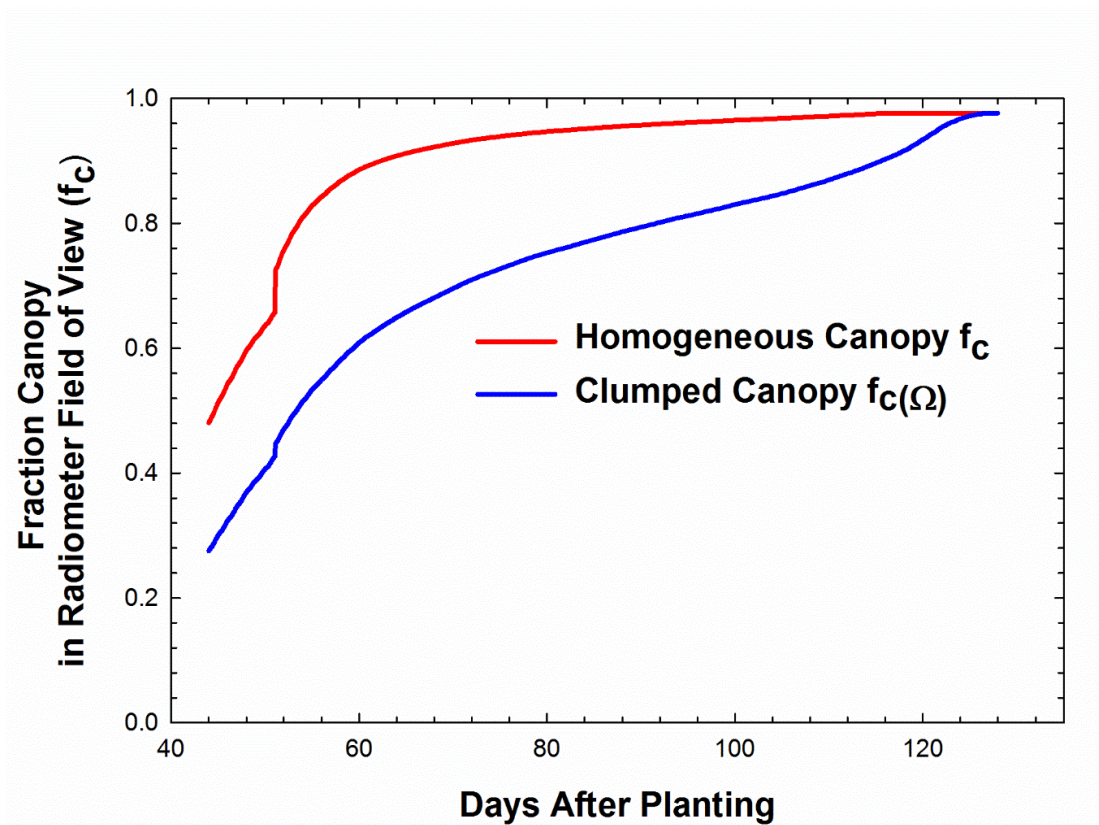
Fig. 3-4: Calculated fraction of canopy in the radiometer field of view using equation (3.1) with LAI multiplied by the clumping index ($f_{c(\Omega)}$) and without (f_c) using data collected from a cotton field in Memphis, TN.
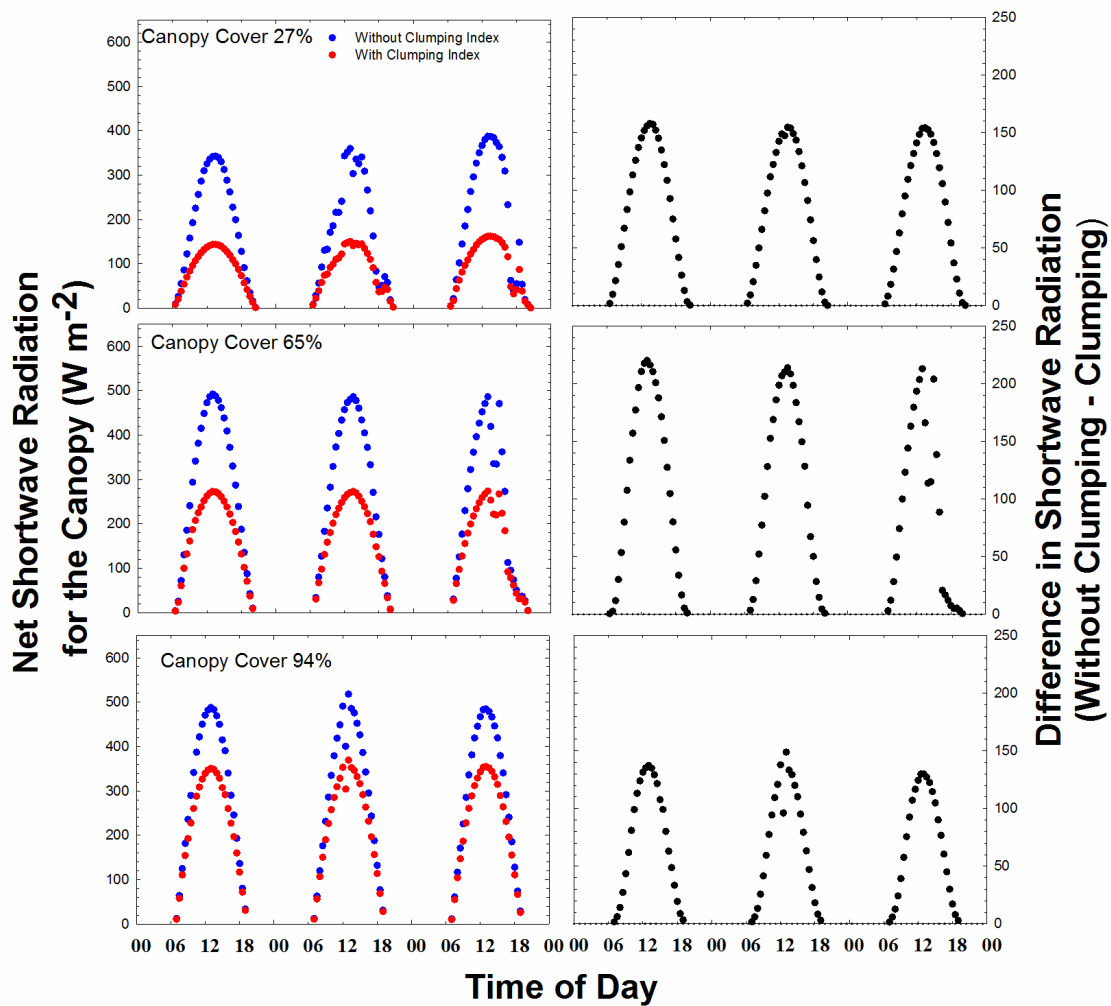
Fig. 3-5: Net shortwave radiation (SW_{nc}) for the canopy with and without the clumping index ($\Omega(\theta)$) included in the calculation of SW_{nc}.
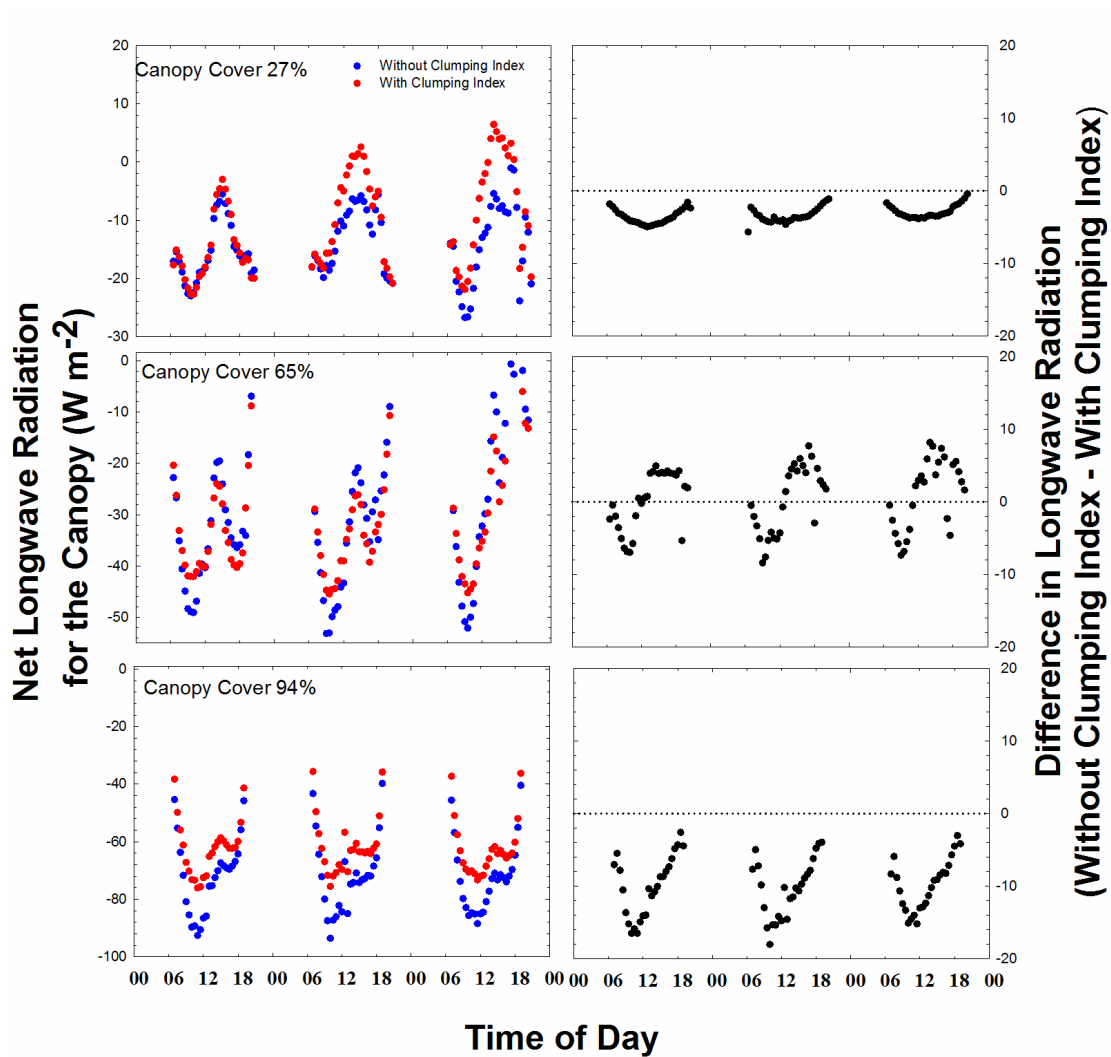
Fig. 3-6: Net longwave radiation (LW$_{nc}$) for the canopy with and without the clumping index ($\Omega(\theta)$) included in the calculation of LW$_{nc}$.
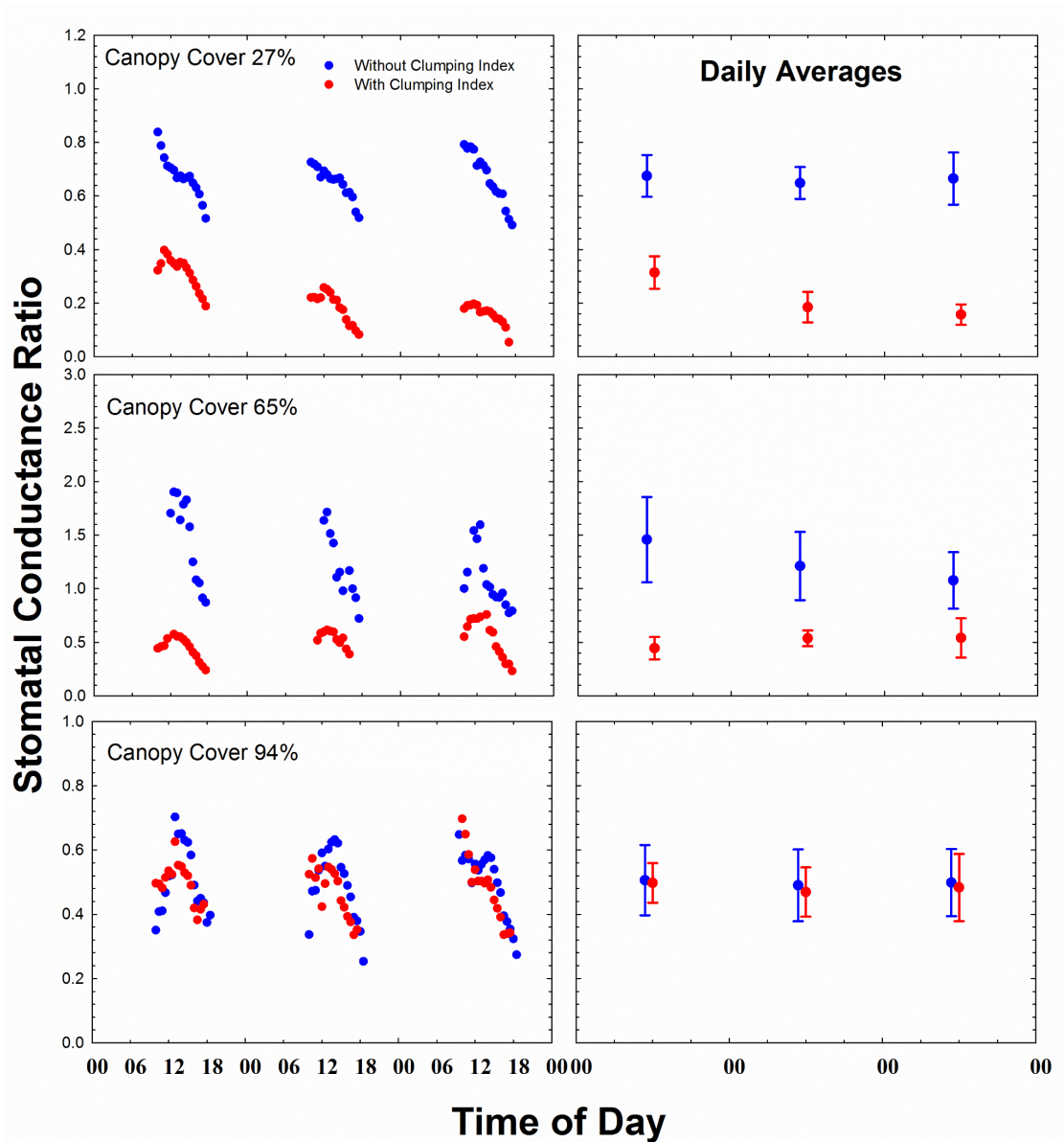
Fig. 3-7: Stomatal conductance ratio (SCR) calculated with and without the clumping index (Ω(θ)) used for radiation partitioning algorithms used in SCR calculation.
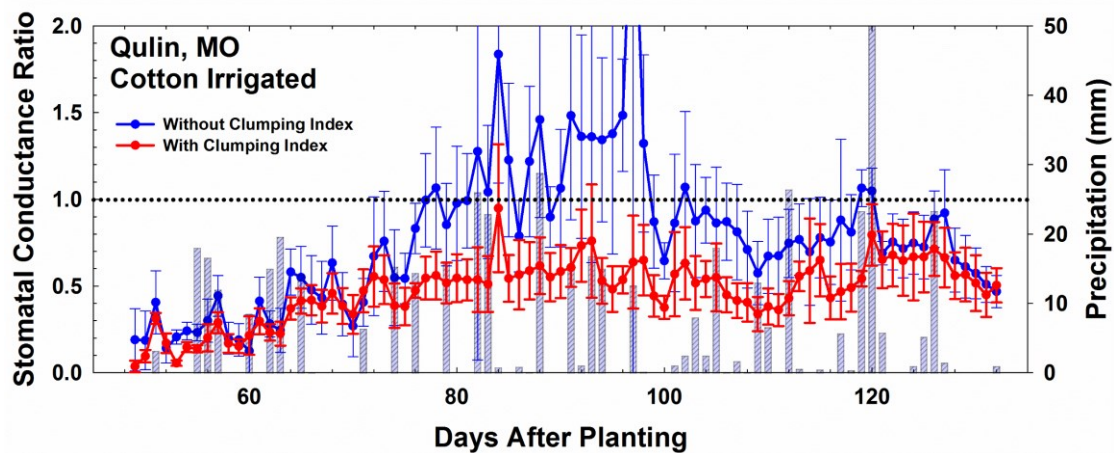
Fig. 3-8: The seasonal stomatal conductance ratio (SCR) average for an irrigated cotton field in Qulin, MO. SCR calculated using the clumping index $(\Omega(\theta))$ is compared to SCR calculated without the clumping index.
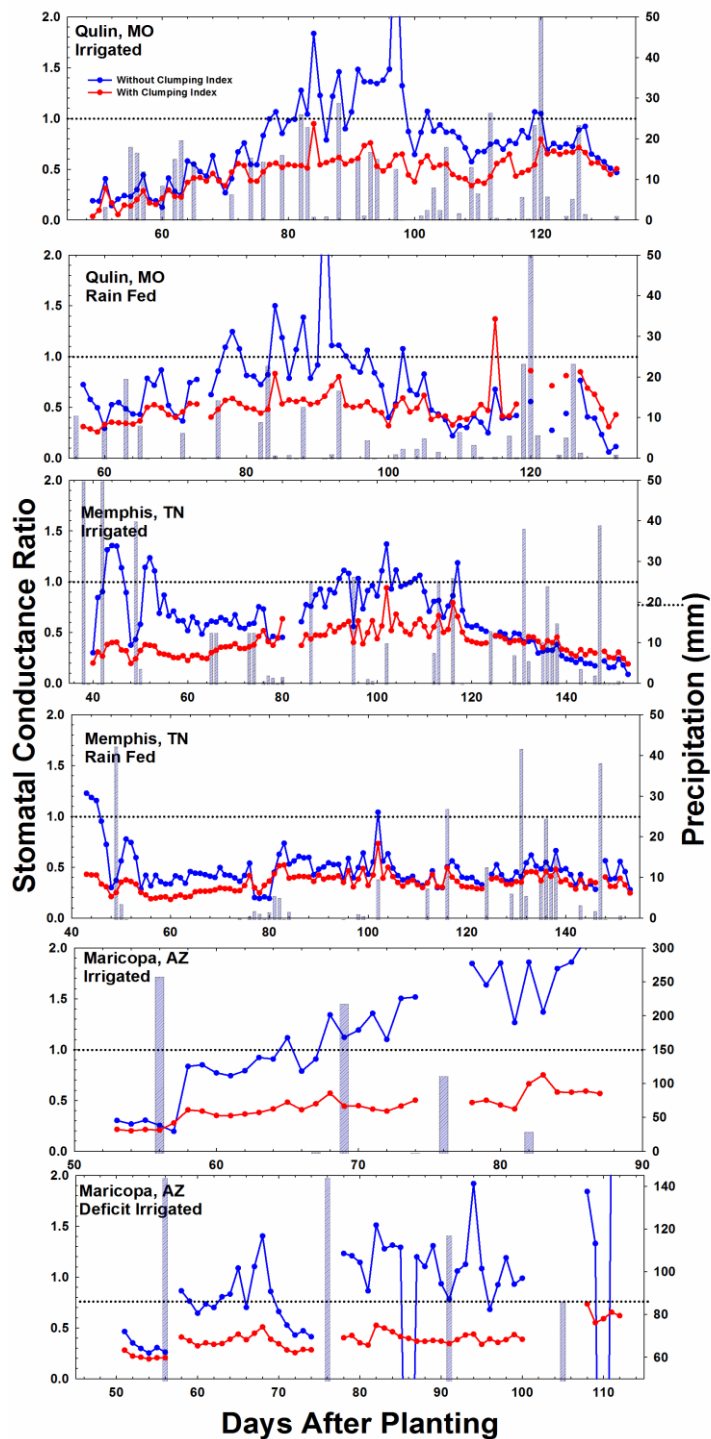
Fig. 3-9: The seasonal stomatal conductance ratio (SCR) average for an irrigated and rain fed/deficit irrigated cotton field in Qulin, MO, Memphis TN, and Maricopa, AZ. SCR calculated using the clumping index is compared to SCR calculated without the clumping index.
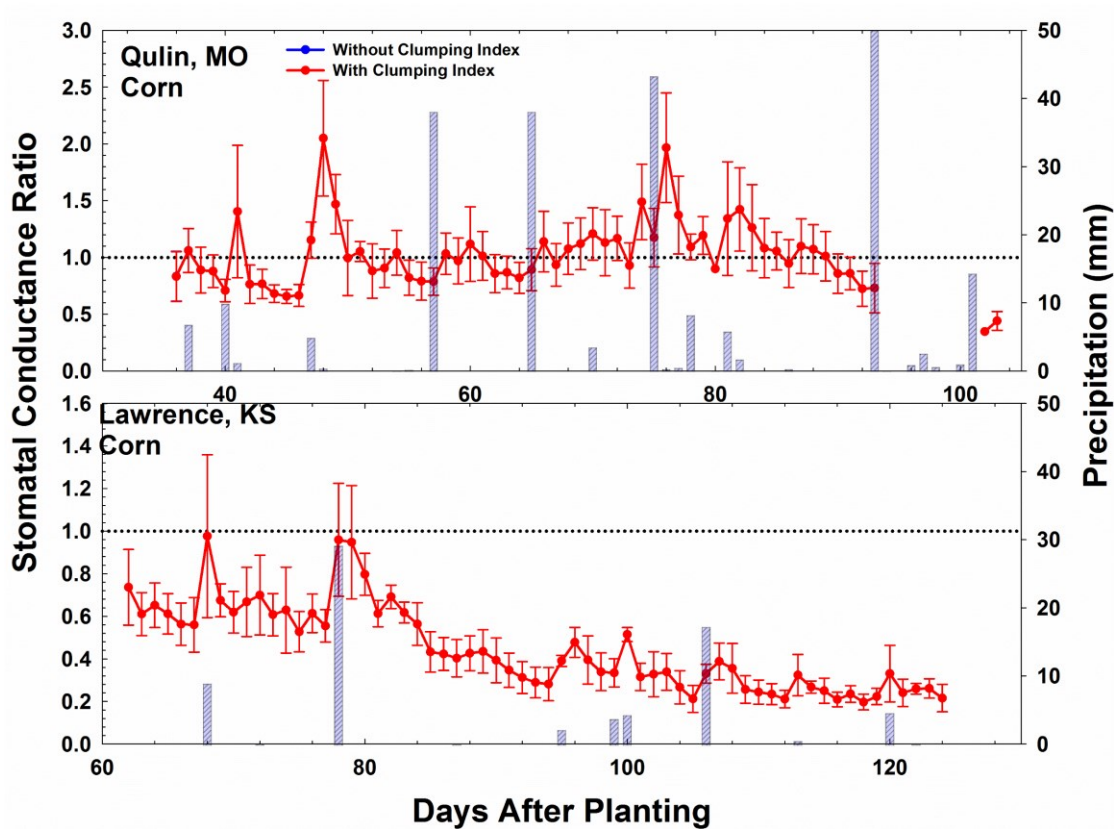
Fig. 3-10: The seasonal stomatal conductance ratio (SCR) average corn fields located in Quilin, MO, and Lawrence, KS. SCR using the clumping index $(\Omega(\theta))$ is compared to SCR calculated without the clumping index. There is no difference between the two methods due to full canopy coverage at the beginning of measurements.

CHAPTER 4

YIELD PREDICTION FROM STOMATAL CONDUCTANCE

4.1. Abstract

Stomatal conductance is a measure of the capacity for CO_2 to diffuse into leaves and supply the substrate for photosynthesis. Increased stomatal conductance thus indicates the capacity for photosynthesis, growth, and ultimately yield. A stomatal conductance ratio (SCR) that is increased over a growing season should thus have increased yield. The relationship between the daily average stomatal conductance ratio and grain yield of corn and lint yield of cotton was analyzed with the goal of developing a predictive yield model. Daily average SCR values were determined starting at the V12 vegetative growth stage through the R3 reproductive growth stage for corn and from 50 to 130 days after planting for cotton from. Growth stages for corn were divided into either 5 groups based on growth stage and a weighting factor for each growth stage was determined from literature values based on crop sensitivity to drought stress during each stage. Seasonal averaged SCR values were calculated using the weighting factors. An average SCR value was calculated for cotton based on one stage that was most sensitive to drought stress. The relationship between average SCR value and yield was determined by regression analysis. The literature based weighting factors yielded an r^2 value of 0.79 for the corn and the average SCR with no weighing factors resulted in an r^2 value of 0.76.   The r^2 value for cotton was as high as 0.93. These results form the basis for predicting yield from water stress measurements in multiple crops.

4.2. Introduction

4.2.1. Stomatal conductance and yield

Canopy conductance is directly related to stomatal aperture and plant water status which affects crop growth and crop yield. Previous studies have shown a relationship between stomatal conductance of water vapor and crop yield (Cornish et al., 1991; Fischer et al., 1998; Lu et al., 1998).

4.2.2. Cotton lint yield response to drought stress

Water-deficit stress can significantly compromise plant development and yield. This decrease in yield is generally caused by a reduction in leaf area and photosynthesis. The reduction in photosynthesis is related to the stomatal closure and a decrease in CO_2 gas exchange. When experiencing water stress, cotton has reduced boll production from fewer flowers and bolls (Gerik et al., 1996).

A greenhouse study showed an increases in stomatal conductance and photosynthetic rates accompanying an increase in cotton lint yield (Cornish et al., 1991). Lu et al. (1998) showed a positive correlation between lint yield of Pima cotton and stomatal conductance with an r value of 0.92. Stomatal conductance was measured at the time of peak flowering and fruiting on cotton grown in Arizona.

4.2.3. Corn grain yield response to drought stress

Corn grain yield is largely dependent on the crop water availability during growth stages that include tasseling, silking, and pollination, being particularly sensitive to drought stress during this time period.

Earl and Davis (2003) and references cited therein describe three main mechanisms that cause a reduction in corn grain yield as a response to drought stress. First, the whole canopy photosynthetically active radiation (PAR) absorption can be reduced by a decrease in leaf rate expansion, leaf wilting or rolling during severe water stress, or early leaf senescence. Second, the radiation use efficiency is reduced. Third, the harvest index may be reduced. Decrease in harvest index is significant if drought stress occurs during the critical development stage around silking. Developing ovaries are prone to failing if there is a lack of carbohydrate available for their growth. Silk receptivity can also be affected by water stress.

Corn grain yield has been correlated with various stress indicators such as the crop water stress index (CWSI), canopy and air temperature differences, applied irrigation water, leaf water potential, and crop evapotranspiration (Otegui et al., 1995; Irmak et al., 2000; Katerji et al., 2004).

4.2.4. Objectives

The objective of this study were to determine if corn grain yield and cotton lint yield were correlated to an average seasonal stomatal conductance ratio (SCR). An averaging period that included the stages of growth sensitive to water stress in determination of yield also needed to be determined for both corn and

cotton. For the averaging periods that included multiple growth stages, this study also sought to determine if weighing factors applied to the growth stages would improve yield to SCR correlation.

4.3. Materials and Methods

4.3.1. Data collection

Weather stations were deployed over corn and cotton fields in the following locations: Corn: Sparta, IL, Lawrence, KS, Qulin, MO, Portland, IN, Rockwood, IL, North Platte, NE, Memphis TN; Cotton: Maricopa, AZ, Memphis, TN, and Qulin, MO. Each cotton location had a weather station setup on an irrigated and non-irrigated field trial. These stations made the required measurements to monitor crop water status by calculating canopy stomatal conductance. Each station was equipped with a datalogger (model CR1000, Campbell Scientific, Logan, UT), a pyranometer (Model SP-110, Apogee Instruments, Logan, UT), a relative humidity probe (Model CS215, Campbell Scientific, Logan, UT), two thermistors (Model ST-100, Apogee Instruments), a cup anemometer (Model Wind Sentry, RM Young Co., Traverse City, MI), and four infrared (IR) radiometers (Model SI-111 or SI-1H1, Apogee Instruments, Logan, UT). Four extendable poles were used as masts for IR sensor placement. The datalogger, anemometer, RH probe, pyranometer, and one of the thermistors were mounted on the "center" mast. The thermistor and RH probe were each placed in naturally ventilated louvered-radiation shields two meters above the crop canopy. The anemometer was also placed two meters above the crop canopy. The pyranometer was mounted at the top of the center

mast. The other thermistor was buried approximately 10 cm below the soil surface. Three of the infrared radiometers measured surface brightness temperature and each were placed on their own mast at an angle of 68 degrees (Models SI-111) or 72 degrees (SI-1H1) above nadir, at a height above canopy that allows the maximum view of the trial plot. The fourth infrared radiometer measured soil brightness temperature and was placed at an angle of 68 degrees above nadir and approximately 30 cm above the soil surface. A tipping bucket rain gauge (Model TE525WS, Campbell Scientific, Logan, UT) was installed at the edge of the crop fields to insure no obstructions from the crop for precipitation measurements.

Measurements of RH, air temperature, soil and canopy brightness temperature, wind speed, soil temperature at 10 cm, and incoming solar radiation were made every ten seconds and averaged over a 30-minute interval. The canopy height was measured at the time of setup and was periodically measured throughout the season. The growth stage of each crop was also periodically recorded over the season.

4.3.2. Experimental outline

The stomatal conductance ratio (SCR) was calculated as outlined in the introduction using data from six cotton and ten corn locations with the necessary modifications needed to account for sparse canopy coverage using the clumping index (Anderson et al., 2005).

4.3.3.   Calculating daily average stomatal conductance ratio

Daily averages of the stomatal conductance ratio (SCR) were calculated to summarize the water status of a crop over a season. These values were calculated as outlined in CHAPTER 1 using equations 1.3, 1.19, and 1.20. The 30-minute values were averaged for each day. This values are graphed with the standard deviation of these 30-minute values (Fig. 3-1).

Figure 4-1 is an example of how the stomatal conductance ratio is calculated using the calculated canopy stomatal conductance values and the reference canopy stomatal conductance values. This graph shows three days that vary in the solar intensity, with water being applied between the second and third day. The stomatal conductance ratio shows the crop at moderate water stress days two and three with an average daily SCR ratio at approximately 0.56 and 0.60 respectively. The decreased solar radiation of the second day decreases the water stress of the canopy. After the irrigation event the canopy is shown to have little water stress with an average SCR at 0.90.

4.3.4. Corn yield and SCR relationship

The corn life cycle was divided into five corn growth stage groups (V12 to V16, V16 to Tassel, R1, R2, R3) for pairing with associated weighting factors. The growth stage for each crop was calculated using growth degree days (GDD) and the relationship between GDD and growth stage published by South Dakota State University Extension (http://www.sdstate.edu/ps/extension/crop-mgmt/corn/upload/Corn-growth-stage-day-and-GDU-calendar10.pdf).

The relationship with growing degree days was originally developed for a 120-day hybrid. Using the maturity days for each site, the relationships between GDD and growth stage were adjusted for each cultivar.   Each day was assigned a growth stage and an associated weighting factor that was multiplied by the SCR index value calculated for that day. The weighted SCR values were averaged for each site from V12 to the Soft Dough stage to obtain a single value for each site to be paired with their corresponding grain yield. Weighting factors were developed from growth stage yield reduction percentages due to drought stress (Fig. 4-2) (Shaw, 1988; Rhoads and Bennett, 1990).

4.3.5. Cotton and yield SCR relationship

To determine the relationship between the stomatal conductance ratio (SCR) and cotton lint yield, the daily SCR values were averaged over the growth stage of flowering and boll development. This is a stage considered to be sensitive to drought stress and one of the few stages that measurements were taken over the majority of the stage for the studied cotton sites. No weighting factors were included as they were for corn due to only one growth stage being used.

It is important to point out that any correlation between yield and SCR assumes that yield is only impacted by drought stress. This is most likely not entirely true due to varying cultivation and management practices of each trial site. The linear regression and r^2 values for the corn and cotton relationship to yield was computed using SigmaPlot software.

4.4. Results and Discussion

4.4.1. Corn yield prediction from SCR

Corn yield for each of the 10 sites studied was graphed with the seasonal averaged SCR values calculated as described above (Fig. 4-3). The SCR vs yield data point for the Qulin, MO site was considered to be an outlier as it varied greatly from the majority of the data set and was not included in the calculation of the coefficient of determination (r^2). The resulting r^2 values were 0.79 using the literature based weighting factors and 0.72 with no weighting factors used in the calculation of a seasonal average SCR.

The resulting r^2 values strongly suggest that the SCR values can be used to predict corn grain yield. The higher r^2 values resulting from the weighted SCR values indicate that corn yield was affected by water stress differently for each growth period. Further research should be done to determine how well each growth stage used could predict grain yield independently. It could be possible to determine from this and further research, on SCR and yield potential, threshold values of the SCR to obtain the best yields given a determined allotment of water for the season. Water could be strategically applied at different rates for each growth stage to maximize yield.

4.4.2. Cotton yield prediction from SCR

Cotton yield for each of the 6 sites studied was graphed with the seasonal averaged SCR values calculated as described above (Fig. 4-4). The SCR vs yield data point for the irrigated Maricopa, AZ site was considered to be an outlier as it varied greatly from the majority of the data set. The SCR values calculated

for this site did not span the growth stage used to calculate an averaged SCR value to compare with yield. This may have been the reason for it being an outlier. Two coefficients of determination (r^2) values were determined, one with and the other without the outlier. The resulting r^2 values were 0.18 when included the determined outlier and 0.96 with it excluded.

The results indicate that the yield obtained for the irrigated Maricopa site was most likely affected by other factors other than water stress. Unfortunately no reason has been found to explain the significant decrease in yield from where it is predicted to be by the regression lined obtained from the other five sites.

When the yield data form the irrigated Maricopa site is excluded the seasonal average SCR shows a very strong correlation to cotton lint yield. This result suggests that for these five sites water stress was the major factor in determining yield.

4.5. Conclusions

The results indicate that the stomatal conductance ratio (SCR) can be used to predict corn and cotton yields and that developing a threshold for daily SCR values may be a good practice to maximize crop yield. More data points are needed to provide further confidence in the prediction relationship between SCR and crop yield from the results provided in this study.

The literature based weighing factors for the five corn growth stages resulted in a better correlation between the SCR and yield than the non-weighted SCR values. This indicates that as predicted by the literature based weighing factors, the reproductive growth stages (R1, R2, and R3) were the most sensitive

to water stress in determining yield. The high correlation with the single growth stage of cotton indicates that other growth stages are not as sensitive to water stress.

The results found in this study can be beneficial to growers who have restrictions on the amount of water they can apply over the season. These results, and further studies, can help growers determine how much water to apply to each growth stage to maximize yield.

4.6. References

Anderson, M.C., Norman, J.M., Kustas, W.P., Li, F.Q., Prueger, J.H., Mecikalski, J.R., 2005. Effects of vegetation clumping on two-source model estimates of surface energy fluxes from an agricultural landscape during SMACEX. Journal of Hydrometeorology 6, 892-909.

Cornish, K., Radin, J.W., Turcotte, E.L., Lu, Z.M., Zeiger, E., 1991. Enhanced Photosynthesis and Stomatal Conductance of Pima Cotton (Gossypium-Barbadense L) Bred for Increased Yield. Plant Physiology 97, 484-489.

Earl, H.J., Davis, R.F., 2003. Effect of drought stress on leaf and whole canopy radiation use efficiency and yield of maize. Agronomy Journal 95, 688-696.

Fischer, R.A., Rees, D., Sayre, K.D., Lu, Z.M., Condon, A.G., Saavedra, A.L., 1998. Wheat yield progress associated with higher stomatal conductance and photosynthetic rate, and cooler canopies. Crop Science 38, 1467-1475.

Gerik, T.J., Faver, K.L., Thaxton, P.M., ElZik, K.M., 1996. Late season water stress in cotton .1. Plant growth, water use, and yield. Crop Science 36, 914-921.

Irmak, S., Haman, D.Z., Bastug, R., 2000. Determination of crop water stress index for irrigation timing and yield estimation of corn. Agronomy Journal 92, 1221-1227.

Katerji, N., van Hoorn, J.W., Hamdy, A., Mastrorilli, M., 2004. Comparison of corn yield response to plant water stress caused by salinity and by drought. Agricultural Water Management 65, 95-101.

Lu, Z.M., Percy, R.G., Qualset, C.O., Zeiger, E., 1998. Stomatal conductance predicts yields in irrigated Pima cotton and bread wheat grown at high temperatures. Journal of Experimental Botany 49, 453-460.

Otegui, M.E., Andrade, F.H., Suero, E.E., 1995. Growth, Water-Use, and Kernel Abortion of Maize Subjected to Drought at Silking. Field Crops Research 40, 87-94.

Rhoads, F.M., Bennett, J.M., 1990. Corn. In: B.A. Stewart and D.R. Nielsen (Editors), Irrigation of agricultural crops. ASA, CSSA, and SSSA, Madison, WI, pp. 569-596.

Shaw, R.H., 1988. Climate Requirement. Corn and Corn Improvement agronomymonogra, 609-638.
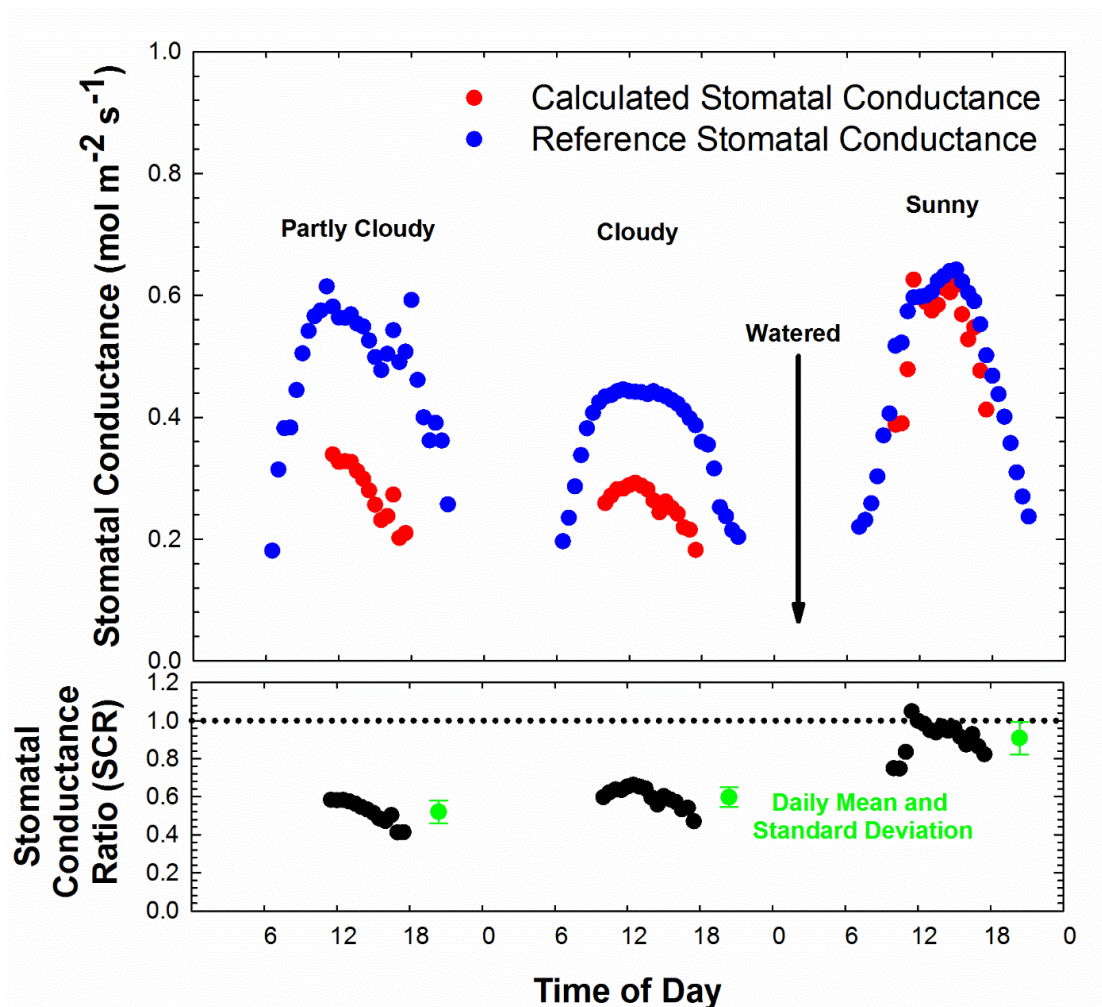
Fig. 4-1: Calculated 30-minute stomatal conductance ratio (SCR) values. The SCR is a ratio of the measured actual stomatal conductance to the reference stomatal conductance. The daily average is shown with error bars representing the standard deviation of each of the 30-minute SCR values.
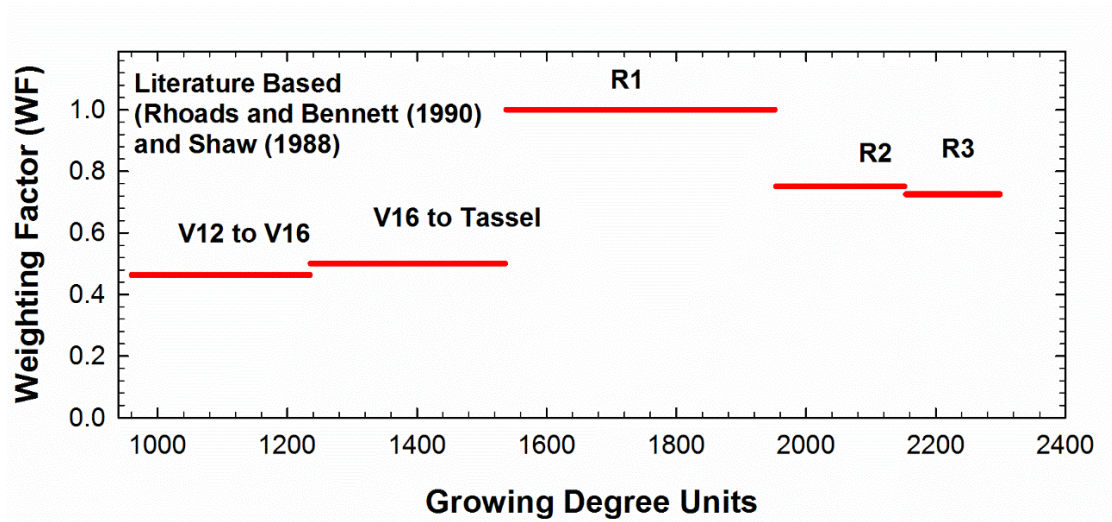
Fig. 4-2: Literature based weighting factors relating sensitivity of corn yield to drought stress for the most sensitive growth stages.
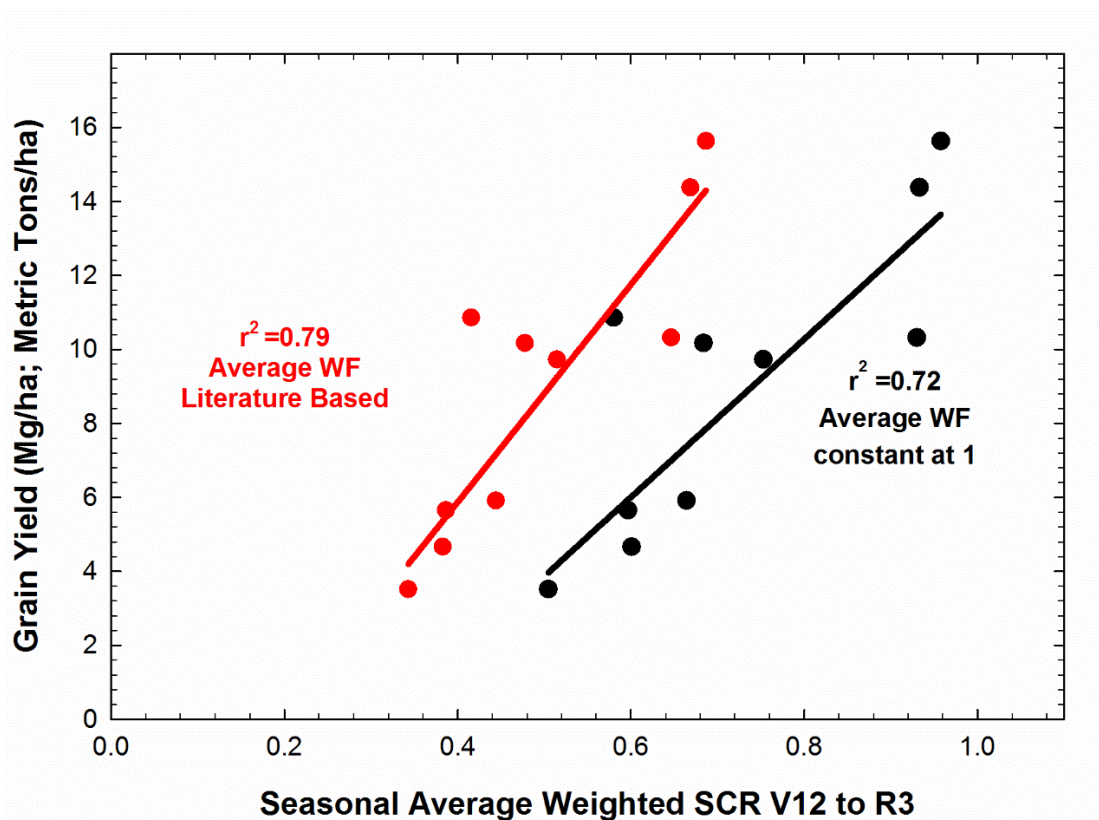
Fig. 4-3: Seasonal average stomatal conductance ratios (SCR) vs corn grain yield. Weighting factors based on growth stage sensitivity to drought stress on grain yield were resulted in an r^2 value of 0.79 and using no weighting factors resulted in an r^2 value of 0.72.
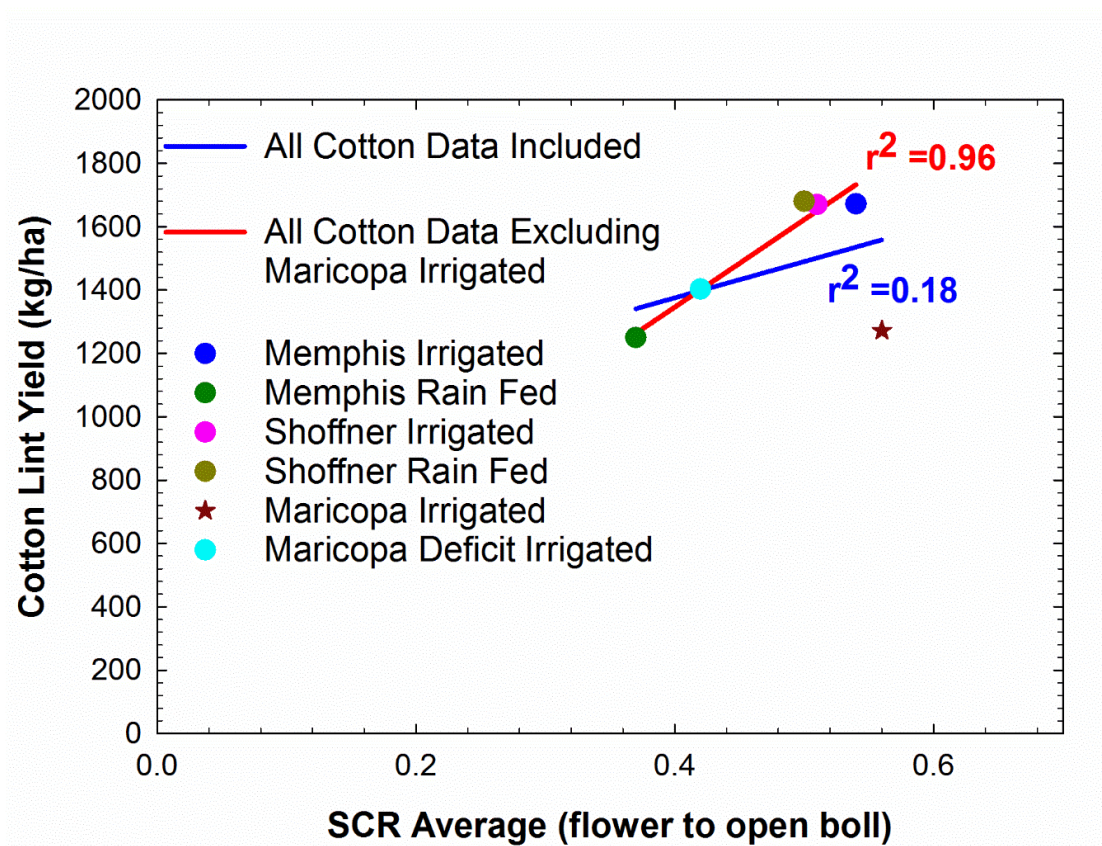
Fig. 4-4: Seasonal average stomatal conductance ratios (SCR) vs cotton lint yield. Seasonal SCR yields vs cotton lint yield resulted in an r^2 value of 0.18 when including a determined outlier (Maricopa Irrigated) and 0.96 when it was excluded from the analysis.

CHAPTER 5

SUMMARY and CONCLUSIONS

The research summarized in this dissertation sought to improve a method using calculations of actual and potential stomatal conductance to detect crop water stress of corn and cotton crops.

Three research studies were reported here: 1) Methods to derive canopy temperature from a composite soil and canopy temperature, and the effects on stomatal conductance calculation; 2) An examination of the effects of implementing a clumping index to a two-source energy balance model; 3) The correlation between a seasonal average stomatal conductance ratio and crop yield.

1) Less erratic and better behaves stomatal conductance values were obtained using canopy temperatures derived from the Priestley-Taylor approximation. Canopy temperature derived using measured soil temperature resulted in stomatal conductance values that did not behave as expected for 30-minute daily values or for daily averaged values over the season. Calculated daily stomatal conductance ratios reacted as expected to irrigation/precipitation events and dry down periods when using Priestley-Taylor derived canopy temperature.

2) Incorporating the clumping index into the radiation divergence algorithms resulted in lower total net radiation values within the canopy when canopy coverage was incomplete. The clumping index had no effect on calculated net radiation values when the canopy was fully closed. Stomatal

conductance ratio values were less erratic in their behavior over the day and season when the clumping index was incorporated into the radiation divergence algorithms.

3) A strong correlation was found between stomatal conductance ratios (SCR) and corn and cotton yields when omitting determined outliers. Coefficient of determination values (r^2) as high as 0.82 for corn and 0.87 for cotton were observed. More data points are needed to provide further confidence in the prediction relationship between SCR and crop yield from the results provided in this study.

The results from the studies in this dissertation suggest that the modifications suggested for calculation of canopy stomatal conductance will give more accurate estimates of crop water status by means of canopy stomatal conductance. To incorporate the modifications crop row spacing and crop width are needed, which should be easily obtained.

Canopy stomatal conductance is strongly related to plant water status and stomatal aperture, which influences crop yield. The calculation of canopy stomatal conductance with the included modifications studied in CHAPTER 2 and CHAPTER 3 has the potential to supplement and improve existing transpiration and evapotranspiration models. Many models use empirically calculated or constant values of stomatal conductance. Calculations of actual stomatal conductance can replace these values to improve estimations of transpiration and evapotranspiration.

Calculation of an actual stomatal conductance compared to a reference value can provide indication crop water status. Better estimates of canopy stomatal conductance with the modifications suggested in this dissertation can improve irrigation scheduling and application. With improved accuracy of crop water status indication, water can be more efficiently used.

No direct measurements of canopy or leaf stomatal conductance were available for any of the sites used in this study. This makes it difficult to validate the daily and seasonal corn and cotton canopy stomatal conductance values calculated. Due to this limitation we determined which approach led to better estimates of canopy stomatal conductance by observing the behavior of the calculated values. Stomatal conductance values were assessed on their response to irrigation/precipitation events, expected daily and seasonal behavior, and the variability throughout the day.

Leaf stomatal conductance measurements made with a leaf porometer are the most commonly made measurements of stomatal conductance in the field. For comparison to the calculated canopy stomatal conductance values made in this study, leaf stomatal conductance measurements would need to be scaled up. There is error and uncertainty associated with the multiple methods used to scale up leaf to canopy stomatal conductance. Even if 30-minute or once-a-day leaf stomatal conductance measurements were made, which would be labor and time intensive, there is no certainty that these values would be the best reference. They could however provide a good relative indication of the expected daily and seasonal trends.

APPENDICES

APPENDIX A

UTAH STATE UNIVERSITY

ENVIRONMENTAL OBSERVATORY PROGRAM

```
'Weather Station
'CR3000 Series Data- logger
'Date: Nov. 3, 2010
'Final Version: July 1, 2014
'Program Author: Chris Parry


SequentialMode                          'may change this if skipped scans occur

PreserveVariables         'retain in memory the values for variables declared by the Dim or
Public statements.

'CH200 Public Variables

Public Check_sum                        'Holds the check sum value of the received CH200
string.
Public xmit_str As String                'Used to catch clutter from the CH200
Public CH200string As String * 140  'Holds the entire status string coming from
theCH200.
Public SDI12command As String            'Used to send 'enclosuretemp' to CH200
Public SDI12result As String        'Result verifying sending of 'SDI12command'
Public totalampusage                    'Daily amps use by entire system as
measured by the CH200
Public totalincomingamp             'Daily incoming amps as measured by the CH200


'Display Public Variables

Public DispError                    'Holds the results of the communication attempt for
display
Public avgserialtemp                'Running average of ambient air temperature for
display
Public serialtemp As Float          'Temperature output to display
Public brightness As Float          'Brightness level of display
Public displaydelay As Float        'Determines delay on display
Units avgserialtemp = °C
Units serialtemp= °C


'Visibility Public Variables

Public visibilitym,visibilitykm
Public OutString As String * 40          'Outgoing Visibility string
Dim CheckVal As Long                     'Checksum value of Visibility Sensor
Public InString As String * 200          'Incoming string Visibility Sensor
Public instringset As String *200
Public CS120NmbrBytes
Public visset As Boolean        'Flag to that sends new command to visibility sensor to turn
dew heaters on or off
Public CS120_Array(19) As String * 20        ' CS120 Return Array
```

```
Public SETCS120_Array(20) As String * 6 'CS120 Command Array
Public StatusDewHeater As Boolean
Public SETCS120Parameters As Boolean


'CS120 Array sent back to logger at 'POLL'

Alias CS120_Array(1)=Message_ID
Alias CS120_Array(2)=Unit_ID
Alias CS120_Array(3)=System_Status
Alias CS120_Array(4)=Interval_Time
Alias CS120_Array(5)=Visibilty_Distance
Alias CS120_Array(6)=Visibility_Units
Alias CS120_Array(7)=Average_Duration
Alias CS120_Array(8)=User_Alarm_1
Alias CS120_Array(9)=User_Alarm_2
Alias CS120_Array(10)=Emitter_Failure
Alias CS120_Array(11)=Emitter_Lens_Dirty
Alias CS120_Array(12)=Emitter_Temperature
Alias CS120_Array(13)=Detector_Lens_Dirty
Alias CS120_Array(14)=Detector_Temperature
Alias CS120_Array(15)=Detector_DC_Saturation_Level
Alias CS120_Array(16)=Hood_Temperature
Alias CS120_Array(17)=Signature_Error
Alias CS120_Array(18)=Flash_Read_Error
Alias CS120_Array(19)=Flash_Write_Error


Public countervisibility        'Counter that adds delay to initial measurement of Visibility
sensor once program in reset
Public visibilitypower As Boolean     'Flag turning on or off visibility sensor measurement


'Time stamps

Public maxtemptime As String *22
Public mintemptime As String *22
Public maxwindtime As String *22


'Relative Humidity

Public RHbox                    'Relative Humidity of Enclosure (%)
Public RH                       'Relative Humidity of Ambient Air (%)
Public RHtemp                        'Ambient Air temperature made with
humidity sensor (HMP110)
Units RHbox = %
Units RH= %
Units RHtemp = C
```

'Yesterday *Public* variables

Public yesterdayprecip
Public yesterdayet
Public yesterdaymaxtemp
Public yesterdaymintemp
Public yesterdayavgtemp
Public yesterdaymaxwind
Units yesterdaymaxtemp = °C
Units yesterdaymintemp = °C
Units yesterdayavgtemp = °C
Units yesterdaymaxwind = m/s
Units yesterdayet= mm/day
Units yesterdayprecip =mm/day

'*Const*ants

Const s = 0.000000056704   'Stefan-Boltzmann *Const*ant
Const scanrate =1   'Main scanrate
Const scanrateslow=10   'Scan rate for slow sequence
measurements
Const slow2scanrate =30   'Scan rate for "slow2" sub
Const solarsetpoint1=300   'Set point in determining power conservation
Const solarsetpoint2=15   'Set point in determining power conservation
Const wattstoMJ=.000001   'conversion of Watts to Mega Joules
Const zero=0   'needed to graph a reference line in RTMC

'Radiation Variables

Public ppftotal 'intermediate variable for ppfdaytotal
Public ppfdaytotal
Public mjswihour   'intermediate variable for mjswihourtotal
Public mjswihourtotal
Public swipaneltoswi 'Ratio of incoming solar radiation at panel to solar radiation
measured by upward Pyranometer
Units ppfdaytotal =µmol/day
Units mjswihourtotal =MJ/hr
Units mjswihour =MJ
Units ppftotal = umol

'*Public* Variables for Fan

Public fanspeed   'Determines duty cycle for PWM of fan
Public fan_frequency   'Speed of the fan

'Array to hold extended data from the PS200/CH200

```
Public CH200_MX(4)
Alias CH200_MX(1) = BattTargV      'Battery charging target voltage.
Alias CH200_MX(2) = DgtlPotSet     'Digital potentiometer setting.
Alias CH200_MX(3) = BattCap        'Present battery capacity.
Alias CH200_MX(4) = Qloss          'Battery charge deficit.


'Array to hold all the data coming from the CH200

Public CH200_M0(9), Panelwatts, batterywatts, loadwatts, netamp
Alias CH200_M0(1)=VBatt            'Battery voltage: VDC
Alias CH200_M0(2)=IBatt            'Current going into, or out of, the battery: Amps
Alias CH200_M0(3)=ILoad            'Current going to the load: Amps
Alias CH200_M0(4)=V_in_chg         'Voltage coming into the charger: VDC
Alias CH200_M0(5)=I_in_chg         'Current coming into the charger: Amps
Alias CH200_M0(6)=Chg_TmpC         'Charger temperature: Celsius
Alias CH200_M0(7)=Chg_State        'Charging state: Cycle, Float, Current
Limited, or None
Alias CH200_M0(8)=Chg_Source       'Charging source: None, AC, or Solar
Alias CH200_M0(9)=Ck_Batt          'Check battery error: 0=normal, 1=check
battery


'Arrays to hold the associated words for the charge state, charge source, and check
battery values.

Dim ChargeStateArr(6) As String
Dim ChargeSourceArr(3) As String
Dim CheckBatteryArr(2) As String


'Variables to hold the words for charge state, charge source, and check battery.

Public ChargeState As String
Public ChargeSource As String
Public CheckBattery As String


'Temperature Sensors

Public Temp109(4)                  '109 Thermistors
Public Temp109f(4)
Public dewpnt                      'Dew point temperature
Public runavgtemp109(4)            'Temperature running average
Public windchillC
Public heatindexC
Public ybdif                       'Difference between yellow bead thermistors from
passive and aspirated shields
Public maxtemp                     'Holds maximum temperature for the day
Public mintemp                     'Holds minimum temperature for the day
```

```
Alias Temp109(2)= GillYellobead
Alias Temp109(4)= AspiratedYellobead
Alias runavgtemp109(2)= runavgGillYellobead
Alias runavgtemp109(4)= runavgAspiratedYellobead
Alias Temp109f(4)= AspiratedYellobeadF
Units GillYellobead=°C
Units AspiratedYellobead=°C
Units dewpnt= °C
```

'Public variables for meteorological calculations

'VPD

```
Public vpda, vpdc
```

'Barometric Temperature

```
Public Vaisalatemporary, pressure, pressureinhg, pressurekpasealevel,
pressureinhgsealevel, pressurerunavg
```

'Co2

```
Public Co2 As String *25, runavgco2, runavgco2long,
Public returnA As String * 25, NBytesReturned, co2string(3), co2temperaturecorrected

Alias co2string(1)=vaisalacorrectedco2
Alias co2string(2)=rawco2
Alias co2string(3)=gastemp
```

```
Public eqt                    'equation of time
Public daylight                         'factor to account for daylight savings time (1 =
daylight savings, 0 = standard time)
Public SolarN              'time of solar noon
Public hrangle                        'Hour angle
Public SolarE           'Solar elevation angle
Public SolarZ           'Solar zenith angle
Public SWa              'Extraterrestrial radiation
Public w                'Precipitable water in the atmosphere
Public kb               'Clearness index for direct beam radiation
Public kd               'Transmissivity index for diffuse radiation
Public SWic             'Clear sky solar radiation
Public SWratio                   'Ratio of incoming solar radiation to clear sky
Public fc               'Cloudiness factor
Public Tbsky            'Sky brightness temperature in the 8-14 um waveband
Public eclear           'Clear sky emissivity
Public ecloudy                   'Cloudy sky emissivity
```

```
Public esky                    'Effective sky emissivity
Public pb                      'Barometric pressure
Public ea                      'Vapor pressure of the air
Public esa                     'Saturation vapor pressure of the air
Public skytemp                     'Sky temperature as calculated from pyrgeometer
Public groundtemp              'Surface temperature as calculated from pyrgeometer
Public Eta, etb, etc, et48, et72      'ET values
Public evapotranspiration, Ro,evapotranspirationdaytotal, etflag As Boolean
Public esc                     'Surface saturation vapor pressure
Public deltat                  'Difference between surface temperature and ambient air
Dim Latr                       'Latitude in radians
Dim dr                         'Inverse relative distance factor for the distance between
the Earth and sun
Dim de                             'Solar declination
Dim j                          'Used in calculation of equation of time

Const Elev = 1458
Const Lat = 41.735
Const Lon = 111.833
Const Lontz = 105.65       'Time Zone Longitude
Const pi = 3.141592654
Const SolarC = 1367.8          'Solar
Const P0 = 101.325         'Standard barometric pressure
Const kt = 1.0             'Atmospheric turbidity coefficient
Const g = 9.80665          'Acceleration of gravity
Public RTime(9)
Alias RTime(1) = Year
Alias RTime(2) = Month
Alias RTime(3) = DayMonth
Alias RTime(4) = Hour
Alias RTime(5) = Minute
Alias RTime(6) = Second
Alias RTime(7) = Microsecond
Alias RTime(8) = Weekday
Alias RTime(9) = DOY

'Datalogger Status

Public PTemp               'Datalogger panel temperature
Public batt_volt           'Voltage going into the datalogger as measured by the
datalogger
Units PTemp= °C
Units batt_volt=Volts

'Incoming Solar Radiation Apogee Pyranometer

Public SWi                 'Incoming solar radiation
Public SWMJi               'Incoming Mega joule power from sun
```

```
Public mjtot                  'Cumulative of incoming Mega Joules
Public mjdaytot               'Day total of Mega joules
Public solarpanelswi          'Incident solar radiation measure at the solar panel
Public solarpaneleff          'Efficiency of the solar panel
Public solarpanelmj           'Incoming Mega joules measured at the solar panel
Units SWi= Watts m-2
Units SWMJi= Mega Joules m-2
Units mjtot = Mega Joules m-2
Units mjdaytot = Mega Joules m-2
Units solarpanelswi = Watts m-2
Units solarpaneleff= %


'UV and Quantum sensor

Public PPF                    'Photosynthetic radiation
Public UV                     'Ultraviolet radiation
Units PPF = umol m-2 s-1
Units UV = umol m-2 s-1



'Wind Measurements

Public WScup_ms, WindDirvane 'Wind Speed and Direction
Public windsonic(4), windsonicavgrun
Alias windsonic(1) = wind_direction
Alias windsonic(2) = wind_speed
Alias windsonic(3) = diag
Alias windsonic(4) = nmbr_bytes_rtrnd
Public winddirection As String
Units wind_direction =  °
Units wind_speed = m s-1

Dim in_bytes_str As String * 21
Dim checksum_flg As Boolean
Dim disable_flg As Boolean
Dim n, x, y , dummy
Units n = samples

Public windgust              'Maximum wind speed in one minute interval
Public  maxwind              'Max wind speed for the day
Public windspeedmph                'Sonic anemometer wind speed measurement in
MPH for USU AP
Public enclosuretemp
'Temperature inside battery enclosure

Units windgust= m s-1
Units maxwind =m s-1
Units windspeedmph =MPH
Units enclosuretemp= °C
```

'Infrared Radiometer variables

'SBTempC = infrared sensor body temperature [C]
'SBTempK = infrared sensor body temperature [K]
'TargmV = voltage output of sensor target detector [mV]
'TargTempK1 = targettemperature [K]
'TargTempC1 = targettemperature [C]
Public SBTempC1, SBTempK1, TargmV1, m1, b1, TargTempK1, TargTempC1
Public SBTempC2, SBTempK2, TargmV2, m2, b2, TargTempK2, TargTempC2,
Public irttargtempdif, TargTempC1avg, TargTempC2avg,

'Calibration Coefficients for SI-111 Infrared Radiometers

'mC2 = 2nd order polynomial coefficient used to calculate m (slope) based on sensor body temperature
'mC1 = 2nd order polynomial coefficient used to calculate m (slope) based on sensor body temperature
'mC0 = 2nd order polynomial coefficient used to calculate m (slope) based on sensor body temperature
'bC2 = 2nd order polynomial coefficient used to calculate b (intercept) based on sensor body temperature
'bC1 = 2nd order polynomial coefficient used to calculate b (intercept) based on sensor body temperature
'bC0 = 2nd order polynomial coefficient used to calculate b (intercept) based on sensor body temperature

'Coefficients for Infrared Radiometer Serial # 2846

Const mC2_1 = 71646.6
Const mC1_1 = 7836350
Const mC0_1 = 1290120000
Const bC2_1 = 21243.7
Const bC1_1 = -118088
Const bC0_1 = 4394980

'Coefficients for Infrared Radiometer Serial # 2810

Const mC2_2 = 65432.4
Const mC1_2 = 8375840
Const mC0_2 = 1411120000
Const bC2_2 = 28071.7
Const bC1_2 = -240833
Const bC0_2 = 3746380

'Storage Variables

Public storageFile As Long

Public errorCode   *'Error code for storage variables*

'Precipitation

Public P   *'Current rainfall measurement*
Public raintotal   *'Cumulative rainfall*
Public raintotalinch   *'Total precipitation inch*
Public rain5mintotal   *'Total rainfall in past 5 minutes*
Public rainrate   *'Tate of rainfall over 5 minute period*
Units P=mm
Units raintotal=mm
Units raintotalinch= inch
Units rain5mintotal= mm
Units rainrate= mm/Minute

'Leaf Wetness Sensors

Public lws(4),LWSDEPTH(4),lwsraw(4)
Units LWSDEPTH=mm

'Net Radiometer Measurements

Public SWUp   *'Incoming shortwave radiation measured by net radiometer*
Public SWDn   *'Reflected shortwave radiation measured by net radiometer*
Public LWUp   *'Incoming sky long wave radiation measured by net radiometer*
Public LWDn   *'Outgoing surface long wave radiation measured by net radiometer*
Public NR01TC   *'Temperature of net radiometer*
Public NR01TK   *'Temperature of net radiometer*
Public NetRSW   *'Net Shortwave radiation measured by net radiometer*
Public NetRLW   *'Net Longwave radiation measured by net radiometer*
Public Albedo   *'Calculated albedo of the surface*
Public UpTot   *'Total incoming solar and emitted longwave radiation from sky*
Public DnTot   *'Total reflected shortwave and emitted longwave radiation from surface*
Public NetTot   *'Net total radiation measured by net radiometer*
Public LWUPRaw   *'Raw longwave radiation from sky not accounting for sensor body temperature*
Public LWDNraw   *'Raw longwave radiation from surface not accounting for sensor body temperature*
Units SWUp=w/m2
Units SWDn=w/m2
Units LWUPRaw=w/m2
Units LWDNraw=w/m2

Units NR01TC= °C
Units NR01TK=k
Units NetRSW=w/m2
Units NetRLW=w/m2
Units Albedo=w/m2
Units UpTot=w/m2
Units DnTot=w/m2
Units NetTot=w/m2
Units LWUp=w/m2
Units LWDn=w/m2

Const SWUpcal = 1000/15.7 *'Calibration Coefficient for Net Radiometer*
Const SWDowncal = 1000/16.3   *'Calibration Coefficient for Net Radiometer*
Const LWUpcal = 1000/9   *'Calibration Coefficient for Net Radiometer*
Const LWDowncal =1000/8.9   *'Calibration Coefficient for Net Radiometer*

'Misc Variables

Public CO2Load,displayload, fanload, CO2Loadrunavg, displayloadrunavg,
fanloadrunavg   *'Sensor*
current loads and averages
Public Finaltrigger

DataTable (wind1,True,1000)

  DataInterval (0,1,Sec,10)

  Sample (1,windsonic(2),FP2)
  Sample (1,windsonic(1),FP2)
  Sample (1,windsonic(3),FP2)
  Sample (1,windsonic(4),FP2)
EndTable

DataTable (Final,Finaltrigger,-1)

  DataInterval (0,scanrateslow,Sec,10)

  Minimum (1,batt_volt,IEEE4,0,False)
  Sample (1,Temp109(2),FP2)
  Sample (1,Temp109(4),FP2)
  Sample (1,RHtemp,FP2)
  Sample(1,RH,FP2)
  Sample (1,enclosuretemp,IEEE4)
  Sample(1, mintemp,IEEE4)
  Sample(1,maxtemp,IEEE4)
  Sample(1,mintemptime,String)
  Sample(1, maxtemptime,String)
  Average (1,windchillC,FP2,False)
  Average(1,heatindexC,FP2,false)
  Sample (1,ybdif,FP2)

Minimum (1,Temp109(2),FP2,Temp109()=NAN,true)
Minimum (1,Temp109(4),FP2,Temp109()=NAN,true)

'Co2

Sample (1,Co2,String)
Sample (1,runavgco2,FP2)
Sample (3,co2string(),FP2)

'Precipitation

Sample (1,lws(1),FP2)
Sample (1,lws(2),FP2)
Sample (1,LWSDEPTH(1),FP2)
Sample (1,LWSDEPTH(2),FP2)
Sample (1,lwsraw(1),FP2)
Sample (1,lwsraw(2),FP2)
Sample (1,lws(3),FP2)
Sample (1,lws(4),FP2)
Sample (1,LWSDEPTH(3),FP2)
Sample (1,LWSDEPTH(4),FP2)
Sample (1,lwsraw(3),FP2)
Sample (1,lwsraw(4),FP2)
Sample (1,raintotal,FP2)
Sample (1,raintotalinch,FP2)
Sample (1,rain5mintotal,FP2)
Sample (1,rainrate,FP2)

'Pressure

Sample (1,pressure,IEEE4)
Sample (1,pressurekpasealevel,IEEE4)

'Power

Sample (6,CH200_M0(),FP2)
Sample (1,Panelwatts,fp2)
Sample (1,batterywatts,fp2)
Sample (1,loadwatts,fp2)
Sample (1,totalampusage,fp2)
Sample (1,totalincomingamp,fp2)
Sample (1,netamp,fp2)
Sample (1,solarpanelmj,fp2)
Sample (1,CheckBattery,String)
Sample (1,ChargeState,String)
Sample (1,BattTargV,FP2)
Sample (1,Qloss,FP2)
Sample (1,CO2Load,FP2)

```
Sample (1,displayload,FP2)
Sample (1,fanload,FP2)
```

'wind

```
Sample (1,wind_direction,FP2)
Sample (1,maxwind,FP2)
Sample (1,wind_speed,FP2)
Maximum (1,windsonic(2),FP2,windsonic(2)=NAN,True)
FieldNames ("finalmaxwind")
Sample (1,maxwindtime,String)
Sample (1,WScup_ms,FP2)
```

'Net Radiation

```
Sample (1,SWDn,FP2)
Sample (1,SWUp,FP2)
Sample (1,LWUp,FP2)
Sample (1,LWDn,FP2)
Sample (1,NetTot,FP2)
Sample (1,NetRSW,FP2)
Sample (1,NetRLW,FP2)
Sample (1,NR01TC,fp2)
Sample (1,solarpanelswi,FP2)
Sample (1,SWic,FP2)
Sample (1,SWi,FP2)
Sample (1,dewpnt,FP2)
Sample (1,TargTempC1,FP2)
Sample (1,TargTempC2,FP2)
Sample (1,PPF,FP2)
Sample (1,UV,FP2)
Sample (1,mjtot,FP2)
Sample (1,ppftotal,FP2)
Sample (1,ppfdaytotal,FP2)
Sample (1,Albedo,FP2)
Sample (1,groundtemp,FP2)
Sample (1,skytemp,FP2)
```

'Visibility

```
Sample (1,visibilitykm,FP2)
```

'misc

```
Sample (1,zero,ieee4)
Average (1,fc,FP2,False)
Sample (1,solarpaneleff,ieee4)
Sample (1,evapotranspiration,FP2)
Sample (1,Ro,FP2)
```

```
Sample (1,evapotranspirationdaytotal,FP2)
Sample (1,swipaneltoswi,fp2)
Sample (1,deltat,ieee4)
Sample (1,vpda,ieee4)
Sample (1,vpdc,ieee4)
Sample (1,fan_frequency,IEEE4)
Average (1,NR01TC,FP2,False)
Sample (1,fanspeed,FP2)
Sample (1,brightness,FP2)
Sample (1,displaydelay,FP2)
```

'yesterdays data

```
Sample (1,yesterdayet,IEEE4)
Sample (1,yesterdayprecip,IEEE4)
Sample (1,yesterdaymaxwind,IEEE4)
Sample (1,yesterdaymaxtemp,IEEE4)
Sample (1,yesterdaymintemp,IEEE4)
Sample (1,et48,ieee4)
Sample (1,et72,ieee4)
Sample (1,yesterdayavgtemp,ieee4)
EndTable

DataTable (ClimateCtrDaily,Finaltrigger,-1)

 Average (1,AspiratedYellobead,FP2,False)
 Maximum (1,AspiratedYellobead,FP2,False,True)
 Minimum (1,AspiratedYellobead,FP2,False,True)
 Average (1,ea,FP2,False)              ' Vapor Pressure
 Maximum (1,RH,FP2,False,True)
 Minimum (1,RH,FP2,False,True)
 Average (1,dewpnt,FP2,False)
 Maximum (1,dewpnt,FP2,False,True)
 Minimum (1,dewpnt,FP2,False,True)
 Totalize (1,SWMJi,FP2,False)
 Totalize (1,NetTot,FP2,False)
 Average (1,PPF,FP2,False)
 Average (1,SWUp,FP2,False)
 Average (1,SWDn,FP2,False)
 Average (1,LWUp,FP2,False)
 Average (1,LWDn,FP2,False)
 WindVector (1,wind_speed,wind_direction,FP2,False,360,0,0)
 FieldNames ("WS_ms,WindD,WindD_SD")
 Average (1,pressure,FP2,False)
 Average (1,pressurekpasealevel,FP2,false)
 Average (1,runavgco2,FP2,False)
 Average (1,vaisalacorrectedco2,FP2,False)
 Average (1,TargTempC1,FP2,False)
```

```
  Average (1,TargTempC2,FP2,False)
  Average (1,visibilitykm,FP2,False)
  Histogram (lwsraw(1),IEEE4,False,1,011,.2777999,274,9999999)
  FieldNames ("LWS1_pct_wet")
  Histogram (lwsraw(2),IEEE4,False,1,011,.2777999,274,9999999)
  FieldNames ("LWS2_pct_wet")
  Histogram (lwsraw(3),IEEE4,False,1,011,.2777999,274,9999999)
  FieldNames ("LWS3_pct_wet")
  Histogram (lwsraw(4),IEEE4,False,1,011,.2777999,274,9999999)
  FieldNames ("LWS4_pct_wet")
  Totalize (1,P,FP2,False)
  Totalize (1,evapotranspiration,IEEE4,False)
EndTable

DataTable (ClimateCTRHourly,True,-1)

  DataInterval (0,60,Min,10)
  Average (1,AspiratedYellobead,FP2,False)
  Maximum (1,AspiratedYellobead,FP2,False,False)
  Minimum (1,AspiratedYellobead,FP2,False,False)
  Average (1,ea,FP2,False)
  Maximum (1,RH,FP2,False,False)
  Minimum (1,RH,FP2,False,False)
  Average (1,dewpnt,FP2,False)
  Maximum (1,dewpnt,FP2,False,False)
  Minimum (1,dewpnt,FP2,False,False)
  Totalize (1,SWMJi,FP2,False)
  Totalize (1,NetTot,FP2,False)
  Average (1,PPF,FP2,False)
  Average (1,SWUp,FP2,False)
  Average (1,SWDn,FP2,False)
  Average (1,LWUp,FP2,False)
  Average (1,LWDn,FP2,False)
  WindVector (1,wind_speed,wind_direction,FP2,False,360,0,0)
  FieldNames ("wind_speed,WindD,WindD_SD")
  Maximum (1,wind_speed,FP2,False,False)
  Sample (1,pressure,FP2)
  Sample (1,pressurekpasealevel,FP2)
  Average (1,runavgco2,FP2,False)
  Average (1,vaisalacorrectedco2,FP2,False)
  Average (1,TargTempC1,FP2,False)
  Average (1,TargTempC2,FP2,False)
  Sample (1,visibilitykm,FP2)
  Average (1,visibilitykm,FP2,False)
  Histogram (lwsraw(1),IEEE4,False,1,011,.2777999,274,9999999)
  FieldNames ("LWS1_pct_wet")
  Histogram (lwsraw(2),IEEE4,False,1,011,.2777999,274,9999999)
  FieldNames ("LWS2_pct_wet")
```

```
  Histogram (lwsraw(3),IEEE4,False,1,011,.2777999,274,9999999)
  FieldNames ("LWS3_pct_wet")
  Histogram (lwsraw(4),IEEE4,False,1,011,.2777999,274,9999999)
  FieldNames ("LWS4_pct_wet")
  Totalize (1,P,FP2,False)
  Sample (1,evapotranspiration,IEEE4)
EndTable

DataTable (Finalxml,1,-1)                'Table used for USU APP

  DataInterval (0,scanrateslow,Sec,10)
  Sample (1,AspiratedYellobeadF,FP2)
  Sample (1,RH,FP2)
  'Precipitation
  Sample (1,raintotalinch,FP2)
  'Pressure
  Sample (1,pressureinhg,IEEE4)
  'wind
  Sample (1,wind_speed,FP2)
EndTable

DataTable (onemintable,1,-1)

  DataInterval (0,60,Sec,10)
  Maximum (1,windsonic(2),IEEE4,windsonic(2)=NAN,False)
  FieldNames ("oneminwindgust")
EndTable

DataTable (Evapo,1,1000)

  DataInterval (0,60,Min,10)
  ETsz (Temp109(4),RH,wind_speed,SWMJi,-
111.81,41.74,1458,4,0,FP2,Temp109(4)=NAN OR wind_speed=NAN OR RH= NAN OR
SWMJi =NAN )
  FieldNames ("ETGrass,SolarRadCalc")
EndTable

DataTable (twentyfour,1,100)

  DataInterval (0,1,Day,10)
  Average (1,Temp109(4),IEEE4,Temp109(4)=NAN)
  Minimum (1,Temp109(4),FP2,Temp109(4)=NAN,true)
  Maximum (1,Temp109(4),FP2,Temp109(4)=NAN,true)
  Totalize (1,P,FP2,False)
  Maximum (1,windsonic(2),FP2,windsonic(2)=NAN,True)
EndTable

DataTable (hourly,1,1000)

  DataInterval (0,scanrateslow,sec,10)
  Minimum (1,Temp109(4),IEEE4,Temp109(4)=NAN,True)
```

```
  FieldNames ("hourtempmin")
  Maximum (1,Temp109(4),IEEE4,Temp109(4)=NAN,True)
  FieldNames ("hourtempmax")
EndTable
```

'Sub routine that saves variables to USR drive on datalogger so they are not lost with a program reset

```
Sub SaveStorage

  storageFile = FileOpen( "usr:maxwind.dat", "w", 0)
  FileWrite (storageFile, maxwind, Len(maxwind))
  FileClose(storageFile)

  storageFile = FileOpen( "usr:maxtemp.dat", "w", 0)
  FileWrite (storageFile, maxtemp, Len(maxtemp))
  FileClose (storageFile)

  storageFile = FileOpen( "usr:mintemp.dat", "w", 0)
  FileWrite (storageFile, mintemp, Len(mintemp))
  FileClose (storageFile)

  storageFile = FileOpen ("usr:raintotal.dat", "w", 0)
  FileWrite (storageFile, raintotal, Len(raintotal))
  FileClose(storageFile)

  storageFile = FileOpen ("usr:maxtemptime.dat", "w", 0)
  FileWrite (storageFile, maxtemptime, Len(maxtemptime))
  FileClose (storageFile)

  storageFile = FileOpen ("usr:mintemptime.dat", "w", 0)
  FileWrite (storageFile, mintemptime, Len(mintemptime))
  FileClose (storageFile)

  storageFile = FileOpen( "usr:maxwindtime.dat", "w", 0)
  FileWrite (storageFile, maxwindtime, Len(maxwindtime))
  FileClose (storageFile)

  storageFile = FileOpen ("usr:yesterdaymaxwind.dat", "w", 0)
  FileWrite (storageFile, yesterdaymaxwind, Len(yesterdaymaxwind))
  FileClose (storageFile)

  storageFile = FileOpen ("usr:yesterdaymaxtemp.dat", "w", 0)
  FileWrite (storageFile, yesterdaymaxtemp, Len(yesterdaymaxtemp))
  FileClose (storageFile)

  storageFile = FileOpen ("usr:yesterdaymintemp.dat", "w", 0)
  FileWrite (storageFile, yesterdaymintemp, Len(yesterdaymintemp))
```

```
  FileClose (storageFile)

  storageFile = FileOpen ("usr:yesterdayavgtemp.dat", "w", 0)
  FileWrite (storageFile, yesterdayavgtemp, Len(yesterdayavgtemp))
  FileClose (storageFile)

  storageFile = FileOpen ("usr:yesterdayprecip.dat", "w", 0)
  FileWrite (storageFile, yesterdayprecip, Len(yesterdayprecip))
  FileClose (storageFile)

  storageFile = FileOpen ("usr:yesterdayet.dat", "w", 0)
  FileWrite (storageFile, yesterdayet, Len(yesterdayet))
  FileClose (storageFile)

  storageFile = FileOpen ("usr:eta.dat", "w", 0)
  FileWrite (storageFile, Eta, Len(Eta))
  FileClose (storageFile)

  storageFile = FileOpen ("usr:etb.dat", "w", 0)
  FileWrite (storageFile, etb, Len(etb))
  FileClose (storageFile)

  storageFile = FileOpen ("usr:etc.dat", "w", 0)
  FileWrite (storageFile, etc, Len(etc))
  FileClose (storageFile)

  storageFile = FileOpen ("usr:evapotranspirationdaytotal.dat", "w", 0)
  FileWrite (storageFile, evapotranspirationdaytotal, Len (evapotranspirationdaytotal))
  FileClose (storageFile)

  storageFile = FileOpen ("usr:yesterdayavgtemp.dat", "w", 0)
  FileWrite (storageFile, yesterdayavgtemp, Len(yesterdayavgtemp))
  FileClose (storageFile)

EndSub

Sub LoadStorage

  storageFile = FileOpen( "usr:maxwind.dat", "r", 0)
  If storageFile =0 Then
    errorCode = "usr:maxwind.dat"
  EndIf
  FileRead (storageFile, maxwind, 250)
  FileClose (storageFile)
  storageFile = FileOpen ("usr:maxtemp.dat", "r", 0)
  If storageFile =0 Then
    errorCode = "usr:maxtemp.dat"
  EndIf
```

```
FileRead (storageFile, maxtemp, 250)
FileClose (storageFile)

storageFile = FileOpen ("usr:mintemp.dat", "r", 0)
If storageFile =0 Then
  errorCode = "usr:mintemp.dat"
EndIf
FileRead (storageFile, mintemp, 250)
FileClose (storageFile)

storageFile = FileOpen ("usr:raintotal.dat", "r", 0)
If storageFile =0 Then
  errorCode = "usr:raintotal.dat"
EndIf
FileRead (storageFile, raintotal, 250)
FileClose (storageFile)

storageFile = FileOpen ("usr:maxtemptime.dat", "r", 0)
If storageFile =0 Then
  errorCode = "usr:maxtemptime.dat"
EndIf
FileRead (storageFile, maxtemptime, 250)
FileClose (storageFile)

storageFile = FileOpen ("usr:mintemptime.dat", "r", 0)
If storageFile =0 Then
  errorCode = "usr:mintemptime.dat"
EndIf
FileRead (storageFile, mintemptime, 250)
FileClose (storageFile)

storageFile = FileOpen ("usr:maxwindtime.dat", "r", 0)
If storageFile =0 Then
  errorCode = "usr:maxwindtime.dat"
EndIf
FileRead (storageFile, maxwindtime, 250)
FileClose (storageFile)

storageFile = FileOpen ("usr:yesterdaymaxwind.dat", "r", 0)
If storageFile =0 Then
  errorCode = "usr:yesterdaymaxwind.dat"
EndIf
FileRead (storageFile, yesterdaymaxwind, 250)
FileClose (storageFile)
storageFile = FileOpen ("usr:yesterdaymaxtemp.dat", "r", 0)
If storageFile =0 Then
  errorCode = "usr:yesterdaymaxtemp.dat"
```

```
EndIf
FileRead (storageFile, yesterdaymaxtemp, 250)
FileClose (storageFile)

storageFile = FileOpen ("usr:yesterdaymintemp.dat", "r", 0)
If storageFile =0 Then
  errorCode = "usr:yesterdaymintemp.dat"
EndIf
FileRead (storageFile, yesterdaymintemp, 250)
FileClose (storageFile)

storageFile = FileOpen ("usr:yesterdayprecip.dat", "r", 0)
If storageFile =0 Then
  errorCode = "usr:yesterdayprecip.dat"
EndIf
FileRead (storageFile, yesterdayprecip, 250)
FileClose (storageFile)

storageFile = FileOpen ("usr:yesterdayet.dat", "r", 0)
If storageFile =0 Then
  errorCode = "usr:yesterdayet.dat"
EndIf
FileRead (storageFile, yesterdayet, 250)
FileClose (storageFile)

storageFile = FileOpen ("usr:eta.dat", "r", 0)
If storageFile =0 Then
  errorCode = "usr:eta.dat"
EndIf
FileRead (storageFile, Eta, 250)
FileClose (storageFile)

storageFile = FileOpen ("usr:etb.dat", "r", 0)
If storageFile =0 Then
  errorCode = "usr:etb.dat"
EndIf
FileRead (storageFile, etb, 250)
FileClose (storageFile)

storageFile = FileOpen ("usr:etc.dat", "r", 0)
If storageFile =0 Then
  errorCode = "usr:etc.dat"
EndIf
FileRead (storageFile,etc, 250)
FileClose (storageFile)
storageFile = FileOpen ("usr:evapotranspirationdaytotal.dat", "r", 0)
If storageFile =0 Then
```

```
    errorCode = "usr:evapotranspirationdaytotal.dat"
  EndIf
  FileRead (storageFile,evapotranspirationdaytotal, 250)
  FileClose (storageFile)

  storageFile = FileOpen ("usr:yesterdayavgtemp.dat", "r", 0)
  If storageFile =0 Then
    errorCode = "usr:yesterdayavgtemp.dat"
  EndIf
  FileRead (storageFile,yesterdayavgtemp, 250)
  FileClose (storageFile)
EndSub
```

'Sub routine for CO2 measurement

```
Sub turnonCO2

  returnA= "send 0" + CHR(13) + CHR(10)
  SerialOpen (35,19200,0,0,50)
  SerialOut (35,returnA,"",0,0)
  SerialIn (Co2,35,100,0,50)
  SplitStr (co2string(),Co2,"",3,0)
  co2temperaturecorrected= (1.26142*rawco2)-(1.53*(25-gastemp))
```
                                                    'CO2 measurement
temperature corrected
```
    AvgRun (runavgco2,1,co2temperaturecorrected,1)
    AvgRun (runavgco2long,1,co2temperaturecorrected,40)
EndSub
```

'Sub routine for CH200 instruction

```
Sub (CH200subroutine)

  SDI12Recorder (CH200_M0(),3,0,"MC!",1.0,0)
  SDI12command = "XT" & FormatFloat (enclosuretemp,"%4.2f") & "!"
  SDI12Recorder (SDI12result,3,0,SDI12command,1.0,0)
```

'Array values start with one. Values for charge state start with -1.
```
  ChargeState = ChargeStateArr(Chg_State + 2)
```
                                                    'Have to shift the value by
two to line it up with the correct words in the array.
```
ChargeSource = ChargeSourceArr(Chg_Source + 1)
```
                                                    'Values for charge source
start with zero. Have to shift the value by one to line it up with   the correct words in the
array.
```
  CheckBattery = CheckBatteryArr(Ck_Batt + 1)
```
'Values for check battery start with zero.
Have to shift the value by one to line it up with the correct words in the array.
```
  SDI12Recorder (CH200_MX(),3,0,"M6!",1.0,0)
  solarpaneleff = ((((I_in_chg*V_in_chg))/.85)/(solarpanelswi*.65))*100
  Panelwatts=V_in_chg*I_in_chg
```

```
batterywatts=VBatt*IBatt
loadwatts=VBatt*(ILoad)
totalampusage=(((ILoad)/3600)*slow2scanrate)+totalampusage
totalincomingamp=(((I_in_chg)/3600)*slow2scanrate)+totalincomingamp
netamp=totalampusage-totalincomingamp
EndSub
```

'Function Creates SET String for CS120

```
Function CS120_SETCommand As String * 100

  Public TempStringFunc As String * 100
  Public CS120CommandString As String * 100
  Public k As Long
  Public CheckValSET As Long
  Public TempString As String * 200


  'Create a string with all values to be SET in CS120

  TempStringFunc="SETNC:0:"
  For k = 1 To 20
    TempStringFunc = TempStringFunc + SETCS120_Array(k) + " "
  Next

  'Create Checksum for string

  CheckValSET = CheckSum (TempStringFunc,1,0 )

  'Create Final String to Output to CS120

CS120CommandString = CHR(2) + TempStringFunc + ":" +
FormatLong(CheckValSET,"%04X") + ":" + CHR(3) + CHR(13) + CHR(10)
  Return (CS120CommandString)
EndFunction
```

'Sub routine for visibility sensor measurement

```
Sub visibilityon

  TempString = "POLL:0:0"
  If visset=1 Then
    SETCS120_Array(17)=0
    SerialFlush (32)
    TempString = CS120_SETCommand()
    SerialOut (32,TempString,"",0,100)
    Delay (1,1,Sec)
    SerialIn (instringset,32,200,0,1000)
    StatusDewHeater=True
  EndIf

  CheckVal=CheckSum (TempString,1,0)
```

```
OutString=CHR(2)+TempString+":"+ Hex(CheckVal)+":"+ CHR(3)+CHR(13)
SerialOut (32,OutString,"",0,100)    ' Send POLL request to the CS120
Delay (1,1,Sec)
SerialIn (InString,32,100,0,1000)    ' Grab retuned data from the POLL command
SplitStr (CS120_Array(),InString," ",19,5)
```

'Separates incoming string
```
EndSub

BeginProg

  SetStatus ("USRDriveSize","30240")
```
                                          'Allocates memory to USR
drive for storage measurements
```
  Call turnonCO2
  Call visibilityon
  visset=0                   'When set to 1 this variable turns on the visibility dew
heaters
  fanspeed=1                 'sets initial duty cycle for aspirated shield
  brightness = 5                    'sets initial brightness for display
  displaydelay=2             'sets initial display delay for display
  visibilitypower=0     'Keeps visibility sensor turned off until it has had time to let
capacitors drain after power is turned off
  countervisibility=0               'counter leading up to turning the visibility sensor back on
after power off
  Finaltrigger=0         'trigger for final table, when set low it allows measurements to be
made before they are called in the final table
```

  'Load arrays with words to associate with the charge state, charge source and check
battery values from the PS/CH200.

```
  ChargeStateArr(1) = "Regulator Fault"
  ChargeStateArr(2) = "No Charge"
  ChargeStateArr(3) = "Current Limited"
  ChargeStateArr(4) = "Cycle Charging"
  ChargeStateArr(5) = "Float Charging"
  ChargeStateArr(6) = "Battery Test"
  ChargeSourceArr(1) = "None"
  ChargeSourceArr(2) = "Solar"
  ChargeSourceArr(3) = "Continuous"
  CheckBatteryArr(1) = "Normal"
  CheckBatteryArr(2) = "Check Battery"
  errorCode =0
```

'Load CS120 settings into array

```
  SETCS120_Array(1)=0               ' Sensor ID
  SETCS120_Array(2)=0               ' Alarm 1 Enable
  SETCS120_Array(3)=0               ' Set Alarm 1 to Greater or Less Than
```

```
SETCS120_Array(4)=0              ' Set Alarm 1 Trigger Distance
SETCS120_Array(5)=0              ' Alarm 2 Enable
SETCS120_Array(6)=0              ' Set Alarm 2 to Greater or Less Than
SETCS120_Array(7)=0              ' Set Alarm 2 Trigger Distance
SETCS120_Array(8)=2              ' Set Baud Rate to 38400bps
SETCS120_Array(9)=0              ' No Entry Required
SETCS120_Array(10)="M"   ' Set Unit Type to Meters
SETCS120_Array(11)=60    ' Set Continuous Output Period
SETCS120_Array(12)=1     ' Set Polling Mode
SETCS120_Array(13)=2     ' Set Full Message Format
SETCS120_Array(14)=0     ' Set RS232 Serial Mode
SETCS120_Array(15)=10    ' Set Averaging Over 10 mins
SETCS120_Array(16)=10    ' Set Sample Timing to 10 sec
SETCS120_Array(17)=1     ' Dew Heaters Off, 0=On, 1=Off
SETCS120_Array(18)=1     ' Hood Heaters Off, 0=On, 1=Off
SETCS120_Array(19)=0     ' Dirty Window Compensation
SETCS120_Array(20)=1     ' Use CRC Checking on incoming command line
StatusDewHeater=False


Call CH200subroutine
Call LoadStorage
SW12(1,1)                        'Turn on power for display

'Initialize serial ports

SerialOpen (Com3,115200,16,0,10000)
                                        'Set up Comport for Display
SerialFlush(Com3)                'clear any characters in the serial input buffer
SerialOpen (Com1,38400,3,0,108)
                                        'Set up Comport for Windsonic
Anemometer
SerialOpen (32,38400,3,0,10000)
                                        'Set up Comport for Visibility Sensor

'Initialize display values

ModbusMaster (DispError,Com3,115200,66,16,brightness,3,1,3,100)
                                        'initiate brightness
ModbusMaster (DispError,Com3,115200,66,16,displaydelay,5,1,3,100)
                                        'initiate delay
ModbusMaster (DispError,Com3,115200,66,16,1,7,1,3,100)
                                        'initiate unit



Scan (scanrate,Sec,10,0)     'Initial scan rate (set at faster rate for windspeed
measurements)
```

```
'Fan control

   PWM (fanspeed,4,50,mSec)
   PulseCount (fan_frequency,1,3,0,1,30,0)
```
                                            'This outputs the frequency in hertz.
Pulsecount cannot be in slowsequence in Pipeline mode
```
   n=1
   'Sonic Anemometer measurement

   SerialInRecord (Com1,in_bytes_str,&h02,0,&h0D0A,nmbr_bytes_rtrnd,01)
   wind_direction = Mid (in_bytes_str,3,3)
   wind_speed = Mid (in_bytes_str,7,6)
   diag = Mid (in_bytes_str,16,2)
   checksum_flg = ( (HexToDec (Mid (in_bytes_str,20,2))) EQV (CheckSum
(in_bytes_str,9,18)) )
   disable_flg = (NOT (checksum_flg) OR (nmbr_bytes_rtrnd=0) OR (diag<>0))
```

   'The following conditional statement sets the etflag low if input variables are not
usable, thus not calculating evapotranspiration
```
   If wind_speed="NAN" OR Temp109(4)="NAN"
     etflag=0
   EndIf
```

   'Wind Sentry Measurements
```
   PulseCount(WScup_ms,1,1,1,1,0.75,0.2)
   If WScup_ms<0.21 Then WScup_ms=0
   BrHalf(WindDirvane,1,mv5000,4,Vx3,1,5000,True,0,_60Hz,352,-66)
   If WindDirvane>=360 OR WindDirvane<0 Then WindDirvane=0
```

   'TB4 Rain Gauge measurement Rain_mm:
```
   PulseCount(P,1,2,2,0,0.1,0)
   rain5mintotal=P+rain5mintotal
   raintotal=P+raintotal                        'cumulative of rain
   raintotalinch =raintotal * 0.0393700787
   If IfTime(1,5,min) Then
     rainrate=rain5mintotal/5 : rain5mintotal=0
   EndIf

   CallTable onemintable
   CallTable twentyfour
   CallTable wind1
 NextScan
```

```
  SlowSequence                                      'Main Slowsequence

 Scan(scanrateslow,Sec,10,0)
  RealTime (RTime)                                  'Turn on LEDs in datalogger enclosure at
night time

'Can't excite CA01 in conditional statement in PipeLinemode, main reason for forcing
program into sequential mode


  If RTime(4)<10 AND RTime(4)>16 Then
  ExciteCAO (CAO1,5000,False )
  ExciteCAO (CAO2,5000,False )
  EndIf

  PanelTemp (PTemp,_60Hz)
  Battery (batt_volt)

   'Visibility Sensor needs time to let capacitors drain when power is turned off(new
program sent), this instruction allows visibility sensor to power down before data is
polled

  If visibilitypower =0 Then
    countervisibility=countervisibility+1
  EndIf
  If countervisibility = 30 Then
    SW12(2,1) : visibilitypower =1 : countervisibility=0
  EndIf

   'Enable Dew Heaters on visibility sensor if AirTC < DewPoint

  If Temp109(4) <= dewpnt  AND StatusDewHeater=False Then
    SETCS120_Array(17)=0
    SerialFlush (Com2)
    TempString = CS120_SETCommand()
    SerialOut (Com2,TempString,"",0,100)
    Delay (1,1,Sec)
    SerialIn (instringset,Com2,100,0,1000)
    StatusDewHeater=True
  EndIf

   'Disable Dew Heaters on visibility sensor if AirTC > DewPoint+3

  If Temp109(4) > dewpnt+3 AND StatusDewHeater=True Then
    SETCS120_Array(17)=1
    SerialFlush (Com2)
    TempString = CS120_SETCommand()
    SerialOut (Com2,TempString,"",0,100)
    Delay (1,1,Sec)
```

```
      SerialIn (instringset,Com2,100,0,1000)
      StatusDewHeater=False
    EndIf


    AvgRun (avgserialtemp,1,AspiratedYellobead,30)
```
                                                                    'temperature
sent to display at a 5 min running average
```
    serialtemp= Round (avgserialtemp,1)

    If serialtemp = Round (avgserialtemp, 0) Then
      serialtemp = avgserialtemp+0.1
    EndIf


    'Power conservation algorithm controlling displaydelay and brightness as well as
fanspeed

    If solarpanelswi> solarsetpoint1
      If (Qloss)>30
        If VBatt >= (BattTargV-.2) Then
          displaydelay=4
          brightness=5

        ElseIf VBatt > 12.6 Then
          displaydelay=5
          brightness=5

        ElseIf VBatt > 12.4 Then
          displaydelay=6
          brightness=5

        ElseIf VBatt> 12.2 Then
          displaydelay= 7
          brightness=5

        ElseIf VBatt> 12.1 Then
          displaydelay= 8
          brightness=5

        ElseIf VBatt> 12 Then
          displaydelay= 15
          brightness=5

        EndIf
      Else
        If VBatt >= (BattTargV-.2) Then
          displaydelay= 1
```

```
      brightness=5
      fanspeed=1
    ElseIf VBatt > 12.6 Then
      displaydelay= 2
      brightness=5


    ElseIf VBatt > 12.4 Then
      displaydelay= 3
      brightness=5


    ElseIf VBatt> 12.2 Then
      displaydelay= 4
      brightness=5


    ElseIf VBatt> 12.1 Then
      displaydelay= 4
      brightness=5


    ElseIf VBatt> 12 Then
      displaydelay= 4
      brightness=1


    EndIf
  EndIf


  ElseIf solarpanelswi<solarsetpoint1 AND solarpanelswi>solarsetpoint2

    If VBatt >= (BattTargV-.2) Then
      displaydelay=2
      brightness=5

    ElseIf VBatt > 12.6 Then
      displaydelay=7
      brightness=5

    ElseIf VBatt > 12.4 Then
      displaydelay=8
      brightness=5

    ElseIf VBatt> 12.2 Then
      displaydelay= 9
      brightness=5

    ElseIf VBatt> 12.1 Then
      displaydelay= 10
      brightness=5
```

```
  ElseIf VBatt> 12 Then
    displaydelay= 11
    brightness=1


  EndIf


  ElseIf solarpanelswi<solarsetpoint2

    displaydelay =6
    brightness=5

  EndIf

  If solarpanelswi<1
    displaydelay =3
    brightness=1
  EndIf

  If VBatt<=12 Then
    SW12(1,0)  : brightness = 0
  EndIf
```

'Vapor Pressure Calculation

```
  esa = 0.6108 * EXP((17.27 *RHtemp) / (237.3 + RHtemp))
  ea = esa * (RH / 100)
  esc=0.6108 * EXP((17.27 *(((TargTempC1+TargTempC2)/2)) / (237.3 +
((TargTempC1+TargTempC2)/2))))
    vpda=esa-ea
    vpdc=esc-ea
```

'Clear Sky Solar Radiation Calculation

```
If DOY > 68 AND DOY < 306 Then
                                                   'Change DOY
depending on Daylight Savings (these DOY numbers may need to change)
    daylight = 1
  Else
    daylight = 0
  EndIf
  Latr = Lat * (pi / 180)
  dr = 1 + 0.033 * COS(((2 * pi) / 365) * DOY)
  de = ASIN(0.39785 * SIN((278.97 + 0.9856 * DOY + 1.9165 * SIN((356.6 + 0.9856 *
DOY) * (pi / 180))) * (pi / 180)))
  j = ((2 * pi * DOY) / 366) + 4.8718
  eqt = (5.0323 - 430.847 * COS(j) + 12.5024 * COS(2 * j) + 18.25 * COS(3 * j) -
100.976 * SIN(j) + 595.275 * SIN(2 * j) +3.6858 * SIN(3 * j) - 12.47 * SIN(4 * j)) / 60
  SolarN = 12 + daylight - (eqt / 60) - ((Lontz - Lon) / 15)
```

```
    hrangle = ((Hour + (Minute / 60)) - SolarN) * (pi / 12)
    SolarE = ASIN(SIN(Latr) * SIN(de) + COS(Latr) * COS(de) * COS(((Hour + (Minute /
60)) - SolarN) * (pi / 12))) * (180 / pi)

    SolarZ = ACOS(SIN(Latr) * SIN(de) + COS(Latr) * COS(de) * COS(((Hour + (Minute /
60)) - SolarN) * (pi / 12))) * (180 / pi)

  If SolarC * dr * COS(SolarZ * (pi / 180)) > 0 Then
    SWa = SolarC * dr * COS(SolarZ * (pi / 180))
  Else
    SWa = 0
  EndIf

  pb = P0 * ((293.15 - 0.0065 * Elev) / 293.15)^(g / (0.0065*287))
  w = 0.15 * ea * pb + 2.0
  kb = 0.98 * EXP(((-0.00146 * pb) / (kt * SIN(SolarE * (pi / 180)))) - 0.075 * (w /
SIN(SolarE * (pi / 180)))^0.4)
  If kb > 0.15 Then
    kd = 0.35 - 0.36 * kb
  Else
    kd = 0.18 + 0.82 * kb
  EndIf
  SWic = (kb + kd) * SWa
  If SWi / SWic < 1 Then
    SWratio = SWi / SWic
  Else
    SWratio = 1
  EndIf
  If 1 - (1.4 * SWratio - 0.4) > 0 Then
    fc = (1 - (1.4 * SWratio - 0.4))*100
  Else
    fc = 0
  EndIf
  If fc < 1 Then
    fc = fc
  Else
    fc = 100
  EndIf

  'Aspirated Shield Control

  If SWi>200   Then              'You can chose the parameters to turn off the fan or
not turn it off
    If fanspeed<1  Then
      fanspeed=1
    EndIf
  ElseIf SWi<200 AND SWi>15
```

```
      fanspeed=.75

   ElseIf SWi<15
     If fanspeed>.5 Then
       fanspeed=.5

     EndIf

   EndIf
```
'Followinf instruction reduces fan speed to not exceed 4500 rpm

```
   If VBatt>13.8  Then
     fanspeed=13.8/VBatt
   EndIf
```

'Measure CS300 Pyranometers

```
   VoltSe (SWi,1,AutoRange,3,0,0,_60Hz,5.0,0)
   If SWi<0 Then SWi=0
   SWMJi=SWi*0.000001*scanrateslow              'Convert watts to MJ/m²s
   mjtot = SWMJi + mjtot                        'total MJ/m²s
   mjswihour=SWMJi+mjswihour
   ppftotal=((PPF*scanrateslow*.000001)+ppftotal)
   VoltSe (solarpanelswi,1,AutoRange,26,0,0,_60Hz,5.0,0)
   If solarpanelswi<0 Then solarpanelswi=0
   swipaneltoswi=solarpanelswi/SWi
   solarpanelmj=((solarpanelswi*scanrateslow)*wattstoMJ)+solarpanelmj

   If IfTime(1439,1440,min) Then
     mjtot=0                                 'reset for next
     totalampusage=0
     totalincomingamp=0
   EndIf
   If IfTime(59,60,min) Then
     mjswihourtotal=mjswihour
     mjswihour=0
   EndIf


   If maxwind < final.finalmaxwind(1,1) Then
     maxwind=final.finalmaxwind(1,1) : maxwindtime =final.wind_speed_Tmx(1,1)
   Else
     maxwind = maxwind
   EndIf
```

'Humidity probe measurements

```
   VoltSe(RHtemp,1,mV5000,27,0,0,_60Hz,.024,-40)
```

```
VoltSe(RH,1,mV5000,28,0,0,_60Hz,.02,0)
If (RH>100) AND (RH<108) Then RH=100

CallTable evapo
 evapotranspiration= evapo.etgrass(1,1)
 Ro=evapo.SolarRadCalc(1,1)

'Infrared Radiometer measurement

 ExciteV (Vx1,2500,0)
 Therm109 (SBTempC1,1,5,Vx1,0,_60Hz,1.0,0)
 Therm109 (SBTempC2,1,6,Vx1,0,_60Hz,1.0,0)

 VoltDiff (TargmV1,1,mV20,4,True ,0,_60Hz,1.0,0)
 m1 = mC2_1 * SBTempC1^2 + mC1_1 * SBTempC1 + mC0_1
 b1 = bC2_1 * SBTempC1^2 + bC1_1 * SBTempC1 + bC0_1
 SBTempK1 = SBTempC1 + 273.15
 TargTempK1 = ((SBTempK1^4) + m1 * TargmV1 + b1)^0.25
 TargTempC1 = TargTempK1 - 273.15

 VoltDiff (TargmV2,1,mV20,5,True ,0,_60Hz,1.0,0)
 m2 = mC2_2 * SBTempC2^2 + mC1_2 * SBTempC2 + mC0_2
 b2 = bC2_2 * SBTempC2^2 + bC1_2 * SBTempC2 + bC0_2
 SBTempK2 = SBTempC2 + 273.15
 TargTempK2 = ((SBTempK2^4) + m2 * TargmV2 + b2)^0.25
 TargTempC2 = TargTempK2 - 273.15
 irttargtempdif=ABS(TargTempC1-TargTempC2)

'set yesterday values

 If IfTime(1439,1440,min) Then
   yesterdayet=evapotranspirationdaytotal :yesterdayprecip=raintotal
:yesterdaymintemp=mintemp :yesterdaymaxtemp=maxtemp :
yesterdaymaxwind=maxwind :  etc=etb : etb=Eta : Eta=evapotranspirationdaytotal
 EndIf

 If IfTime(0,1440,min) Then
   evapotranspirationdaytotal=0 : raintotal=0   : maxwind=0 :  ppfdaytotal=ppftotal :
ppftotal=0:solarpanelmj=0
 EndIf

 If IfTime(1,1440,min) Then
   maxtemp=AspiratedYellobead  :mintemp=AspiratedYellobead
:maxtemptime="12:00": mintemptime="12:00":
yesterdayavgtemp=twentyfour.aspiratedyellobead_avg(1,1)

 EndIf
```

'NR01 Net Radiometer measurements

```
VoltDiff(SWUp,1,mV50,8,True,0,_60Hz,SWUpcal,0)
If SWUp<0 Then SWUp =0

If SWUp<10 Then PPF=0
If SWUp<10 Then UV=0

VoltDiff(SWDn,1,mV50,9,True,0,_60Hz,SWDowncal,0)
VoltDiff(LWUPRaw,1,mV20,10,True,0,_60Hz,LWUpcal,0)
VoltDiff(LWDNraw,1,mV20,11,True,0,_60Hz,LWDowncal,0)
Resistance (NR01TK,1,mV200,12,Ix2,1,1675,True ,True,0,_60Hz,1.0,0)
NR01TK=NR01TK/100
PRT(NR01TK,1,NR01TK,1,273.15)
NR01TC=NR01TK-273.15
NetRSW=SWUp-SWDn
NetRLW=LWUp-LWDn

Albedo=SWDn/SWUp
If SWUp<5 Then Albedo=0
LWUp=LWUPRaw+(5.67*10^-8)*NR01TK^4
LWDn=LWDNraw+(5.67*10^-8)*NR01TK^4
UpTot=SWUp+LWUp
DnTot=SWDn+LWDn
NetTot=UpTot-DnTot

groundtemp=((LWDn/(s*.96))^.25)-273.15
skytemp=((LWUp/(s*1))^.25)-273.15
```

'Vaisala Barometer measurement
```
VoltSe (Vaisalatemporary,1,AutoRange,25,False,0,_60Hz,.240,500)
pressure= Vaisalatemporary *.1*1.0037     'Pressure converted from mb to kPa
pressureinhg=pressure* .2953
pressurekpasealevel=pressure*(101.3/85.8)
pressureinhgsealevel=pressurekpasealevel*.2953
AvgRun (pressurerunavg,1,pressure,60)
```

'Leaf wetness sensors

```
BrHalf (lwsraw(1),4,mv5000,11,Vx4,4,2500,False,10000,_60Hz,2500,184)'Leaf
Wetness sensor measurement
'Conversion of Leaf Wetness sensors output to a depth (mm):

lws(1)=(lwsraw(1)/93.1)-4.77
lws(2)=(lwsraw(2)/93.1)-4.77
lws(3)=(lwsraw(3)/93.1)-4.77
lws(4)=(lwsraw(4)/93.1)-4.77
LWSDEPTH(1)=(lwsraw(1)*.047-20.895)/100
```

```
LWSDEPTH(2)=(lwsraw(2)*.047-20.895)/100
LWSDEPTH(3)=(lwsraw(3)*.047-20.895)/100
LWSDEPTH(4)=(lwsraw(4)*.047-20.895)/100


  CallTable hourly
  If evapotranspirationdaytotal="NAN" Then
    evapotranspirationdaytotal=0
  EndIf
  If evapo.output(1,1) Then
    evapotranspirationdaytotal=evapotranspirationdaytotal+ evapotranspiration
  EndIf

  If maxtemp< AspiratedYellobead Then
    maxtemp=AspiratedYellobead :maxtemptime= final.timestamp(1,1)
  Else
    maxtemp=maxtemp
  EndIf

  If mintemp> AspiratedYellobead Then
    mintemp=AspiratedYellobead :mintemptime= final.timestamp(1,1)
  Else
    mintemp=mintemp
  EndIf

  ybdif=Temp109(2)-runavgtemp109(4)
  deltat=((TargTempC1avg+TargTempC2avg)/2)- runavgtemp109(4)
  et48=Eta+etb
  et72=Eta+etb+etc

  'Call tables

  CallTable final

  CallTable ClimateCtrDaily

  CallTable ClimateCtrHourly

  CallTable finalxml

  CallTable twentyfour

  CallTable onemintable

NextScan

'Multiplexer Measurements

SlowSequence                       'Multiplexer measurements measured at
"scanrateslow"
Scan (scanrateslow,Sec,3,0)
```

```
PortSet (7,1)                          'Turn on Am16/32 Multiplexer (2x32 mode)
Delay (0,150,mSec)                     'add delay
```

'Begin Thermistor measurements

```
PulsePort (8,20000)
Delay (0,20,mSec)
Therm109 ( Temp109(3),2,1,Vx2,0,_60Hz,1.0,0)

PulsePort (8,20000)
Delay (0,20,mSec)
Therm109 ( Temp109(1),2,1,Vx2,0,_60Hz,1.0,0)
```

'Solar Measurements

'Quantum sensor

```
PulsePort (8,20000)
Delay (0,20,mSec)
VoltDiff (PPF,1,mV1000,1,True ,0,_60Hz,5.25,-4)'adjusted by 5% to match clear sky
```
calculator

'UV sensor

```
PulsePort (8,20000)
Delay (0,20,mSec)
VoltDiff (UV,1,mV50,1,True ,0,_60Hz,4,-5)
```

'battery Enclosure Temperature

```
PulsePort (8,20000)
Delay (0,20,mSec)
Therm109 (enclosuretemp,1,1,Vx2,0,_60Hz,1.0,0)
```

'Sensor loads measured with shunt resistors

```
PulsePort (8,20000)
Delay (0,20,mSec)
VoltDiff (CO2Load,1,mV20,1,True ,0,_60Hz,100,0)

PulsePort (8,20000)
Delay (0,20,mSec)
VoltDiff (displayload,1,mV20,1,True ,0,_60Hz,100,0)

PulsePort (8,20000)
Delay (0,20,mSec)
VoltDiff (fanload,1,mV20,1,True ,0,_60Hz,100,0)
```
'Enclosure Relative Humidity

```
PulsePort (8,20000)
Delay (0,20,mSec)
VoltSe (RHbox,1,mV5000,1,1,0,_60Hz,.1,0)

Delay (0,20000,uSec)
PortSet (7,0) 'Turn off Am16/32 Multiplexer (2x32 mode)

AvgRun (CO2Loadrunavg,1,CO2Load,60)
AvgRun (displayloadrunavg,1,displayload,60)
AvgRun (fanloadrunavg,1,fanload,60)
AvgRun (runavgtemp109(),4,Temp109(),20)
Temp109f (4)=Temp109(4)*1.8+32 'Convert from Celcius to Farenheight for USU App

'Display Instructions

SerialOpen (Com3,115200,16,0,10000)
SerialFlush (Com3)
ModbusMaster (DispError,Com3,115200,66,16,brightness,3,1,3,5,0)
ModbusMaster (DispError,Com3,115200,66,16,displaydelay,5,1,3,5,0)
Delay (1,100,mSec)
ModbusMaster (DispError,Com3,115200,66,16,serialtemp,1,1,3,5,0)


Finaltrigger=1 'Trigger to initiate 'Final Table'
NextScan

'SlowSequence with SDI-12 measurements AND Temperature Measurements on
AM16/32

SlowSequence
Scan (slow2scanrate,Sec,2,0)
  Call CH200subroutine
  Call savestorage
NextScan
'Request Data from CS120 "POLL"

SlowSequence
Scan (1,Min,3,0)
  If visibilitypower=1 Then
    Call visibilityon
  EndIf

  If IfTime(0,1,min) Then
    Call turnonCO2
  EndIf
  visibilitym = CS120_Array(5) 'Visibilty reported in meters
  visibilitykm=visibilitym*.001 'Convert meters to Kilometers
NextScan
```

APPENDIX B

IN SITU MEASUREMENT OF LEAF CHLOROPHYLL CONCENTRATION:

ANALYSIS OF THE OPTICAL/ABSOLUTE RELATIONSHIP[1]

---

[1] The content of this chapter has been published elsewhere under the following reference: "Parry, C., Blonquist, J.M, & Bugbee, B. 2014. In situ measurement of leaf chlorophyll concentration: analysis of the optical/absolute relationship. *Plant, Cell & Environment* DOI: 10.1111/pce.12324." Reprint permission forms from the authors not listed on the title page of this dissertation and from the journal, Plant, Cell and Environment, are included in an appendix.

Abstract

In situ optical meters are widely used to estimate leaf chlorophyll concentration, but non-uniform chlorophyll distribution causes the optical measurement to vary widely among species for the same chlorophyll concentration. Over 30 studies have sought to quantify the *in situ/in vitro* (optical/absolute) relationship, but neither chlorophyll extraction nor measurement techniques for *in vitro* analysis have been consistent among studies. Here we: 1) review standard procedures for measurement of chlorophyll, 2) estimate the error associated with non-standard procedures, and 3) implement the most accurate methods to provide equations for conversion of optical to absolute chlorophyll for 22 species grown in multiple environments. Tests of five Minolta (model SPAD-502) and 25 Opti-Sciences (model CCM-200) meters, manufactured from 1992 to 2013, indicate that differences among replicate models are less than 5 %. We thus developed equations for converting between units from these meter types. There was no significant effect of environment on the optical/absolute chlorophyll relationship. We derive the theoretical relationship between optical transmission ratios and absolute chlorophyll concentration and show how non-uniform distribution among species causes a variable, non-linear response. These results more rigorously link *in situ* optical measurements with *in vitro* chlorophyll concentration and provide insight to strategies for single-leaf radiation capture among diverse species.

Introduction

Leaf chlorophyll concentration is most accurately measured by extraction of chlorophyll in a solvent followed by in vitro measurements in a spectrophotometer. However, non-destructive, *in situ*, optical techniques have become widely used to provide a relative indication of leaf chlorophyll concentration. Two commercially available meters are widely used (Minolta, model SPAD-502; and Opti-Sciences, model CCM-200) and results from these meters have been reported in over 30 studies. Neither meter has a linear relationship with chlorophyll concentration, and the reported optical/absolute chlorophyll concentration relationship has varied widely, sometimes even within the same species.

Measurement of absolute chlorophyll concentration *in vitro*

The extraction method, extraction solvent, spectrophotometric equation, and spectrophotometer resolution must match to accurately determine chlorophyll *in vitro* (Wellburn, 1994). More than 30 studies have been conducted, but few have used the appropriate combination of analytical procedures.

Seven organic solvents have been widely used for chlorophyll extraction: acetone, methanol, ethanol, chloroform, diethyl-ether, dimethyl-formamide (DMF), and dimethyl-sulphoxide (DMSO). Acetone has been the most widely used solvent because it has sharp chlorophyll peaks, but it is considered to be less efficient at chlorophyll extraction than methanol and ethanol (Holmhansen and Riemann, 1978; Ritchie, 2006). Acetone, methanol, and ethanol require grinding of leaf tissue for complete extraction of chlorophyll. DMF and DMSO

have an advantage over other solvents in that they allow for immersion of intact leaf tissue for chlorophyll extraction. However, even with these solvents, immersion may not be effective for all plant tissues. Schaper and Chacko (1991) were not able to completely extract chlorophyll from Cashew and Mango leaf discs using DMSO. DMSO is less toxic than DMF, and extracted solutions are stable up to 7 days in the dark at 4 °C (Barnes et al., 1992). These advantages have led to increasing use of DMSO as an extraction solvent, but it is absorbed through the skin and gloves should be worn when handling it (Barnes et al., 1992).

Matching extraction solvent with spectrophotometric equation to convert absorption values to chlorophyll concentration

Wellburn (1994) emphasized the importance of using spectrophotometric equations that have been derived from accurate extinction coefficients determined in a reliable reference solution. Extinction coefficients from Smith and Benitez (1955) derived for diethyl-ether are generally accepted as accurate and are recommended for use in deriving extinction coefficients for other extraction solvents using the procedures described in Porra et al. (1989). Based on the magnesium concentration of a known chlorophyll a and b solution, Porra et al. (1989) confirmed the extinction coefficients of Smith and Benitez (1955) for both chlorophyll a and b in diethylether. They found that the error in the original Smith and Benitez (1955) equation was less than 1 %. Several equations developed for DMSO and DMF solvents have failed to follow the appropriate Porra et al. (1989)

procedure (Moran and Porath, 1980; Moran, 1982; Inskeep and Bloom, 1985; Barnes et al., 1992).

The equations developed by Arnon (1949) have often been used to quantify chlorophyll a and b concentration in higher plants and green algae. These equations were developed for use with 80 % acetone in water. Several authors (Lichtenthatler and Wellburn, 1983; Barnes et al., 1992; Porra, 2002) have reported that equations from Arnon (1949) are inaccurate because they used the less accurate extinction coefficients of Mackinney (1941). Also, the chlorophyll a/b ratios obtained from the equations of Arnon (1949) underestimate the true a/b chlorophyll ratio (Porra et al., 1989; Wellburn, 1994). Porra et al. (1989) developed an equation to convert a/b chlorophyll ratios determined by the equations of Arnon (1949) to correct values.

Several authors have used DMSO as an extracting solvent, but used spectrophotometric chlorophyll equations developed for 80 % acetone (Monje and Bugbee, 1992; Richardson et al., 2002). This is has been justified by citing other publications that suggest that absorption spectra for chlorophyll a and b are identical for 90 % acetone and DMSO (Shoaf and Lium, 1976; Hiscox and Israelstam, 1979; Ronen and Galun, 1984). However, equations from Arnon (1949) were developed for 80 % (not 90 %) acetone. Furthermore, Barnes et al. (1992) showed that the peak absorption wavelength for chlorophyll a and b is at a longer wavelength in DMSO than 80 % acetone and found that equations from Arnon (1949) underestimated chlorophyll concentration using DMSO extracts by approximately 10 %.

Matching spectrophotometric chlorophyll equations with instrument resolution

Wellburn (1994) discussed differences in chlorophyll measurement among spectrophotometers with differing spectral bandwidth resolution. Early spectrophotometer models used to derive equations were capable of only 1 to 4 nm resolution. High quality modern spectrophotometers have a resolution of 0.1 to 0.5 nm and have been used to derive recently developed spectrophotometric chlorophyll equations. Wellburn (1994) compared three types of spectrophotometers (Uvikon model 941 Plus, 0.5 nm resolution; Hewlett-Packard model HP8452A, diode-array 2 nm fixed resolution; and Pye Unicam model SP30, 1 to 4 nm variable resolution) and determined chlorophyll concentrations in six solvents. He omitted data from the diode array spectrophotometer because it had values that almost always deviated more than 10 % from values of the other two instruments. Wellburn (1994) concluded that diode array spectrophotometers are not appropriate for use with equations derived by non-diode array spectrophotometers, and emphasized that equations derived with one spectrophotometer should not be used with a spectrophotometer with a different spectral resolution.

Although the goal of previous studies has been to develop standard curves to convert optical measurements to absolute chlorophyll concentration, measurement techniques vary widely. Predicted chlorophyll concentration from optical measurements of wheat leaves, measured with the same model of meter,

has varied up to 80 % between studies (Monje and Bugbee, 1992; Uddling et al., 2007). These differences have not been widely acknowledged in the literature.

Optical meters used to determine chlorophyll concentration

The two most widely-used chlorophyll concentration meters are the Konica Minolta, model SPAD-502 (Konica Minolta Sensing, Inc., Sakai, Osaka, Japan) and the Opti-Sciences, model CCM-200 (Opti-Sciences, Inc., Hudson, New Hampshire, USA). Both meters measure the transmission of two wavelengths of radiation through plant leaves: red at approximately 650 nm, and near infrared (NIR) at approximately 900 nm. Increased chlorophyll concentration increases the absorption of red radiation. All plants transmit a high fraction of NIR radiation since these wavelengths are not absorbed by photoreceptors and this transmission is used as a reference wavelength.

Another hand-held, optical chlorophyll meter was recently introduced, the Dualex 4 Scientific (Dx4) (FORCE-A, Orsay, France). This meter measures the transmission of radiation at 710 and 850 nm and converts the measurement into a value of chlorophyll in $\mu g\ cm^{-2}$.

The sampling area differs between meters. The CCM-200 samples 71 mm^2, the SPAD-502 samples 6 mm^2 and the Dx4 samples 20 mm^2. Larger areas provide a larger spatial average, but smaller areas can measure narrower leaves.

Description of the optical differences between meters

The output of the CCM-200 is the ratio of transmission of radiation from an LED centered at 931 nm to transmission of radiation from an LED centered at

653 nm (CCM-200 user manual). This ratio is defined as the chlorophyll content index (CCI).

$$CCI = \frac{\%transmission\ 931\ nm}{\%transmission\ 653\ nm} \qquad (1)$$

The SPAD-502 measures radiation centered at 940 and 650 nm (Minolta manual), but the equation to convert these measurements to a "SPAD" value has been reported differently in four publications. The most complete equation is given by Naus et al. (2010):

$$SPAD = k * log\left(\frac{\%transmission\ 940\ nm}{\%transmission\ 650\ nm}\right) + C \qquad (2)$$

where k is a confidential slope coefficient and C is a confidential offset value. Three other publications have reported less complete equations to calculate the SPAD value. Uddling et al. (2007) reported this equation, but without the C offset. Cerovic et al. (2012) and Markwell et al. (1995) reported the equation without either k or C. Since the slope and offset values are confidential, it is not possible to derive SPAD values from transmission measurements, and it is not possible to mathematically derive a conversion equation between meters. However, since both the SPAD values and the CCI are based on a ratio of the transmission at two closely related wavelengths:

$$SPAD \approx k * log(CCI) + C \qquad (3)$$

Studies on the optical/absolute chlorophyll concentration relationship

Four studies have reported empirical relationships that relate optical measurements to absolute chlorophyll concentration for a meter (model SPAD-501) that was a predecessor to the SPAD-502 (Yadava, 1986; Marquard and

Tipton, 1987; Fanizza et al., 1991; Schaper and Chacko, 1991). The SPAD-501 used slightly different wavelengths and is thus not directly comparable to the SPAD-502.

Monje and Bugbee (1992) appear to have been the first to develop an equation that relates the output from the SPAD-502 to absolute chlorophyll concentration in mg m^{-2}. Since then, numerous other relationships for a range of species have been proposed (Schaper and Chacko, 1991; Markwell et al., 1995; Xu et al., 2000; Bindi et al., 2002; Netto et al., 2002; Richardson et al., 2002; Yamamoto et al., 2002; Esposti et al., 2003; Wang et al., 2004; Cartelat et al., 2005; Jifon et al., 2005; Netto et al., 2005; Uddling et al., 2007; Marenco et al., 2009; Coste et al., 2010; Imanishi et al., 2010; Naus et al., 2010; Ling et al., 2011; Cerovic et al., 2012). The acronym "SPAD" refers to the division of Minolta that developed the meter, Special Products Analysis Division. As the acronym implies, SPAD has no direct relationship to chlorophyll concentration.

Like SPAD, CCI values returned by the CCM-200 are only relative indicators of chlorophyll concentration, as CCI has no direct relationship to chlorophyll concentration. Several studies have also developed chlorophyll prediction equations using CCI measurements from the CCM-200 meter (Richardson et al., 2002; van den Berg and Perkins, 2004; Jifon et al., 2005; Goncalves et al., 2008; Cerovic et al., 2012).

Variation in experimental techniques among studies

Extraction and measurement techniques have not been consistent among studies. Because chlorophyll concentration can have significant spatial variation

it is important to remove the leaf disk from exactly the same location as the optical measurement. This precaution has not always been described in experimental procedures. Multiple extraction solvents, measurement wavelengths, spectrophotometric equations, and instruments with varying resolution have been used to measure absolute chlorophyll. Sampling and measurement differences likely have caused significant variation among studies.

Most studies that have sought to determine the optical/absolute relationship have used only a single meter with the assumption that all meters of the same model are uniform. In an early study, Marquard and Tipton (1987) found 5 % differences between two SPAD-501 meters. Markwell et al. (1995), mentioned that three SPAD-502 meters at the same university differed by ± 5 % and recommended that separate equations be developed for individual meters, but they did not indicate if optics in the meters had been cleaned before use. A comprehensive evaluation of uniformity among replicate meters has not been done. Two studies have attempted to estimate the prediction error associated with an individual measurement. Richardson et al. (2002) examined the error associated with individual optical measurements for paper birch leaves. They compared CCM-200 and SPAD-502 meters and found similar errors for both meters (19 % for the SPAD meter and 20 % for the CCM-200 meter). This relative error was calculated by dividing the root mean square error (RMSE) by average chlorophyll concentration across all samples. Cerovic et al. (2012) compared the Dx4 meter to SPAD-502 and CCM-200 meters and reported similar root mean square errors for all three meters.

Differences among plant groups and species

Related species may share leaf optical properties. Monocots have a larger fraction of vascular tissue per unit surface area and dicots have a thicker adaxial cuticle with more palisade and spongy tissue. Cerovic et al. (2012) measured two monocot and two dicot species, and suggested that optical/absolute chlorophyll relationships could be grouped into separate monocot and dicot categories.

Chlorophyll a/b ratio

Considering that chlorophyll a and b can be easily distinguished in vitro, there has been a surprising lack of literature reporting differences among species. Few of the 30 studies on the optical/absolute relationship have reported the a/b chlorophyll ratio. Chang and Troughton (1972) pointed out that the chlorophyll a/b ratio can be affected by the species, environment, phase of leaf and plant growth, and nutrient status on the chlorophyll a/b ratio. Their data indicate that chlorophyll a/b ratios are higher in C_4 than C_3 plants.

Chlorophyll a/b ratios are known to decrease during leaf senescence (Castro & Sanchez-Azofeifa, 2008, Watts & Eley, 1981), but several studies have found that drought stress has no effect on the chlorophyll a/b ratio (Martin and Warner, 1984; Mafakheri et al., 2010). Several authors have suggested that chlorophyll a/b ratio should increase as leaf nitrogen content decreases, and the data of Kitajima & Hogan (2003) support this conclusion.

Cultivar differences within a species

Markwell et al. (1995) developed a single optical/absolute chlorophyll relationship for multiple strains of soybeans and maize, Uddling et al. (2007)

found that a single curve could be used for multiple wheat cultivars grown over multiple seasons, and Dwyer et al. (1991) found that six maize (corn) hybrids had similar relationship curves. However, significantly different relationships were observed among citrus cultivars (Jifon et al., 2005). Cate and Perkins (2003), Richardson et al. (2002), and van den Berg and Perkins (2004) have all cautioned against treating a single optical/absolute chlorophyll relationship as universal.

The objectives of this study were:

1) estimate the magnitude of differences associated with the use of non-standard combinations of solvents and equations, 2) to implement the most correct methods for chlorophyll measurement to provide improved equations for conversion of optical measurements to absolute chlorophyll concentration, 3) to examine uniformity among two meter models (Opti-Sciences, model CCM-200; and Minolta, SPAD-502) manufactured from 1992 to 2013, 4) to develop equations for inter-converting between units (Chlorophyll Content Index and SPAD units) from the two most common chlorophyll meters (Opti-Sciences, model CCM-200; and Minolta, SPAD-502), 5) estimate environmental effects on the optical/absolute chlorophyll concentration relationship, and 6) use optical and mathematical principles to better understand the underlying causes of non-linearity in the optical/absolute chlorophyll concentration relationship.

Materials and Methods

Collection and extraction of samples

Leaves of multiple ages and intensity of green color were measured and sampled from 22 plant species (five monocots and 17 dicots, 11 deciduous species, and 11 annual crop plants) grown in greenhouse and field environments. Leaves were visually selected for a wide range of the intensity of greenness, which varied due to leaf age, position on the plant, and nutrient deficiencies. A common nutrient deficiency was lack of either nitrogen or iron, which was caused by high root-zone pH. Measurements were made near mid-day to minimize potential effects of light intensity on chloroplast movement.

Chlorophyll content index (CCI), using a CCM-200 meter, was measured at least three times in the same location on each leaf and averaged. A leaf disk was extracted from the exact same location as the measurement. Leaf disks were immediately extracted using a number 4 cork borer with an area of 90 mm^2 to replicate the area measured by the chlorophyll meter and placed in a vial containing 10 mL of DMSO. Vials were incubated in an oven at 65 °C until all of the chlorophyll was in solution and the disk became transparent. This extraction occurred in less than 30-minutes for some species, but required 3 hours for other species. After incubation, a 3 mL aliquot was transferred to an optical-grade analysis cell to measure light absorbance at 646.6 and 663.6 nm (Porra, 1989 acetone equation), and at 649.1 and 665.1 nm (Wellburn, 1994 DMSO equation) using a Shimadzu UV-2401PC spectrophotometer with a resolution of 0.1 nm. Chlorophyll a and b concentrations were determined from spectral measurements using the equations developed by Wellburn (1994) for DMSO and for 0.1 to 0.5 nm spectral resolution:

$$Chlorphyll\ a\ (\mu g\ mL^{-1})$$

(4)

$$= 12.47 * A(665.1nm) - 3.62 * A(649.1nm)$$

$$Chlorphyll\ b\ (\mu g\ mL^{-1})$$

(5)

$$= 25.06 * A(649.1nm) - 6.5 * A(665.1nm)$$

Where A is the absorption at the referenced wavelength and chlorophyll a and b are summed to obtain the total chlorophyll concentration.

Because several publications have extracted with DMSO, but incorrectly used the equation of Porra et al. (1989) that was developed for 80 % acetone, chlorophyll was calculated using both procedures to determine the magnitude of error between equations.

Uniformity among meters

Five replicate Minolta SPAD-502 meters, manufactured from 1992 to 2008, and 25 replicate Opti-Sciences CCM-200 meters, manufactured from 2007 to 2013, were examined for uniformity of output by making replicate measurements on six colored filters. These filters provided a consistent, uniform standard over a range of readings from 2 to 72 CCI units and from 6 to 62 SPAD units. The filters were Roscolux filters: #88, "Light Green"; #3204, "Half Blue"; #86, Pea Green; #92, "Turquoise"; #89, "Moss Green"; and #4490, "CalColor 90 Green".

Conversion between meters

Optical measurements were made in multiple identical locations on leaves of 10 plant species using a SPAD-502 and a CCM-200 meter. These measurements were supplemented with measurements made on 16 Roscolux

filters to provide a wide range of SPAD and CCI values. Measured SPAD values were plotted against corresponding CCI measurements to obtain a relationship curve for the output of the two meters.

Multiple wheat cultivars

Four diverse wheat cultivars (Golden Spire, Lewjain, Greenville, and Wanser) were grown in a greenhouse under three nutrient treatments: optimal nutrient availability, nitrogen deficient, and iron deficient to determine relationships among cultivars and environmental conditions.

Results

Summary of previous studies

Relationships between SPAD-502 and CCM-200 meters and absolute chlorophyll concentration from 17 previous studies indicate a wide range of relationships among species (Figure B-1 A and B).

Relationships among similar species in different studies

Wheat is the most widely studied species with four SPAD-502 curves reported in four studies (Cartelat et al., 2005; Cerovic et al., 2012; Monje and Bugbee, 1992; Uddling et al., 2007). The difference in the optical/absolute relationship among studies was as high as 80 % between Uddling et al. (2007) and Monje and Bugbee, (1992) (Figure B-2).

Some of our measurements on wheat were made with the SPAD-502 meter; others were made with the CCM-200 meter. All data were converted to SPAD units to develop a comprehensive curve for wheat (Figure B-2). No

significant difference among cultivars or nutrient stress treatments was found in the optical/absolute chlorophyll relationship. Our measurements were close to the average of the other studies across all chlorophyll concentrations.

Mean percent difference between relationship curves of this study and others was also calculated for soybean (29 %) (Markwell et al., 1995) and sorghum (40 %) (Yamamoto et al., 2002) (data not shown).

Paper Birch was the only species that was common among studies using the CCM-200 meter. Richardson et al. (2002) used DMSO as the extractant, and the equation of Porra et al. (1989) that was developed for acetone extractants. We determined the magnitude of the error associated with this incorrect match of extraction solvent and spectrophotometric equation. Based on calculations for each of the 22 species in this study, we found that the mean difference between absolute chlorophyll concentrations calculated for a DMSO extractant using the DMSO equation of Wellburn (1994) and the acetone equation of Porra (1989) is 7.84 % (Stdev 0.28 %; data not shown). We thus corrected the equation from Richardson et al. (2002) for Paper Birch by multiplying it by 7.84 %. This correction resulted in a nearly identical fit to our derived equation for Paper Birch (Figure B-3).

Differences among species

The 22 species in this study had a wide range of optical/absolute chlorophyll relationships (Figure B-4 A). A single universal relationship for all species was derived (Figure B-4 B), along with individual equations for each species (Table B-2).

Although it appears that some cultivars within a species can be expressed by a single relationship, we found significantly different optical/absolute chlorophyll concentration relationships between two lettuce cultivars (cv. Waldman's Green and cv. Buttercrunch; *Lactuca sativa*) (Figure B-5). However, our data indicate that the monocots barley, wheat, and rice have a similar optical/absolute chlorophyll concentration relationship (Figure B-5).

Uniformity of replicate meters

Output from each individual meter was plotted against the mean of all meters of the same type to determine variation among studies due to variation among replicate meters (Figure B-6). Mean coefficient of variation was 2.60 % for the CCM-200 meter and 1.10 % for the SPAD-502 meter.

Inter-conversion between Units

Our results indicate that that universal relationships can be used to inter-convert between CCI and SPAD units (Figure B-7 A & B; r^2 = 0.98, 0.99). A similar relationship was developed by Richardson et al. (2002) for converting SPAD units to CCI units (r^2 = 0.97). However, the meter conversion relationship created by Richardson et al. (2002) was based on measurements on Paper Birch leaves with a narrow range of chlorophyll (SPAD units of zero to 40). It was also developed for a prototype CCM-200 meter, which had a different wavelength for the red absorption wavelength. This meter was replaced with the current version in late 2002. The meter conversion curves for this study were developed from multiple species over a wide range of chlorophyll concentrations.

Monocot and dicot species differences

The absolute/optical relationships between CCI and chlorophyll concentration for the mean of five monocot species and the mean of 17 dicot species were not significantly different as indicated by the 95 % prediction intervals (Figure B-8).

Chlorophyll a/b ratio

The mean chlorophyll a/b ratio for C_3 and C_4 plants was 3.2 and 6.3 respectively (Table 2). These results are similar to the values of Chang and Troughton (1972) when corrected for the underestimation of the Arnon (1949) equation (C_3: 3.9 and C_4: 5).

There was a small positive relationship between chlorophyll concentration and the a/b ratio. The coefficient of determination between absolute chlorophyll concentration and a/b ratio was 0.68 for Lilac, 0.48 for Japanese Maple and less than 0.20 for all other species (data not shown).

Discussion

Relationship between transmission and absolute chlorophyll and cell wall content of leaves

Output of both Minolta SPAD-502 and Opti-Sciences CCM-200 meters is based on the ratio of transmission of NIR to red wavelengths. Transmission of radiation is non-linearly related to the amount of absorbing compound in leaf tissue and linearly related to the absorbance of compound (Atkins, 1990). Absorbance is the negative log of transmittance.

Non-chlorophyll compounds (primarily cell walls) absorb radiation similarly at both red and NIR wavelengths, so transmission of red light is similarly affected by both compounds. Transmission of NIR radiation is not affected by chlorophyll and is thus primarily determined by the amount of non-chlorophyll compounds. Assuming a uniform distribution of chlorophyll in leaves, the absolute amount of cell wall and chlorophyll in leaves can be determined from the ratio of percent transmission by the following relationship based on the Beer-Lambert law:

$$CCI = \frac{\%Transmission\ NIR}{\%Transmission\ RED} \approx \frac{e^{-[cell\ wall]}}{e^{-[chlorophyll+cell\ wall]}}$$

$$= \frac{e^{[chlorophyll+cell\ wall]}}{e^{[cell\ wall]}} \tag{6}$$

$$CCI = e^{[chlorophyll+cell\ wall]} - e^{[cell\ wall]} \tag{7}$$

$$ln(CCI) = ln(e^{[chlorophyll+cell\ wall]})$$
$$- ln(e^{[cell\ wall]}) \tag{8}$$

$$ln(CCI) = [chlorophyll + cell\ wall]$$
$$- [cell\ wall] \tag{9}$$

$$SPAD \approx ln(CCI) = [chlorophyll] \tag{10}$$

As shown by the final equation, if chlorophyll is uniformly distributed, SPAD values would be linearly related to chlorophyll concentration of leaves and CCI values would be related to chlorophyll concentration as a logarithmic function. Chlorophyll, however, is not uniformly distributed in leaves and this causes concentration estimates based on transmission measurements to deviate from the equations shown above. The optical changes caused by non-uniform distribution are caused by the sieve and detour effects.

The sieve effect and the detour effect

The transmission of light through a leaf is affected by pigment concentration and pigment spatial distribution in leaves. Non-uniform chlorophyll distribution (clumping of chlorophyll molecules) decreases transmission of light at lower chlorophyll concentrations and increases transmission of light at higher chlorophyll concentrations. Distribution of chlorophyll within a leaf is influenced by structural organization of grana within chloroplasts, chloroplasts within cells, and cells within tissue layers (Fukshansky et al., 1993). When light passes through leaf tissue without encountering an absorber it is known as the sieve effect, which increases with increasing non-uniformity of chloroplasts. As chloroplast uniformity increases, efficiency of red light absorption increases.

The detour effect (light scattering) increases the optical path-length through the leaf, which reduces light transmission. The leaf reflectance at the reference NIR wavelength is much higher than the leaf reflectance at the red chlorophyll absorption wavelength. This causes the detour effect to be more pronounced for the reference NIR wavelength. The detour effect reduces transmission per unit chlorophyll (Monje and Bugbee 1992, Naus et al. 2010, Uddling et al. 2007). Differing optical/absolute chlorophyll relationships among species are likely due to different chlorophyll distribution patterns and thus differing sieve and detour effects.

The sieve effect causes transmission to increase and thus the optical chlorophyll measurement is lower than a sample with uniform chlorophyll distribution (Monje and Bugbee, 1992; Richardson et al., 2002; Jifon et al., 2005;

Uddling et al., 2007; Marenco et al., 2009). The detour effect decreases transmission of light compared to a sample with uniform chlorophyll distribution and thus increases the optical chlorophyll measurement (Uddling et al., 2007). Uddling et al. (2007) observed a noticeable deviation caused by the sieve affect above a SPAD value of 20 and a relatively larger deviation caused by the detour effect below a SPAD value of 20. The combined effects of these relationships on the optical/absolute chlorophyll relationship cause a predictable deviation from the theoretical relationship (Figure B-9).

Environmental effects on optical measurements

Changes in leaf environment have the potential to alter leaf morphology, leaf thickness, and chloroplast distribution. Changes in specific leaf area, often caused by water or temperature stress, have the potential to alter the optical/absolute chlorophyll relationship. Light scatter is higher in thicker leaves (Naus et al., 2010); however, unlike other studies (Campbell et al., 1990; Jifon et al., 2005), we did not find a different optical/absolute chlorophyll relationship between leaves of the same species (tomatoes, peppers, maize, peas) grown in greenhouse vs. outdoor environments. Our data for Paper Birch leave match the corrected data of Richardson et al. (2002), in spite of measurements made on seedlings in a greenhouse (Richardson et al., 2002) and our measurements on mature trees in an arid environment in Utah. Collectively, these findings do not suggest a significant environmental effect on the optical/absolute chlorophyll concentration relationship.

Light-Dependent Chloroplast Movement

Light intensity can alter chloroplast orientation (Hoel and Solhaug, 1998; Naus et al., 2010), which can affect the optical/absolute chlorophyll relationship. Davis et al. (2011) found that the effects of chloroplast movement were greatest in shade species and found that mean maximum percent change in red light transmission between low and high light acclimation was 6.3 % (Stdev 4.7 %) for shade-grown leaves and 2.1 % (Stdev 1.6 %) for sun-grown leaves. This change in chloroplast orientation in response to light is small, but potentially significant in the optical/absolute chlorophyll relationship.

Davis et al. (2011) hypothesized that the amount of chlorophyll movement was correlated with cell diameter. Narrower, more columnar cells of sun leaves may have a greater restriction on chloroplast movement than shade leaf cells. Leaf cell size and shape differ greatly with species (Lee et al., 2000), which may explain varying degrees of chloroplast movement among species. All measurements in this study were made in high light to minimize effects from light dependent chloroplast movement.

Differences among replicate meters

Previous studies on differences among meters have not provided a comprehensive test of meter variability (Markwell et al., 1995; Marquard and Tipton, 1987). Our results indicate that differences among replicate meters were minimal, suggesting differences among studies in the optical/absolute chlorophyll concentration relationship are not caused by different meters.

Most of the variability among optical/absolute chlorophyll concentration relationships of similar species is likely due to the variability of extraction

methods, extraction solvents, chlorophyll concentration equations, and the resolution of spectrophotometers. Some studies have determined chlorophyll concentration using diode array spectrophotometers with methanol extinction coefficients from Porra (1989) (e.g. Cerovic et al. 2012). This is contrary to the recommendations of Wellburn (1994) and would likely lead to errors in determination of absolute chlorophyll concentration. Porra et al (1989) used a Hitachi 3200 spectrophotometer with a spectral resolution of 0.1-0.5 nm over the visible spectrum for extract extinction coefficient determination. Spectrophotometers with similar resolution should be used for best accuracy.

Differences among cultivars of the same species

Many studies have shown that cultivars within species have similar optical/absolute chlorophyll concentration relationships, but this is not always the case. There were significant differences in the optical/absolute chlorophyll relationship for the two lettuce cultivars in this study. This difference can most likely be attributed to the difference in leaf morphology and anatomy in these two cultivars.

Relationship between monocots and dicots

On the basis of measurements in two monocot and two dicot species, Cerovic et al. (2012) suggested that there may be a difference between monocots and dicots. However, no significant difference was found between monocot and dicot curves for the five monocot and 17 dicot species in this study (Figure B-8). In spite of anatomical differences, it does not appear that monocot

and dicot species have different optical/absolute chlorophyll concentration relationships.

Chlorophyll a/b ratio

Chlorophyll a/b ratios are often reported to be a 3 to 1 ratio, but this ratio has not been widely studied. Chang and Troughton (1972) reported typical ratios of C_3 plants as 3 to 1; and ratios in C_4 plants as 5 to 1. They suggest that the a/b ratio is affected by both genetics and by biotic and abiotic factors. We found a similar difference in the ratios for C_3 and C_4 plants (Table 2). We did not find a difference in the optical/absolute chlorophyll relationship between C_4 and C_3 plants in spite of the anatomical difference between these plant groups, and a significant difference in the a/b chlorophyll ratio.

The slope of the optical/absolute relationship indicates differences in chlorophyll distribution and radiation capture

Species with a steep slope in the optical/absolute relationship poorly intercept light per unit chlorophyll; species with a low slope efficiently intercept light per unit chlorophyll. It is likely that increasing non-uniformity of chlorophyll leads to a steeper slope of this relationship. This study highlights the enormous differences in chlorophyll distribution among species and even within species. The lettuce cultivar (Buttercrunch) had one of the lowest slopes and the other (Waldman's Green) had one of the highest slopes.

References

Arnon D.I. (1949) Copper enzymes in isolated chloroplasts. *Plant Physiology*, **24**, 1-15.

Atkins P.W. (1990) *Physical chemistry*. (4th ed.). Freeman, New York.

Barnes J.D., Balaguer L., Manrique E., Elvira S. & Davison A.W. (1992) A reappraisal of the use of dmso for the extraction and determination of chlorophylls-a and chlorophylls-b in lichens and higher-plants. *Environmental and Experimental Botany*, **32**, 85-100.

Bindi M., Hacour A., Vandermeiren K., Craigon J., Ojanpera K., Sellden G., Hogy P., Finnan J. & Fibbi L. (2002) Chlorophyll concentration of potatoes grown under elevated carbon dioxide and/or ozone concentrations. *European Journal of Agronomy*, **17**, 319-335.

Campbell R.J., Mobley K.N., Marini R.P. & Pfeiffer D.G. (1990) Growing conditions alter the relationship between SPAD-501 values and apple leaf chlorophyll. *Hortscience*, **25**, 330-331.

Cartelat A., Cerovic Z.G., Goulas Y., Meyer S., Lelarge C., Prioul J.L., Barbottin A., Jeuffroy M.H., Gate P., Agati G. & Moya I. (2005) Optically assessed contents of leaf polyphenolics and chlorophyll as indicators of nitrogen deficiency in wheat (triticum aestivum l.). *Field Crops Research*, **91**, 35-49.

Cate T.M. & Perkins T.D. (2003) Chlorophyll content monitoring in sugar maple (acer saccharum). *Tree Physiology*, **23**, 1077-1079.

Cerovic Z.G., Masdoumier G., Ben Ghozlen N. & Latouche G. (2012) A new optical leaf-clip meter for simultaneous non-destructive assessment of leaf chlorophyll and epidermal flavonoids. *Physiologia Plantarum*, **146**, 251-260.

Coste S., Baraloto C., Leroy C., Marcon E., Renaud A., Richardson A.D., Roggy J.C., Schimann H., Uddling J. & Herault B. (2010) Assessing foliar chlorophyll contents with the SPAD-502 chlorophyll meter: A calibration test with thirteen tree species of tropical rainforest in french guiana. *Annals of Forest Science*, **67**.

Davis P.A., Caylor S., Whippo C.W. & Hangarter R.P. (2011) Changes in leaf optical properties associated with light-dependent chloroplast movements. *Plant Cell and Environment*, **34**, 2047-2059.

Dwyer L.M., Tollenaar M. & Houwing L. (1991) A nondestructive method to monitor leaf greenness in corn. *Canadian Journal of Plant Science*, **71**, 505-509.

Esposti M.D.D., de Siqueira D.L., Pereira P.R.G., Venegas V.H.A., Salomao L.C.C. & Machado J.A. (2003) Assessment of nitrogenized nutrition of citrus rootstocks using chlorophyll concentrations in the leaf. *Journal of Plant Nutrition*, **26**, 1287-1299.

Fanizza G., Dellagatta C. & Bagnulo C. (1991) A nondestructive determination of leaf chlorophyll in vitis-vinifera. *Annals of Applied Biology*, **119**, 203-205.

Fukshansky L., Vonremisowsky A.M., Mcclendon J., Ritterbusch A., Richter T. & Mohr H. (1993) Absorption-spectra of leaves corrected for scattering and distributional error - a radiative-transfer and absorption statistics treatment. *Photochemistry and Photobiology*, **57**, 538-555.

Goncalves J.F.C., dos Santos Jr U.M. & E.A. d.S. (2008) Evaluation of a portable chlorophyll meter to estimate concentrations in leaves of tropical wood species from amazonian forest. *Hoehnea*, **35**, 185-188.

Hiscox J.D. & Israelstam G.F. (1979) Method for the extraction of chlorophyll from leaf tissue without maceration. *Canadian Journal of Botany-Revue Canadienne De Botanique*, **57**, 1332-1334.

Hoel B.O. & Solhaug K.A. (1998) Effect of irradiance on chlorophyll estimation with the minolta SPAD-502 leaf chlorophyll meter. *Annals of Botany*, **82**, 389-392.

Holmhansen O. & Riemann B. (1978) Chlorophyll a determination - improvements in methodology. *Oikos*, **30**, 438-447.

Imanishi J., Nakayama A., Suzuki Y., Imanishi A., Ueda N., Morimoto Y. & Yoneda M. (2010) Nondestructive determination of leaf chlorophyll content in two flowering cherries using reflectance and absorptance spectra. *Landscape and Ecological Engineering*, **6**, 219-234.

Inskeep W.P. & Bloom P.R. (1985) Extinction coefficients of chlorophyll-a and chlorophyll-b in n,n-dimethylformamide and 80-percent acetone. *Plant Physiology*, **77**, 483-485.

Jifon J.L., Syvertsen J.P. & Whaley E. (2005) Growth environment and leaf anatomy affect nondestructive estimates of chlorophyll and nitrogen in citrus sp leaves. *Journal of the American Society for Horticultural Science*, **130**, 152-158.

Kitajima K. & Hogan K.P. (2003) Increases of chlorophyll a/b ratios during acclimation of tropical woody seedlings to nitrogen limitation and high light. *Plant Cell and Environment*, **26**, 857-865.

Lee D.W., Oberbauer S.F., Johnson P., Krishnapilay B., Mansor M., Mohamad H. & Yap S.K. (2000) Effects of irradiance and spectral quality on leaf structure and function in seedlings of two southeast asian hopea (dipterocarpaceae) species. *American Journal of Botany*, **87**, 447-455.

Lichtenthatler H.K. & Wellburn A.R. (1983) Determinations of total carotenoids and chlorophylls a and b of leaf extracts in different solvents. *Biochemical Society Transactions*, **603**, 591-592.

Ling Q.H., Huang W.H. & Jarvis P. (2011) Use of a SPAD-502 meter to measure leaf chlorophyll concentration in arabidopsis thaliana. *Photosynthesis Research*, **107**, 209-214.

Mackinney G. (1941) Absorption of light by chlorophyll solutions. *Journal of Biological Chemistry*, **140**, 315-322.

Mafakheri A., Siosemardeh A., Bahramnejad B., Struik P.C. & Sohrabi E. (2010) Effect of drought stress on yield, proline and chlorophyll contents in three chickpea cultivars. *Australian Journal of Crop Science*, **4**, 580-585.

Marenco R.A., Antezana-Vera S.A. & Nascimento H.C.S. (2009) Relationship between specific leaf area, leaf thickness, leaf water content and SPAD-502 readings in six amazonian tree species. *Photosynthetica*, **47**, 184-190.

Markwell J., Osterman J.C. & Mitchell J.L. (1995) Calibration of the minolta SPAD-502 leaf chlorophyll meter. *Photosynthesis Research*, **46**, 467-472.

Marquard R.D. & Tipton J.L. (1987) Relationship between extractable chlorophyll and an insitu method to estimate leaf greenness. *Hortscience*, **22**, 1327-1327.

Martin C.E. & Warner D.A. (1984) The effects of desiccation on concentrations and a/b ratios of chlorophyll in leucobryum glaucum and thuidium delicatulum. *New Phytologist*, **96**, 545-550.

Monje O.A. & Bugbee B. (1992) Inherent limitations of nondestructive chlorophyll meters - a comparison of 2 types of meters. *Hortscience*, **27**, 69-71.

Moran R. (1982) Formulas for determination of chlorophyllous pigments extracted with n,n-dimethylformamide. *Plant Physiology*, **69**, 1376-1381.

Moran R. & Porath D. (1980) Chlorophyll determination in intact tissues using n,n-dimethylformamide. *Plant Physiology*, **65**, 478-479.

Naus J., Prokopova J., Rebicek J. & Spundova M. (2010) SPAD chlorophyll meter reading can be pronouncedly affected by chloroplast movement. *Photosynthesis Research*, **105**, 265-271.

Netto A.T., Campostrini E., de Oliveira J.G. & Bressan-Smith R.E. (2005) Photosynthetic pigments, nitrogen, chlorophyll a fluorescence and SPAD-502 readings in coffee leaves. *Scientia Horticulturae*, **104**, 199-209.

Netto A.T., Campostrini E., de Oliveira J.G. & Yamanishi O.K. (2002) Portable chlorophyll meter for the quantification of photosynthetic pigments, nitrogen, and the possible use for assesment of the photochemical process in carica papaya l. Braz. *Plant Physiology*, **14**, 203-210.

Porra R.J. (2002) The chequered history of the development and use of simultaneous equations for the accurate determination of chlorophylls a and b. *Photosynthesis Research*, **73**, 149-156.

Porra R.J., Thompson W.A. & Kriedemann P.E. (1989) Determination of accurate extinction coefficients and simultaneous-equations for assaying chlorophyll-a and chlorophyll-b extracted with 4 different solvents - verification of the concentration of chlorophyll standards by atomic-absorption spectroscopy. *Biochimica Et Biophysica Acta*, **975**, 384-394.

Richardson A.D., Duigan S.P. & Berlyn G.P. (2002) An evaluation of noninvasive methods to estimate foliar chlorophyll content. *New Phytologist*, **153**, 185-194.

Ritchie R.J. (2006) Consistent sets of spectrophotometric chlorophyll equations for acetone, methanol and ethanol solvents. *Photosynthesis Research*, **89**, 27-41.

Ronen R. & Galun M. (1984) Pigment extraction from lichens with dimethylsulfoxide (dmso) and estimation of chlorophyll degradation. *Environmental and Experimental Botany*, **24**, 239-245.

Schaper H. & Chacko E.K. (1991) Relation between extractable chlorophyll and portable chlorophyll meter readings in leaves of 8 tropical and subtropical fruit-tree species. *Journal of Plant Physiology*, **138**, 674-677.

Shoaf W.T. & Lium B.W. (1976) Improved extraction of chlorophyll-a and chlorophyll-b from algae using dimethyl-sulfoxide. *Limnology and Oceanography*, **21**, 926-928.

Smith J. & Benitez A. (1955) Chlorophylls: Analysis in plant materials. In: *In: Modern Methods of Plant Analysis*, pp. 142-196. Springer-Verlag, Berlin.

Uddling J., Gelang-Alfredsson J., Piikki K. & Pleijel H. (2007) Evaluating the relationship between leaf chlorophyll concentration and SPAD-502 chlorophyll meter readings. *Photosynthesis Research*, **91**, 37-46.

van den Berg A.K. & Perkins T.D. (2004) Evaluation of a portable chlorophyll meter to estimate chlorophyll and nitrogen contents in sugar maple (acer saccharum marsh.) leaves. *Forest Ecology and Management*, **200**, 113-117.

Wang Q.B., Chen M.J. & Li Y.C. (2004) Nondestructive and rapid estimation of leaf chlorophyll and nitrogen status of peace lily using a chlorophyll meter. *Journal of Plant Nutrition*, **27**, 557-569.

Wellburn A.R. (1994) The spectral determination of chlorophyll-a and chlorophhyll-b, as well as total carotenoids, using various solvents with spectrophotometers of different resolution. *Journal of Plant Physiology*, **144**, 307-313.

Xu W., Rosenow D.T. & Nguyen H.T. (2000) Stay green trait in grain sorghum: Relationship between visual rating and leaf chlorophyll concentration. *Plant Breeding*, **119**, 365-367.

Yadava U.L. (1986) A rapid and nondestructive method to determine chlorophyll in intact leaves. *Hortscience*, **21**, 1449-1450.

Yamamoto A., Nakamura T., Adu-Gyamfi J.J. & Saigusa M. (2002) Relationship between chlorophyll content in leaves of sorghum and pigeonpea determined by extraction method and by chlorophyll meter (SPAD-502). *Journal of Plant Nutrition*, **25**, 2295-2301.

Table B-1: Summary of publications on the optical/absolute chlorophyll concentration relationship.

Meter Type	Author	Year	Species
SPAD-501			
	Yadava	1986	22 unrelated species
	Marquard and Tipton	1987	12 unrelated species
	Schaper and Chacko	1991	eight tropical and subtropical fruit-tree species
	Dwyer et al.	1991	maize
	Fanizza et al.	1991	12 wine-grape cultivars
SPAD-502			
	Gratani	1992	six sclerophyllous species
	Monje and Bugbee	1992	rice, soybean, wheat
	Markwell et al.	1995	soybean and maize
	Xu et al.	2000	sorghum
	Bindi et al.	2002	potato
	Richardson et al.	2002	paper birch
	Netto et al.	2002	papaya
	Yamamoto et al.	2002	sorghum and pigeonpea
	Esposti et al.	2003	four citrus species
	Wang et al.	2004	peace lily
	Netto et al.	2005	coffee
	Jifon et al.	2005	six citrus species
	Cartelat et al.	2005	wheat
	Uddling et al.	2007	birch, wheat, and potato
	Marenco et al.	2009	six amazonian tree species
	Naus et al.	2010	tobacco
	Imanishi et al.	2010	flowering cherry
	Coste et al.	2010	thirteen tree species of tropical rainforest
	Ling et al.	2011	Arabidopsis thaliana
	Cerovic et al.	2012	kiwi, grape, wheat, and maize
CCM-200			
	Richardson et al.	2002	paper birch
	van den Berg & Perkins	2004	sugar maple
	Jifon et al.	2005	6 citrus species
	Goncalves et al.	2008	four tropical wood species

Table B-2: Equations to determine chlorophyll concentration (µmol m^{-2}) from chlorophyll content index (CCI), r^2 values for each equation, and mean chlorophyll a/b ratio for 22 species. Species are listed in order of increasing slope of the optical/absolute chlorophyll relationship. The mean chlorophyll a/b ratio was not correlated with the optical/absolute chlorophyll relationship. The two species (maize and sorghum) with C$_4$ photosynthesis had the highest a/b ratio.

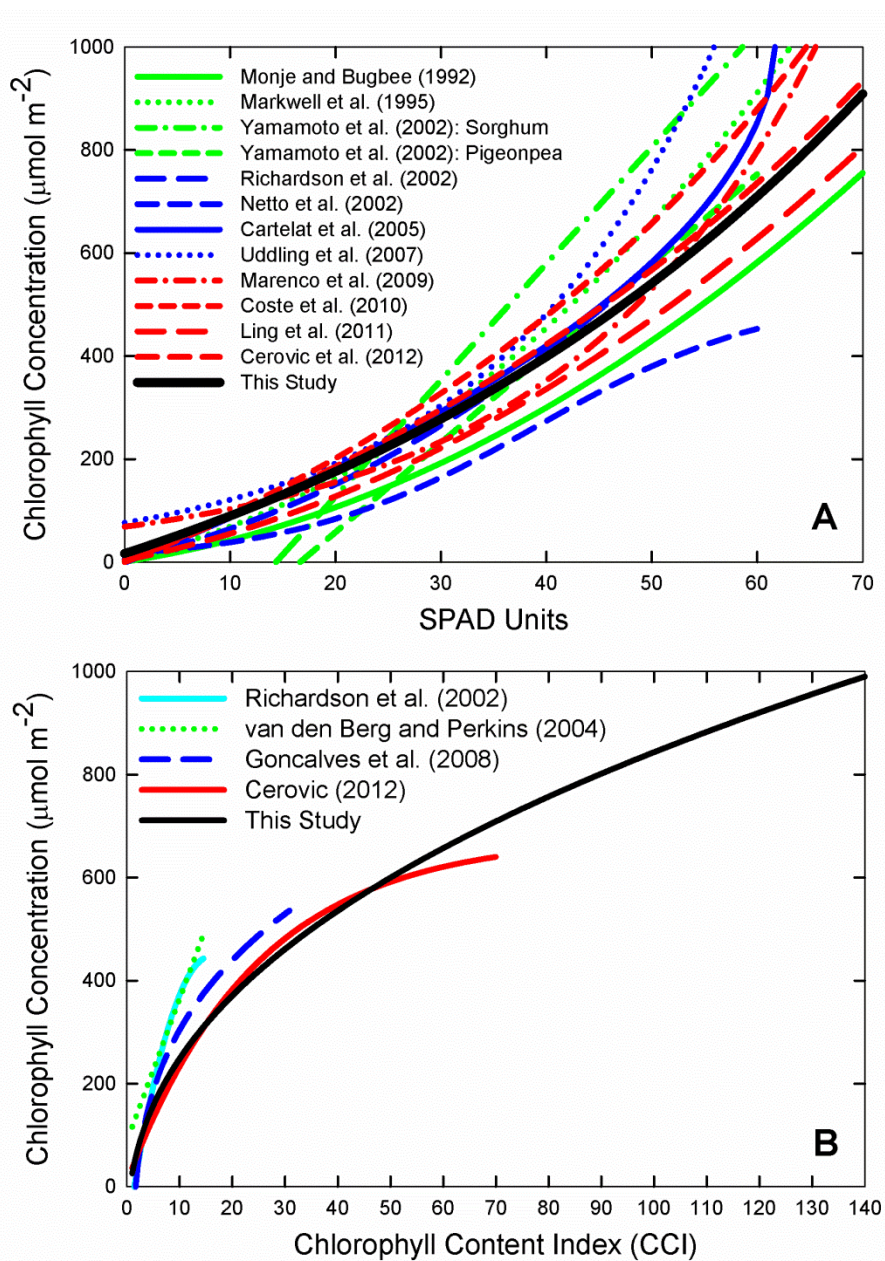|	Chlorophyll Concentration Equation (µmol m^{-2}) from CCI	r^2	Mean Chlorophyll a/b ratio	Standard Devia of a/b ratio
Deciduous Species				
European Birch	$-76 + 85*(CCI)^{0.64}$	0.89	3.3	0.5
Lilac	$-98 + 93*(CCI)^{0.51}$	0.95	2.6	0.5
Norway Maple	$-95 + 96*(CCI)^{0.57}$	0.94	3.9	0.7
Quaking Aspen	$-128 + 106*(CCI)^{0.50}$	0.92	3.3	0.3
Purple Leaf Sand Cherry	$-144 + 113*(CCI)^{0.55}$	0.96	2.5	0.7
Crab Apple	$-124 + 117*(CCI)^{0.47}$	0.93	4.4	1.4
Paper Birch	$-120 + 135*(CCI)^{0.48}$	0.94	2.5	0.4
Crimson King Maple	$-160 + 144*(CCI)^{0.50}$	0.90	2.6	0.3
Japanese Maple	$-150 + 150*(CCI)^{0.43}$	0.97	1.9	0.1
Boxelder	$-191 + 182*(CCI)^{0.38}$	0.92	2.7	0.3
Forsythia	$-486 + 477*(CCI)^{0.18}$	0.93	2.6	0.5
Annual Crop Plants				
Sorghum (C$_4$)	$-8 + 29*(CCI)^{0.80}$	0.90	6.9	2.0
Pepper	$-19 + 39*(CCI)^{0.69}$	0.92	3.7	0.7
Rice	$-64 + 57*(CCI)^{0.68}$	0.82	5.0	1.5
Wheat	$-84 + 79*(CCI)^{0.60}$	0.87	4.3	0.4
Soybean	$-103 + 123*(CCI)^{0.47}$	0.95	4.2	0.6
Maize (C$_4$)	$-121 + 129*(CCI)^{0.42}$	0.84	5.7	1.4
Barley	$-132 + 146*(CCI)^{0.43}$	0.95	3.1	0.7
Kohlrabi	$-150 + 162*(CCI)^{0.34}$	0.83	3.1	0.8
Tomato	$-328 + 304*(CCI)^{0.26}$	0.87	2.9	0.7
Pea	$-334 + 316*(CCI)^{0.24}$	0.84	3.8	0.9
Lettuce				
Waldman's Green	$-2204 + 2204*(CCI)^{0.04}$	0.98	2.7	0.2
Buttercrunch	$-29 + 32*(CCI)^{0.74}$	0.98	2.5	0.2

Figure B-1: Relationship between meter output and chlorophyll concentration (μmol m^{-2}). (A) Twelve representative studies using SPAD units, and (B) four studies and this study using chlorophyll content index (CCI). Species and analytical methods differed among studies.
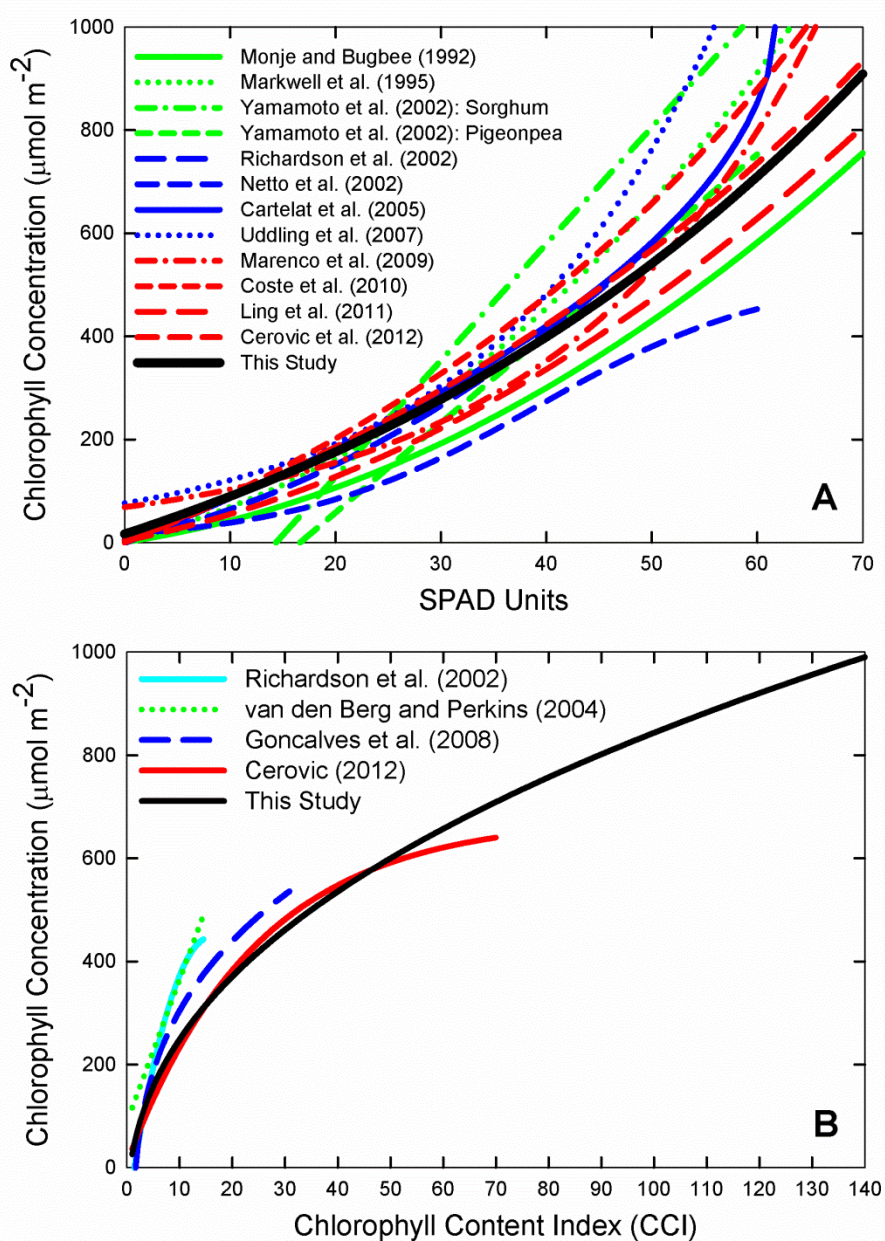
Figure B-2: Relationship between SPAD units and chlorophyll concentration (μmol m^{-2}) for wheat from four prior studies and this study. The CCI relationship from this study was converted for use with SPAD units using the equation in Fig. C-7A.
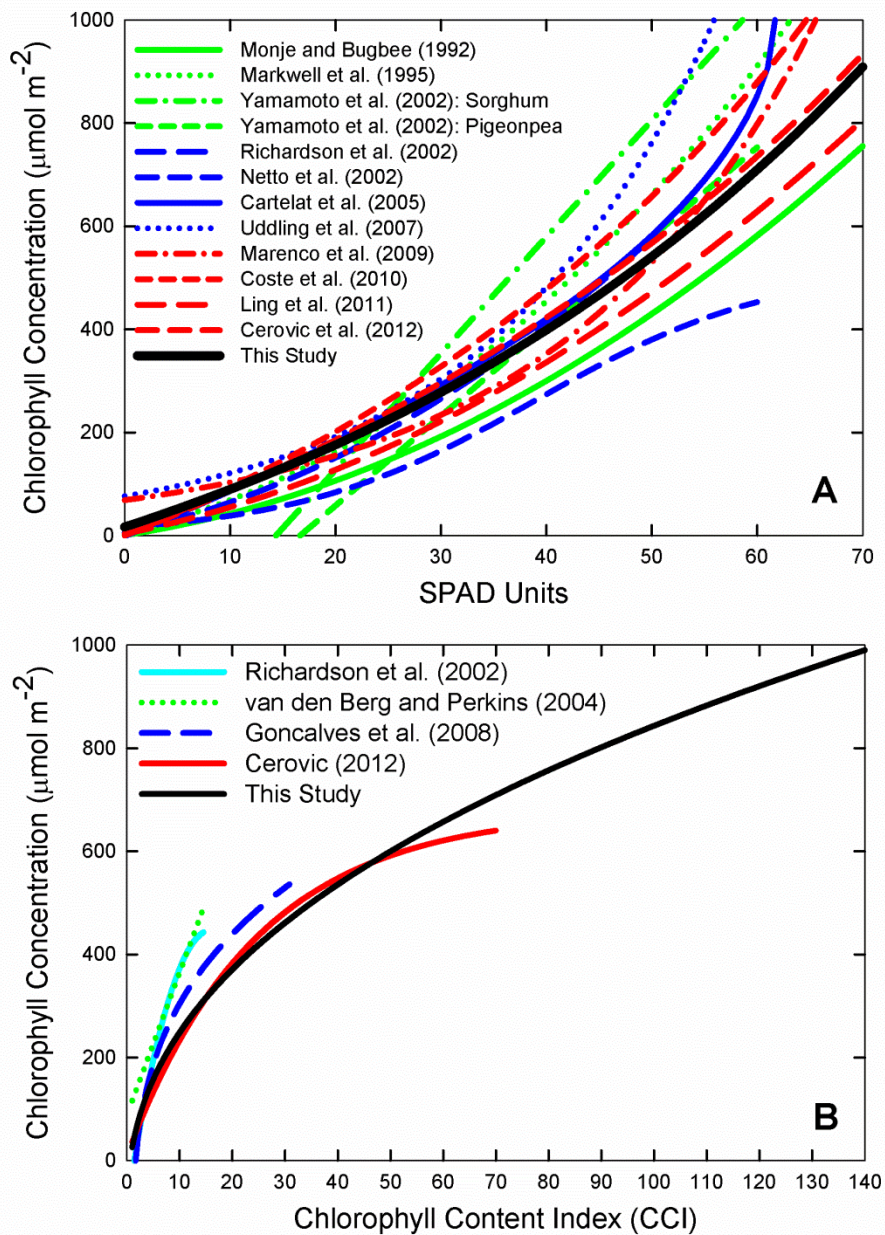
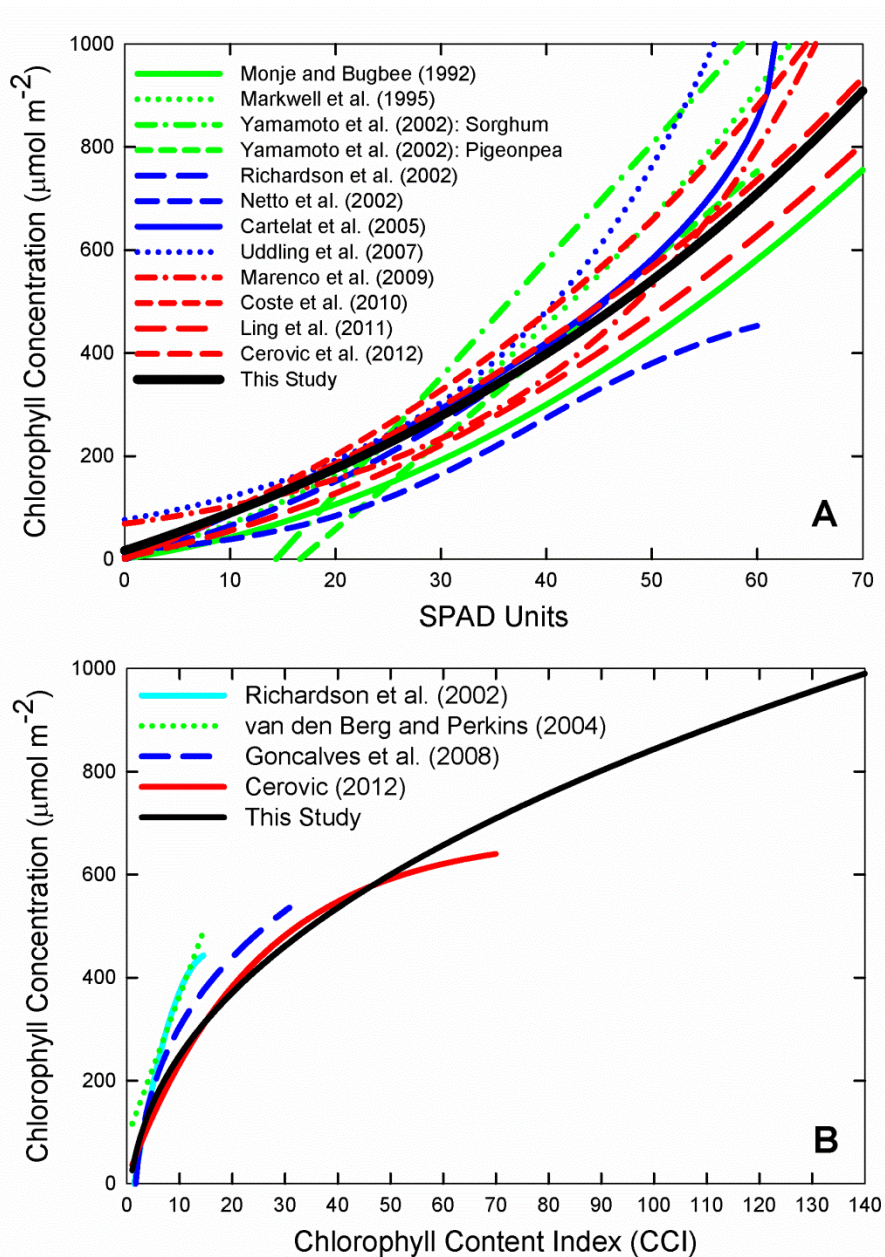Figure B-3: Relationship between chlorophyll content index (CCI) and chlorophyll concentration (µmol m^{-2}) for paper birch (*Betula papytifera*) leaves from two studies. The original relationship from Richardson et al. (2002) was corrected for the underestimation of chlorophyll concentrations derived from the equation of Porra et al. (1989) for DMSO extractants.

Figure B-4: Relationship between chlorophyll content index (CCI) and chlorophyll concentration (µmol m^{-2}) for (A) 22 individual species and (B) all 22 species combined. The molar mass of the chlorophyll molecule is about 900 grams per mole. These measurements can easily be converted to mass per unit area.
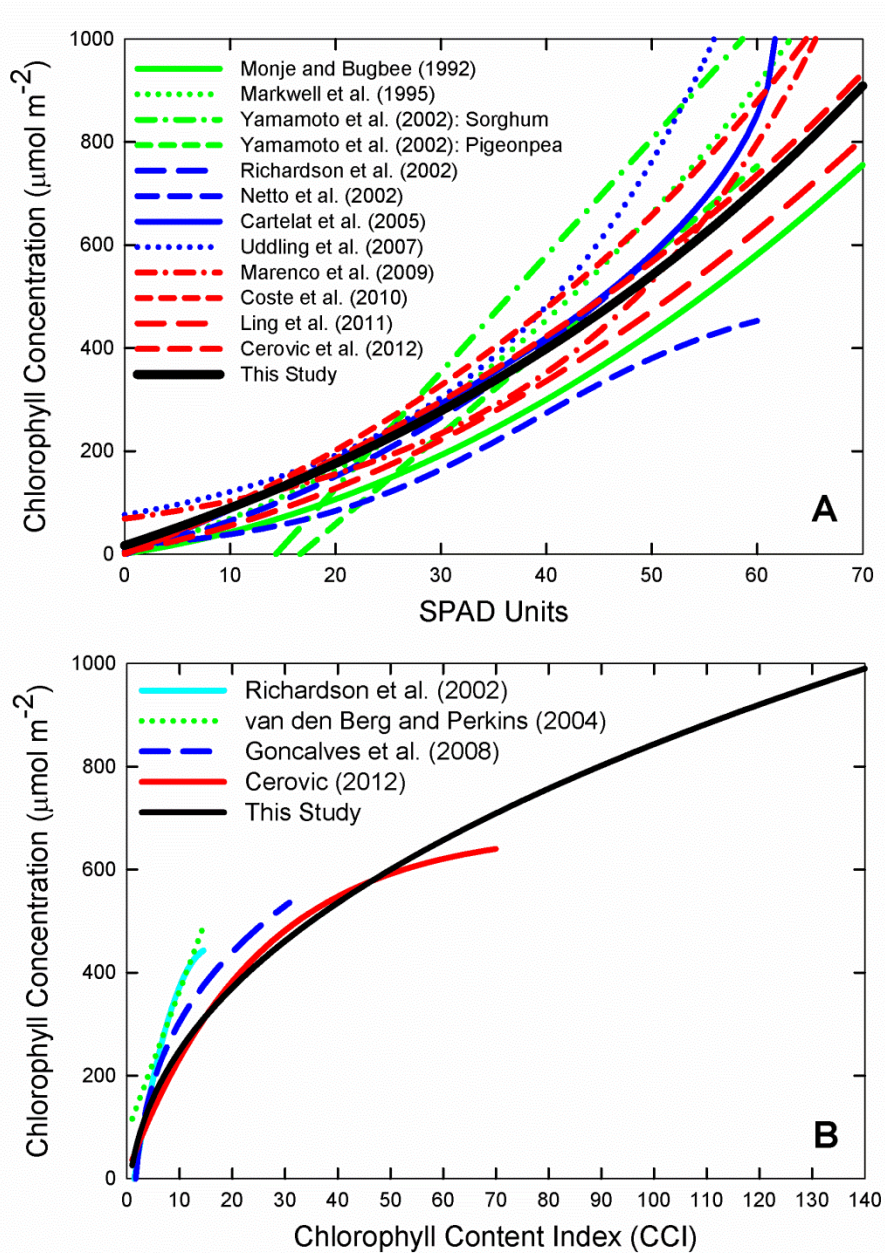
Figure 5-5: Relationship between chlorophyll content index (CCI) and chlorophyll concentration (μmol m^{-2}) for 22 species. Equations for each relationship are provided in Table 2.
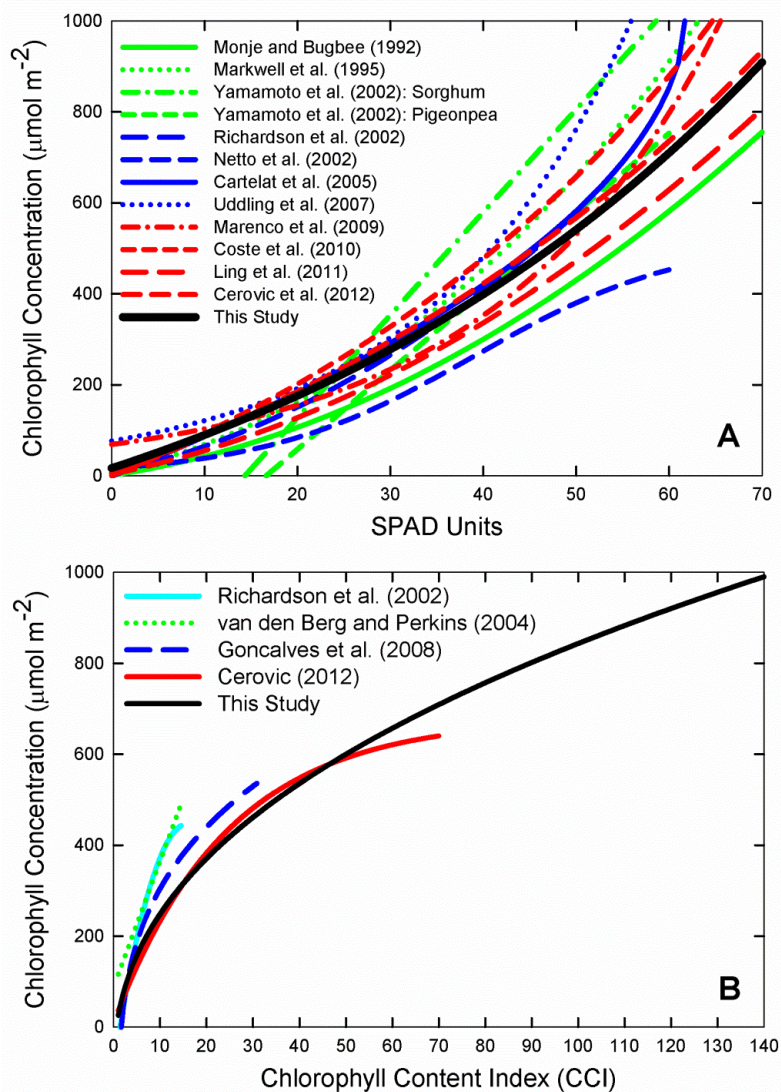
Figure B-6: Uniformity of the two most common chlorophyll meters. The output of individual meters was compared to the mean of all meters of the same type. Measurements were made on colored filters to provide a uniform reference. (A) Five Minolta model SPAD-502 meters with Special Products Analog Division (SPAD) output manufactured from 1992 to 2008. (B) 25 Opti-Sciences model CCM-200 meters with chlorophyll content index (CCI) output manufactured from 2007 to 2013. The Coefficient of Variation (standard deviation / mean) was 1.1 % among meters with SPAD unit output, and 2.6 % among meters with CCI output. Both types of meters were highly uniform and differences among meters are much smaller than differences in genetic, environmental, and extraction/analytical techniques.
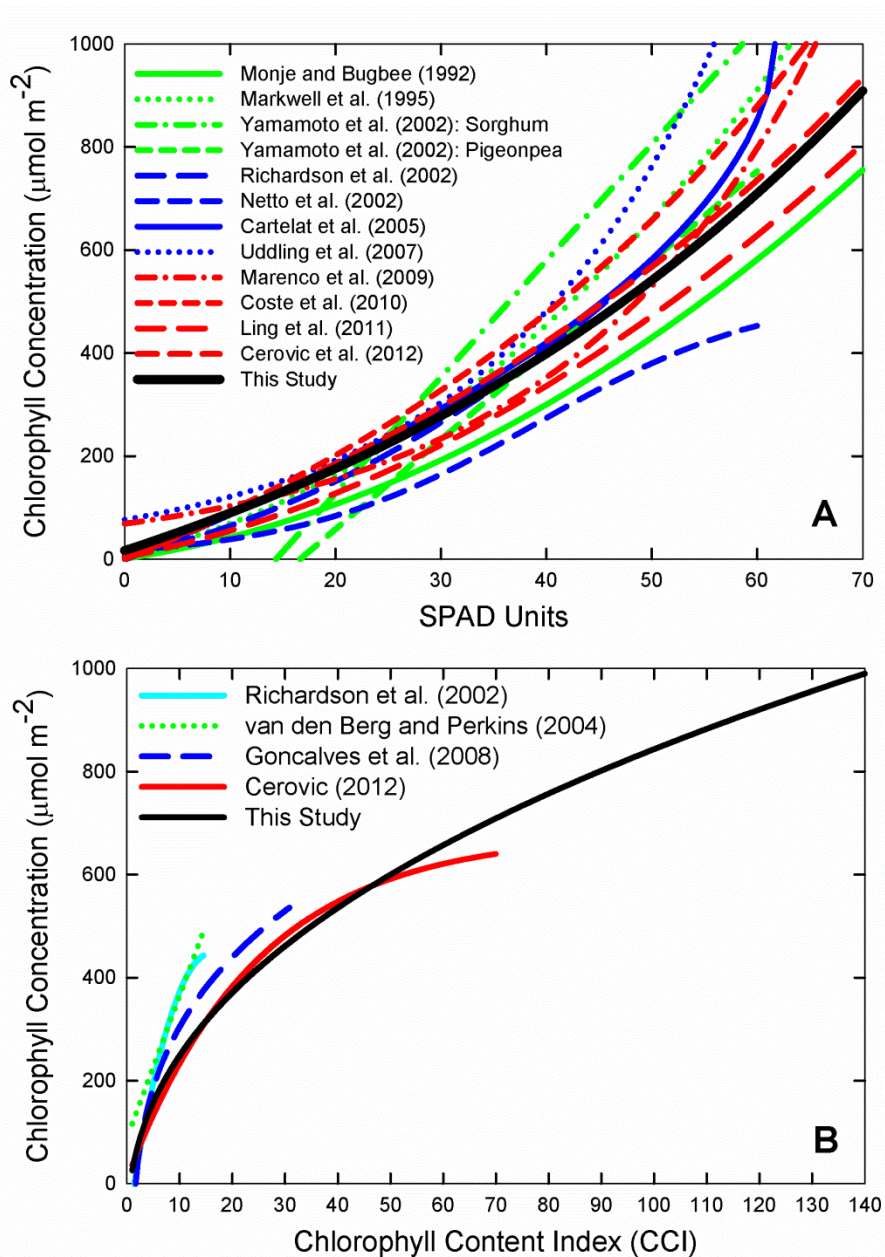
Figure B-7: Equations to convert (A) SPAD units to chlorophyll content index (CCI) and (B) CCI to SPAD units. Data are from replicate measurements of multiple species. Each comparison measurement was made on the same spot on each leaf.
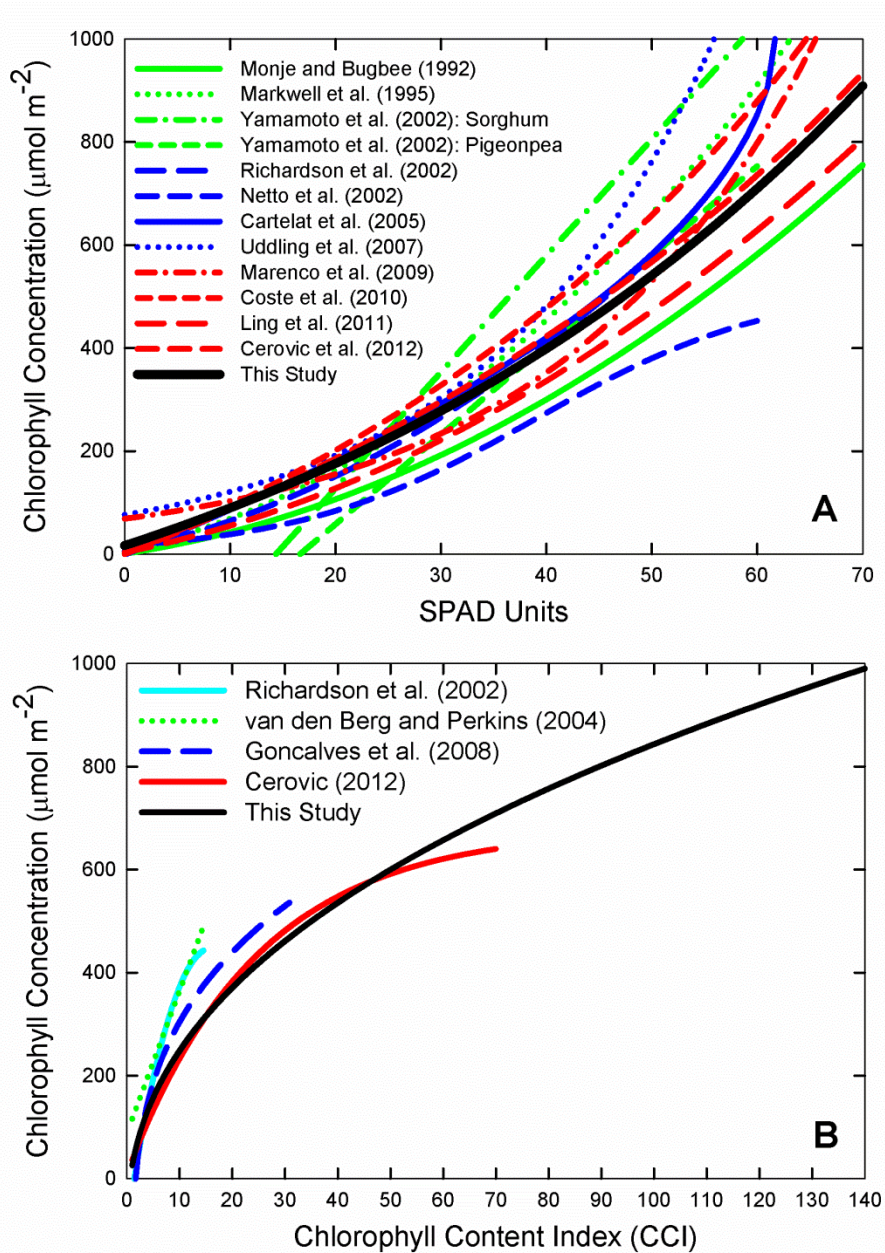
Figure B-8: Relationship between chlorophyll content index (CCI) and chlorophyll concentration (µmol m^{-2}) for the mean of five monocot species and 17 dicot species. In spite of leaf anatomical differences among species there was no significant difference between these diverse plant groups.
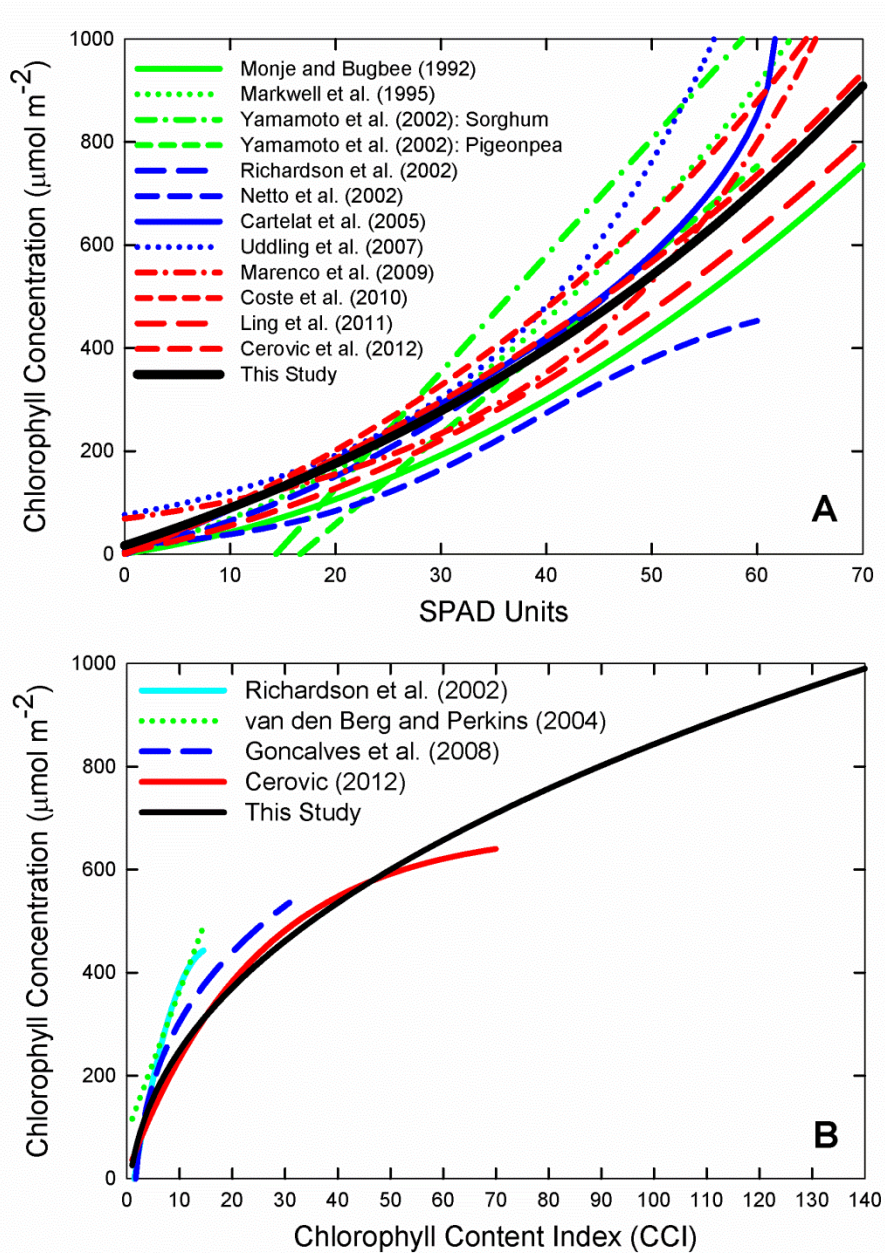
Figure B-9: Impact of the detour (light scattering) and sieve effects (non-uniform chlorophyll distribution) on the optical/absolute chlorophyll concentration relationship for (A) SPAD units and (B) chlorophyll content index (CCI). The black line indicates the theoretical relationship if chlorophyll was uniformly distributed in the leaf.

APPENDIX C

DERIVATION OF THE STOMATAL

CONDUCTANCE EQUATION

Derivation of the Canopy Stomatal Conductance Equation from Energy Balance Components

J.M. Blonquist Jr., J.M. Norman, B. Bugbee, 2009. Automated measurement of canopy stomatal conductance based on infrared temperature. Agricultural and Forest Meteorology 149: 1931-1945.

Developed and formatted by Christopher Parry,
Crop Physiology Laboratory, Utah State University

$$R_{nC} = H_C + \lambda E_C + A_n$$ (1) Energy balance equation for a plant canopy

$$H_C = g_H C_P (T_C - T_A)$$ (2) Sensible heat (Campbell and Norman, 1998)

$$\lambda E_C = g_T \lambda \left(\frac{e_{SC} - e_A}{P_B} \right)$$ (3) Latent heat (Campbell and Norman, 1998)

$$g_T = \frac{1}{(1/g_V) + (1/g_C)} = \frac{g_V g_C}{g_C + g_V}$$ (4) Total conductance = Boundary layer and stomatal conductance in series

List of Symbols:
Equation (1):

R_{nC} = net radiation divergence in the canopy (W m^{-2})

H_C = sensible heat flux (W m^{-2})

λE_C = latent heat flux (W m^{-2})

A_n = net assimilation (W m^{-2})

Equation (2):

g_H = boundary layer heat conductance [mol m^{-2} s^{-1}]

C_P = heat capacity of air (29.17 J mol^{-1} C^{-1})

T_C = aerodynamic canopy temperature [ºC]

T_A = air temperature [ºC]

Equation (3):

g_T = total water vapor conductance [mol m^{-2} s^{-1}]

λ = latent heat of vaporization [J mol^{-1}]

e_{SC} = saturated vapor pressure [kPa]

e_A = vapor pressure [kPa]

P_B = barometric pressure [kPa]

Equation (4):

g_V = boundary layer water vapor conductance [mol m^{-2} s^{-1}]

g_C = canopy stomatal conductance to water vapor [mol m^{-2} s^{-1}]

Substituting for g_T in equation (3) we get:

$$\lambda E_C = \left(\frac{g_V g_C}{g_C + g_V} \right) \lambda \left(\frac{e_{SC} - e_A}{P_B} \right)$$

We then substitute H_C, λE_C, in equation (1) and obtain:

$$R_{nC} = g_H C_P (T_C - T_A) + \left(\frac{g_V g_C}{g_C + g_V} \right) \lambda \left(\frac{e_{SC} - e_A}{P_B} \right) + A_n$$

In 4 steps of subtraction and division we get g_C on one side:

Step 1: subtract $g_H C_P (T_C - T_A)$ and A_n from both sides

$$R_{nC} - g_H C_P (T_C - T_A) - A_n = \left(\frac{g_V g_C}{g_C + g_V} \right) \lambda \left(\frac{e_{SC} - e_A}{P_B} \right)$$

Step 2: divide both sides by $\lambda \left(\dfrac{e_{SC} - e_A}{P_B} \right)$

$$\left(\frac{g_V g_C}{g_C + g_V} \right) = \frac{R_{nC} - g_H C_P (T_C - T_A) - A_n}{\lambda \left(\dfrac{e_{SC} - e_A}{P_B} \right)}$$

Step 3: multiply both sides by $(g_C + g_V)$

$$g_V g_C = \frac{(g_C + g_V)(R_{nC} - g_H C_P (T_C - T_A) - A_n)}{\lambda \left(\dfrac{e_{SC} - e_A}{P_B} \right)}$$

Step 4: divide both sides by g_V

$$g_C = \frac{(g_C + g_V)(R_{nC} - g_H C_P (T_C - T_A) - A_n)}{g_V \lambda \left(\dfrac{e_{SC} - e_A}{P_B} \right)}$$

Simplify by multiplying the denominator and numerator of the left side by P_B we obtain:

$$g_C = \frac{P_B(g_C + g_V)(R_{nC} - g_H C_P(T_C - T_A) - A_n)}{g_V \lambda(e_{SC} - e_A)}$$

Expanding the right side numerator by multiplying out $(g_C + g_V)$ produces:

$$g_C = \frac{g_C P_B[(R_{nC} - A_n) - g_H C_P(T_C - T_A)] + g_V P_B[(R_{nC} - A_n) - g_H C_P(T_C - T_A)]}{g_V \lambda(e_{SC} - e_A)}$$

We still have g_c on the right side, to isolate g_c on one side we separate the right side into two parts by using the common denominator:

$$g_C = \frac{g_C P_B[(R_{nC} - A_n) - g_H C_P(T_C - T_A)]}{g_V \lambda(e_{SC} - e_A)} + \frac{g_V P_B[(R_{nC} - A_n) - g_H C_P(T_C - T_A)]}{g_V \lambda(e_{SC} - e_A)}$$

We subtract the section with g_c from both sides:

$$g_C - \frac{g_C P_B[(R_{nC} - A_n) - g_H C_P(T_C - T_A)]}{g_V \lambda(e_{SC} - e_A)} = \frac{g_V P_B[(R_{nC} - A_n) - g_H C_P(T_C - T_A)]}{g_V \lambda(e_{SC} - e_A)}$$

Multiply g_c by $g_V \lambda(e_{SC} - e_A)/g_V \lambda(e_{SC} - e_A)$ to obtain common denominator:

$$\frac{g_C[g_V \lambda(e_{SC} - e_A)]}{g_V \lambda(e_{SC} - e_A)} - \frac{g_C P_B[(R_{nC} - A_n) - g_H C_P(T_C - T_A)]}{g_V \lambda(e_{SC} - e_A)} = \frac{g_V P_B[(R_{nC} - A_n) - g_H C_P(T_C - T_A)]}{g_V \lambda(e_{SC} - e_A)}$$

Simplify by combing the left side using the common denominator:

$$\frac{g_C[g_V \lambda(e_{SC} - e_A)] - g_C P_B[(R_{nC} - A_n) - g_H C_P(T_C - T_A)]}{g_V \lambda(e_{SC} - e_A)} = \frac{g_V P_B[(R_{nC} - A_n) - g_H C_P(T_C - T_A)]}{g_V \lambda(e_{SC} - e_A)}$$

Bring out g_c to multiply the group:

$$\frac{g_C\{g_V \lambda(e_{SC} - e_A) - P_B[(R_{nC} - A_n) - g_H C_P(T_C - T_A)]\}}{g_V \lambda(e_{SC} - e_A)} = \frac{g_V P_B[(R_{nC} - A_n) - g_H C_P(T_C - T_A)]}{g_V \lambda(e_{SC} - e_A)}$$

Again isolate g_C by division and multiplication:

$$g_C = \frac{g_V P_B\left[(R_{nC} - A_n) - g_H C_P(T_C - T_A)\right]}{g_V \lambda(e_{SC} - e_A)} \times \frac{g_V \lambda(e_{SC} - e_A)}{g_V \lambda(e_{SC} - e_A) - P_B\left[(R_{nC} - A_n) - g_H C_P(T_C - T_A)\right]}$$

Cross out, canceling units to simplify:

$$g_C = \frac{g_V P_B\left[(R_{nC} - A_n) - g_H C_P(T_C - T_A)\right]}{g_V \lambda(e_{SC} - e_A) - P_B\left[(R_{nC} - A_n) - g_H C_P(T_C - T_A)\right]} \qquad (5)$$

(This is equation 8 in Blonquist , Norman, and Bugbee, 2009)

APPENDIX D

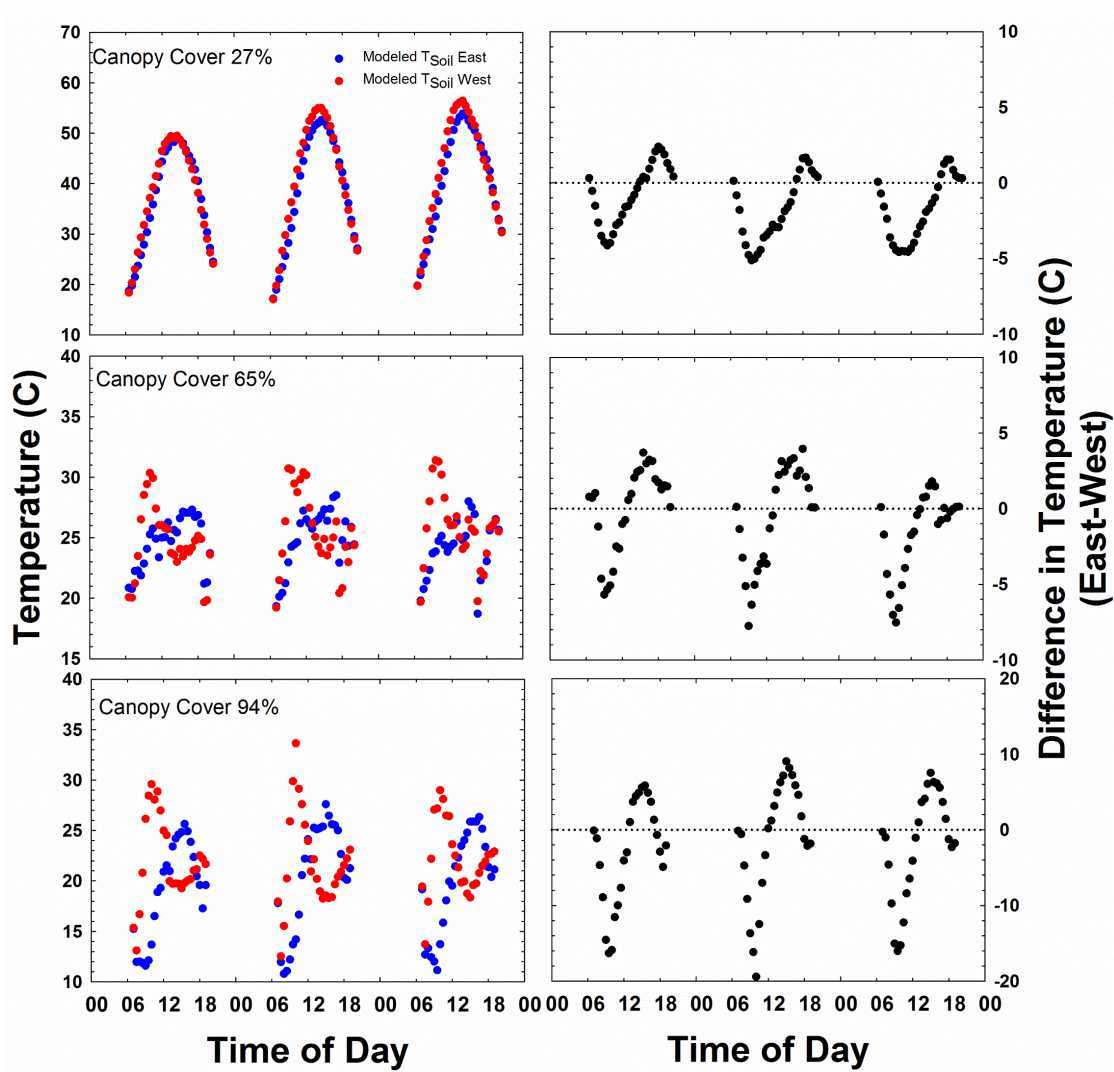UTAH STATE UNIVERSITY

SUPPLEMENTAL FIGURES FOR CHAPTER 2

Figure D-1: Comparison of soil temperature modeled from east and west-facing radiometers.
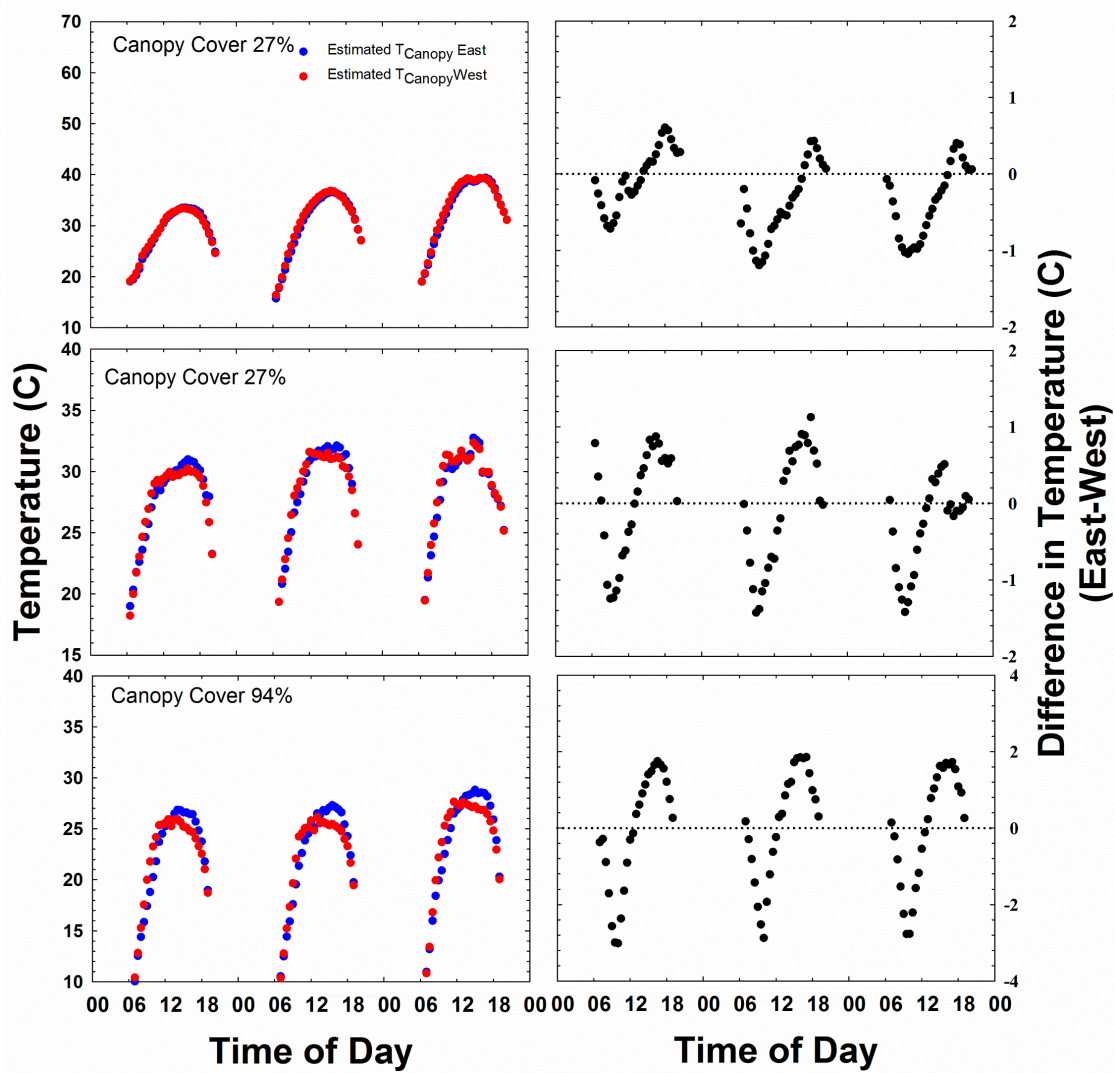
Figure D-2: Comparison of canopy temperature modeled from east and west-facing radiometers.
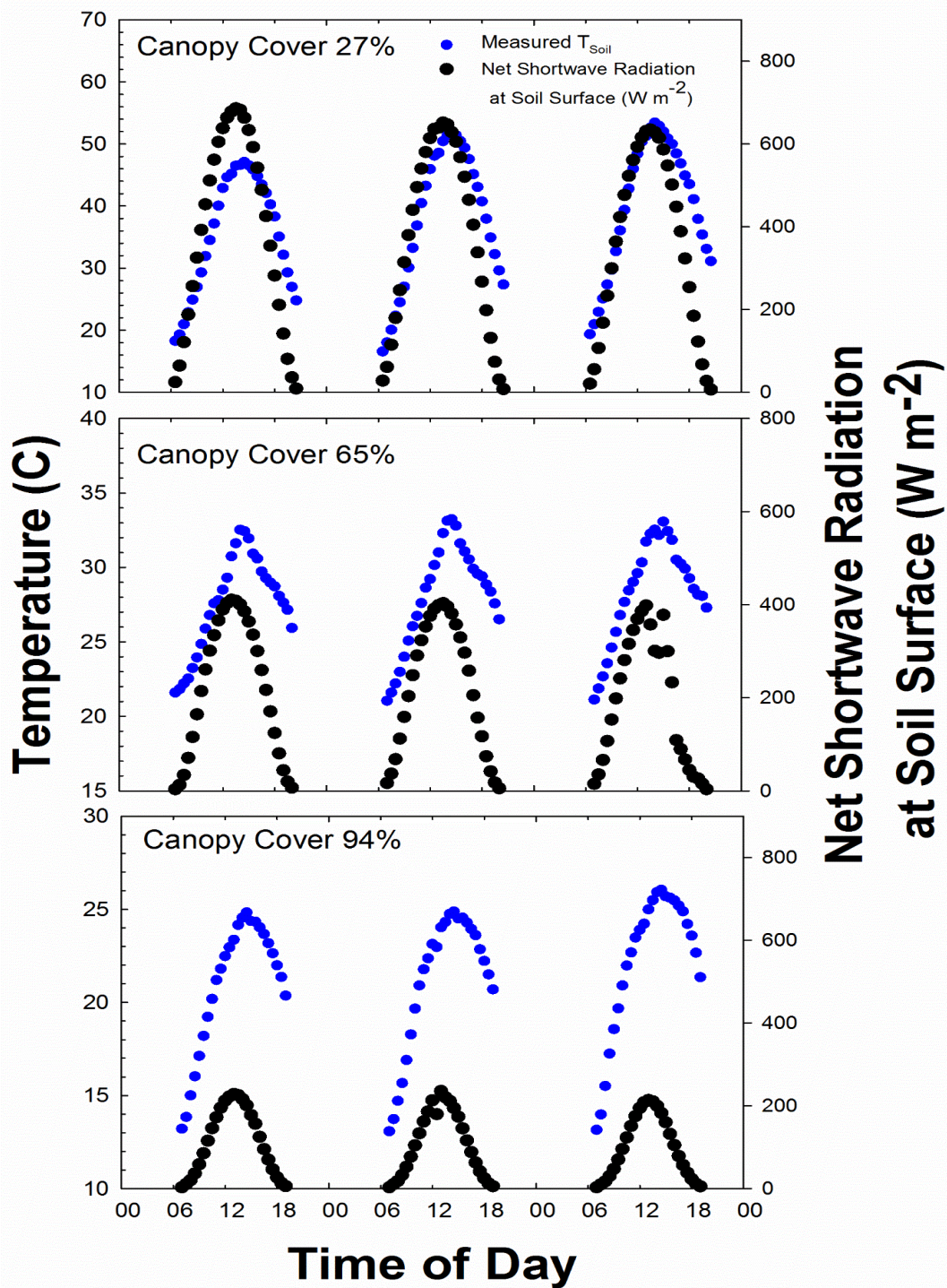
Figure D-3: The effect of net shortwave radiation (SW$_{ns}$) at the soil surface on the measured soil temperature.

APPENDIX E

REPRINT PERMISSION

JOHN WILEY AND SONS LICENSE
TERMS AND CONDITIONS

Jul 09, 2014

This is a License Agreement between Chris K Parry ("You") and John Wiley and Sons ("John Wiley and Sons") provided by Copyright Clearance Center ("CCC"). The license consists of your order details, the terms and conditions provided by John Wiley and Sons, and the payment terms and conditions.

All payments must be made in full to CCC. For payment instructions, please see information listed at the bottom of this form.

License Number	3424851498951
License date	Jul 09, 2014
Licensed content publisher	John Wiley and Sons
Licensed content publication	Plant, Cell & Environment
Licensed content title	In situ measurement of leaf chlorophyll concentration: analysis of the optical/absolute relationship
Licensed copyright line	© 2014 John Wiley & Sons Ltd
Licensed content author	CHRISTOPHER PARRY,J. MARK BLONQUIST,BRUCE BUGBEE
Licensed content date	May 5, 2014
Start page	n/a
End page	n/a
Type of use	Dissertation/Thesis
Requestor type	Author of this Wiley article
Format	Print and electronic
Portion	Full article
Will you be translating?	No
Title of your thesis / dissertation	Biophysically-based measurement of plant water status using canopy temperature
Expected completion date	Aug 2014

CURRICULUM VITAE

Christopher K.
Parry

57 S 1000 E
Hyrum, UT 84319
801-628-8933
chris.k.parry@aggiemail.usu.edu

Education

PhD in Plant Science (Crop Physiology), August 2014, GPA 3.91 Utah State University, Logan, Utah
Dissertation: *Biophysically-Based Measurement of Plant water Status Using Canopy Temperature*

BS in Horticulture Science, Dec. 2008, GPA 3.84 Utah State University, Logan, Utah

Primary Research Interests

Whole-plant physiology; soil-plant-atmosphere continuum; biophysical measurements and principles; crop water status monitoring; yield enhancement; optical and absolute chlorophyll analysis; and stress physiology.

Professional Focus

Measurement and modeling of the Soil-Plant-Atmosphere continuum
Environmental parameters and their effect on plant physiological responses
In situ measurement of leaf chlorophyll concentration

Work Experience

Graduate Research Assistant, Doctoral, 2009 to present Utah State University Crop Physiology Lab, Logan, Utah

- Research on crop water status using biophysical principles and energy balance methods
- Measurement of leaf chlorophyll concentration and the analysis of the optical/absolute relationship

- Programming and assembling the USU Environmental Observatory
- Measurement of plant growth response to ethylene and 1-MCP (1-methylcyclopropene) treatments

Undergraduate Research Assistant, 2008 to 2009
Utah State University Crop Physiology Lab, Logan, Utah

- Research on the effects of low phosphorous fertilizer on iron uptake in container grown corn
- Effects of soil pH on iron uptake in container grown corn
- Assist in research on slow release fertilizers in soilless media

Undergraduate Research Assistant, 2007 to 2008
Utah State University Plant Stress Physiology Lab, Logan, Utah

- Perform plant DNA extraction, PCR analysis, and gel electrophoresis
- Researching key proteins and their role in abiotic stress on plants
- Salinity, osmotic, drought, and stress testing

Publications

Parry, C., Blonquist Jr J.M. & Bugbee B. In situ measurement of leaf chlorophyll concentration: Analysis of the optical/absolute relationship. *Plant, Cell & Environment*, DOI: 10.1111/pce.12324

Skills

CRBasic datalogger programming
Matlab programming
Sigmaplot graphing software
Environmental Instrumentation
Excellent problem solving skills

Professional Presentations

Parry, C., Blonquist, J.M., Bugbee, B. 2013. Automated measurement of crop water status using canopy temperature and biophysical principles. ASA, CSSA, SSSA Annual Meetings, Tampa, FL. Poster presentation

Parry, C., Bugbee, B. 2011. Challenges of air temperature measurement. Intermountain Graduate Research Symposium, Logan, UT. Poster presentation (Placed 2nd)

Parry, C., Bugbee, B. 2010. Leaf Chlorophyll concentration: Linking relative and absolute measurements. NCERA-101 Conference on Controlled Environment Plant Studies, Madison, WI. Poster presentation

Parry, C., Bugbee, B. 2010. Leaf Chlorophyll concentration: Linking relative and absolute measurements. Intermountain Graduate Research Symposium, Logan, UT. Poster presentation (Placed 1st)

Parry, C., Bugbee, B. 2009. Iron nutrition of corn in soilless media. NCERA-101 Conference on Controlled Environment Plant Studies, Park City, UT. Poster presentation.

Teaching Experience

Teaching Assistant, Environmental Physiology (PSC 6200), USU Spring Semester 2011 Teaching Assistant, Environmental Physiology (PSC 6200), USU Spring Semester 2010 Teaching Assistant, Environmental Instrumentation (PSC 6000), USU Fall Semester 2011

Fellowships and Scholarships

Bertrand D. Tanner/Campbell Scientific Fellowship, 2013 Bertrand D. Tanner/Campbell Scientific Fellowship, 2011 Bertrand D. Tanner/Campbell Scientific Fellowship, 2010 John Shaw Welch Fellowship, 2012
Noelle and John Cockett Graduate Fellowship, 2010 Melvin E. Anderson Scholarship, 2008
Plant, Soils, Biometeorology Scholarship, 2007
Utah State University Presidential Scholarship 2005-2008

Professional Memberships

American Society of Agronomy (ASA)
Crop Science Society of America (CSSA)
Soil Science Society of America (SSSA)